# Development of Effective and Efficient Acoustic Emission Based Gear Fault Diagnosis Methods and Tools

BY

YONGZHI QU
B.S., Wuhan University of Technology, 2008
M.S., Wuhan University of Technology, 2011

THESIS

Submitted as partial fulfillment of the requirements for the degree of
Doctor of Philosophy in Industrial Engineering and Operations Research
In the Graduate College of the
University of Illinois at Chicago, 2014

Chicago, Illinois

Defense Committee:

David He, Chair and Advisor
Michael Scott,
Houshang Darabi,
Lin Li,
Eric Bechhoefer, GPMS LLC

*This dissertation is dedicated to my parents, Qu Zhongtong and Dong Shuli, for their unconditional love and endless support; to my grandfather, Dong Licai, for his support on my education over all the years. I also dedicate this dissertation to my girlfriend, Fengjiao Wang, for her encouragement and support, without whom the PhD grind would be lonely and depressed.*

## ACKNOWLEDGMENTS

I need first to thank my academic advisor—Dr. David He—for his supervising, guidance and support. He provided advices in all areas that help me accomplish my research goals and enjoy myself in the process. I would like to show my gratitude to Dr. He for his contribution of time, ideas, and funding for my PhD research. Without these support, I would not complete the dissertation. Also, his working attitude and life philosophy lead me to grow and become a better engineer and a better person overall. Dr. He will be my lifetime mentor in academia and life.

I would like to thank my dissertation committee members, Dr. Eric Bechhoefer, Dr. Michael Scott, Dr. Houshang Darabi, and Dr. Lin Li, , for their time spent on my dissertation and the valuable suggestions.

Specifically, I want to thank Dr. Eric Bechhoefer, for his valuable ideas and suggestions. In particular, I want to thank Dr. Bechhoefer for providing me the TSA codes and the heterodyne function. The generous support from Dr. Bechhoefer has helped me a great deal to complete my research. I gratefully thank Dr. Bechhoefer for the precious opportunity to learn and get inspiration from him.

I would like to show my gratitude to my colleagues, Brandon Van Hecke, Jae Yoon, and Junda Zhu for their helpful discussions and time spent on my data collection. I am glad that we have such a great and friendly lab. I enjoyed all the time working together with them. I sincerely thank them for the long time cooperation and I believe we can keep cooperating in the future.

I would like to thank David Mecha and his colleagues in the mechanics shop, who solved many of my test rig problems. They were always there when I had mechanic troubles.

I would like to thank Alan, Evelyn, Iris, Veronica for the help with my paper work and other things during my PhD study.

Qu Yongzhi

## TABLE OF CONTENTS

## LIST OF FIGURES

## LISTS OF TABLES

## LIST OF ABBREVIATIONS

| | |
|---|---|
| AE | Acoustic emission |
| CBM | Condition based maintenance |
| CI | Condition Indicator |
| DAQ | Data acquisition system |
| EMD | Empirical mode decomposition |
| EO | Energy Operator |
| FFT | Fast Fourier transform |
| PZT | Piezoelectric |
| RMS | Root mean square |
| RPM | Revolutions per minute |
| SK | Spectral kurtosis |
| STFT | Short-time Fourier transform |
| STG | Split torque gearbox |
| TSA | Time synchronous average |

## SUMMARY

Acoustic emission (AE) based sensing technology is considered an emerging technique for rotating machine fault diagnosis even though it has been successfully applied to non-destructive testing of static structures for many years. In comparison with the widely used vibration based techniques, it has numerous advantages. For example, it is capable of incipient fault detection. It is sensitive to the location of the faults and therefore could be used for fault location detection. However, there are a number of challenges in order to apply AE based technology for rotating machine fault diagnosis. In comparison with other sensors such as vibration sensors, AE sensors require a much higher sampling rate. The characteristic frequency of AE signals generally falls in the range of 100 kHz to several MHz, requiring a sampling rate of at least 2 MHz for AE data acquisition. AE data acquired with such a high sampling rate would add a tremendous burden on data storage and analysis for machine health monitoring, fault diagnosis and prognosis. In addition, there is a lack of well-developed signal processing methods that could effectively take advantage of the known structures of the machinery for fault diagnosis.

In this dissertation, effective and efficient AE based methods and tools for gearbox fault diagnosis have been developed and validated with gearbox seeded fault tests on a notational split torque gearbox. Specifically, a frequency reduction method has been developed based on the heterodyne technique commonly used in telecommunication to reduce the AE data sampling rate to as low as 20 kHz. By heterodyning, the AE signal frequency can be reduced from several hundred kHz to below 50 kHz. Also through heterodyning, the AE signals can be demodulated to remove less useful high frequency components while keeping the fault characteristic frequency components in the demodulated AE signals. As a result, the demodulated AE signals can be sampled at a low rate comparable to that of vibration sensors. In order to extract useful features

from AE signals sampled at a low rate, an effective AE signal processing method for gearbox fault diagnosis based on time synchronous average (TSA) has been developed. This is the first reported research effort in developing a physics based gearbox fault diagnosis method using AE sensors.

The developed AE based gearbox fault diagnosis methods and tools have several significant advantages. First, the heterodyne based frequency reduction method could down shift the sampling rate to that comparable to the vibration signals. The original meshing frequencies of the gearbox can be retained in the AE signals sampled at a low rate. This enables well developed vibration analysis methods to be applied efficiently in practice to the AE signals for gearbox fault diagnosis, which is one of the major contributions of this work. Also, this could reduce the storage and computational burden for further signal processing so that great cost reduction can be achieved. By using TSA, the knowledge of the physical structure of the gearbox can be utilized effectively and efficiently for fault diagnosis. This is different from any of the previous data driven methods which completely rely on a black box type of reasoning for gearbox fault diagnosis.

A comparative study between vibration analysis and AE analysis has also been performed. Different levels of tooth cut faults have been seeded and tested with both vibration and AE data collected. Results have shown that AE based approach has the potential to differentiate gear tooth cut levels in comparison with vibration based approach. While vibration signals are easily affected by mechanical resonance and background noises, the AE signals show more stable performance.

The effectiveness of AE analysis under low sampling rate has also been investigated. The results have shown that AE sampling rate could be as low as 20 kHz without serious performance degradation.

# CHAPTER 1
# INTRODUCTION

## 1.1 Machinery Fault Diagnosis and Health Monitoring

Machinery fault diagnosis has received tremendous attention since the 1960s. Especially, as computing power continues to expand, machinery diagnosis has entered the intelligent stage. Multiple techniques have been adopted by fault diagnosis, such as data mining based methods, statistical analysis and numerous other signal processing techniques. Fault diagnosis has played a critical role in industry. A lot of the mechanical systems in industry have incorporated health monitoring and diagnosis systems. Machinery diagnosis is defined as the technique of understanding the health condition of the running machine, and then identifying whether there is any fault associated with the entire system or critical parts within. Early stage fault detection is always preferred because maintenance could be scheduled when required and also could help avoid total machine failure.

Before emphasizing the importance of machinery diagnosis and monitoring, it is better to take a look at machine maintenance. The maintenance of a machine is classified into three categories: breakdown maintenance, time based maintenance, and condition based maintenance (CBM).

The first maintenance type, breakdown maintenance, is already out of date. Each machine failure could cause disaster or an industrial accident, and cause huge economic costs. The second type, time based maintenance, is widely adopted in industry. This is a relatively simple style of maintenance because the overhaul is performed on a time schedule. No sophisticated monitoring system is needed for this kind of maintenance system. Timely replacement of the critical parts could prevent most major catastrophes, and therefore, avoid the loss of life and property. However, the drawback of this kind of maintenance is that it is based on a blind schedule. Even

if the machine is still in a healthy condition, it might be replaced due to scheduled repair. Thus, it can be a huge waste of production time and money. On the other hand, CBM is an ideal dynamic maintenance strategy. With the help of a health monitoring system, the health condition of the system is tracked all of the time and maintenance is scheduled when required. In order to implement the CBM system, it is crucial to develop an efficient and effective health monitoring or fault diagnosis system.

There are three basic steps in performing fault diagnosis. The first is data acquisition. Data acquisition is generally accomplished by sensors. Various parameters could be collected, such as temperature, velocity, vibration, pressure, and so on. For machinery health diagnosis, traditional sensors include speed sensors, accelerometers, eddy sensors, etc. New sensors, like optical fiber sensors, laser sensors, and acoustic emission (AE) sensors, have attracted a lot of attention recently.

The second step is signal extraction and signal processing. Most of the data collected from the working environment contains a lot of noise. In order to extract the fault features, it is necessary to remove the noise and keep the signal of interest. Since the 1950s, a lot of methods have emerged as powerful tools for this purpose. Hilbert transform, power density spectrum, time synchronous averaging (TSA), and wavelet analysis are among the most popular techniques.

The third step is health condition decision making. Based on the features extracted from the above mentioned steps and previous experience, the judgments of current health status are made. Data mining methods, like classification and clustering, can help with the recognition of machine health status. Neural networks are also used for fault identification.

Currently, most of the machine fault diagnosis systems are based on vibration signal analysis. It is generally accepted that when there is any fault in the machine, the vibration amplitude will increase. Also, the vibration signal phase will be modulated accordingly as reported by McFadden (1986). By analyzing the vibration features, most machine faults can be identified.

AE was first applied to the testing of static structural objects, such as concrete bridges, pipeline systems, and large steel vessels, etc. Since the 1990s, AE sensors have been studied as potential tools for rotating machinery fault detection. However, the practical use of AE is still rare as of today.

### 1.2 Gear Fault Diagnosis

Gearboxes are applied to almost all of the transmission systems and power systems. Wind turbine systems and helicopter impetus systems are two types of systems that rely heavily on gearboxes. A wind turbine gearbox and a helicopter gearbox are shown in Figure 1 and Figure 2, respectively. According to the existing literature, gear failure plays a critical role in the overall failure modes of gearbox and transmission systems. Published in a gearbox reliability report by Link *et al*. (2011) on wind turbines, in 37 failure incidents, 36 involved with bearing failures and 22 have included gear failures. That means that approximately 59% of the failure modes involved gear failure. Another report shows that 19.1% of the failures of a helicopter transmission system included gear failure (Astridege, 1989). For industrial gearbox failure breakdown, it is reported by Liao (1995) that among parts failure in gearboxes, 60% is attributed to gears, while bearings account for 19%, shaft 10%, gearbox case 7%, fastener parts 4%, and oil seal 1%.

Figure 1. Gearbox schematic diagram of a wind turbine (Bosch Rexroth, 2011)

To accurately detect gear failure, a comprehensive understanding of the failure modes is essential. Sometimes, it is impossible to determine the exact cause of failure unless the condition of each tooth is completely checked. It is advised to understand the condition of the teeth, and keep monitoring the operating conditions.

The principal causes for gear failure could be attributed to design error, manufacturing error and application errors. During application, factors like mounting, installation, cooling, and maintenance could all affect the health and lifetime of the gears. As shown in Table 1, the American Gear Manufacturers Association (AGMA) has recognized the four basic types of gear failures, with a fifth to comprehensively cover everything (DeLange, 2000).

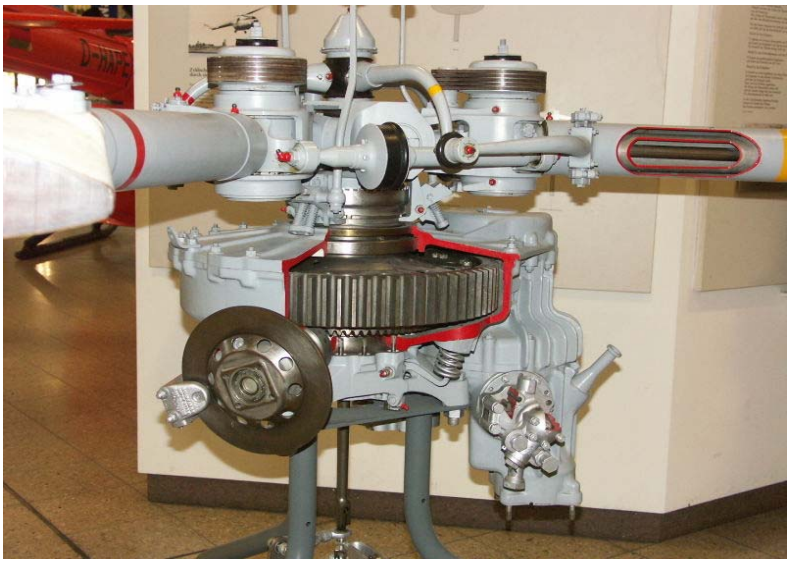

Figure 2. Helicopter bristol 171 sycamore main gearbox (Donzey, 2006)

Table 1. Gear failure mode classification

| | |
|---|---|
| **Wear Failure** | Moderate Wear |
| | Abrasive Wear |
| | Corrosive Wear |
| | Scoring |
| **Surface Fatigue Failure** | Pitting |
| | Spalling |
| | Micro-pitting |
| | Case Crushing |
| **Plastic Flow Failure** | Rippling |
| | Ridging |
| **Breakage Failure** | Bending Fatigue Breakage |
| | Overload Breakage |
| | Random Fracture |
| **Associated Gear Failures** | Quenching Cracks |
| | Grinding Cracks |
| | Rim and Web Failures |
| | Electric Current Damage |

Some examples of gear failures are shown in Figure 3.

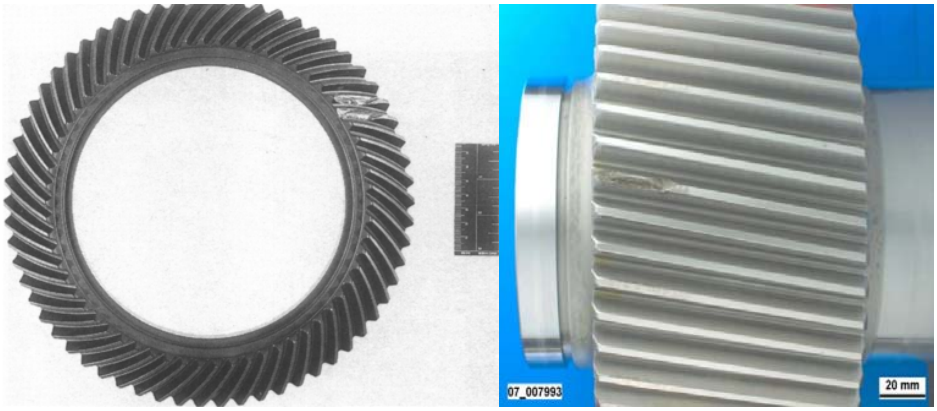


Figure 3. Gear failure graph

Among the above mentioned gear failure modes, tooth breakage accounts for 41%, surface fatigue 31%, surface wear failure 10%, abrasive wear 10%, and others 8% (Liao, 1995). Therefore, breakage failure, for example root breakage failure, is the dominant failure in gear fault.

### 1.3 Gear Noise and Vibration

When there is force variation, the components will generate a vibration. This vibration is then transmitted to the surrounding structure, and therefore noise and vibration will be generated on the gearbox (Smith, 1999). Transmission error (TE) is generally considered to be the primary excitation mechanism for gear noise and vibration. Transmission error is defined as "The difference between the actual position of the output gear and the position it would occupy if the gear drive were perfectly conjugate" (Åkerblom, 2001). Vibration signal analysis is an important tool when experimentally investigating gear noise because gears generate noise at specific frequencies, which are related to the number of teeth and the rotational speed of the gear. Gear conjugating involves several kinds of stress, among which two basic stresses are: contact stress and root bending stress (Li, 2013; Tiwari and Joshi, 2012). Excessive contact stress causes surface pitting/wear, while the latter causes tooth breakage or tooth root crack. On the contrary,

when a tooth crack fault is present, it also affects the contact stress on the broken tooth. The process of gear mating is complex. Numerous papers studied the numerical models and performed extensive experiments to identify the dominant cause of gear noise. The major factors contributing to gear noise include tooth stiffness, manufacturing error, tooth profile, backlash, and asperity ratio. These factors determine the smoothness of the gear meshing and therefore cause the vibration and AE signals.

In this dissertation, gears with partial tooth cut were used in the validation tests. In general, backlash and contact ratio are two major factors that are affected by tooth cut fault. Backlash, in the context of gears and gear trains, is the amount of clearance between mated gear teeth. It is the gap that can be seen when the direction of movement is reversed and the slack or lost motion is taken up before the reversal of motion is complete. The presence of backlash has a significant effect on the impact dynamics of meshing gear teeth-pair. It is one of the most common faults found in gear systems and is essential for gear transmission in the sense that too little backlash may result in interference between the teeth while excessive backlash would cause looseness during gear mating. Generally, the greater transmission accuracy required, the smaller backlash needed. The presence of excessive backlash can result in larger impact energy than normal. The initial contact can be modeled as an impact phenomenon when backlash exists between mating gears. Gear impact is generally approximated by a linear model (Sarkar *et al*., 1997).

Several recent gear mechanics studies regarding backlash will be briefly reviewed here. De La Cruz and Rahnejat (2008) described a model based on classic Hertzian impact for gear mating under medium to heavy load. They modeled the instantaneous geometry of the contact and prevailing kinematics of contiguous surface for helical teeth pairs. Theodossiades and Natsiavas (2000), analyzed dynamic response of a gear pair system with periodic stiffness characteristics and backlash. The study provided an explanation for intermittent chaos and other complicated

dynamic behaviors observed in previous experimental studies. Impact-induced vibration analysis was performed theoretically and experimentally by (Gnanakumarr *et al*., (2005). The results showed that remote impact of meshing transmission teeth through backlash induced high frequency components in drivetrain vibrational response.

Tuma (2009) gave an overall review on the practical techniques and procedures employed to quiet gearboxes and transmission units. He concluded that sufficiently rigid housing, shafts and gears, and high contact ratio gears are important to reduce gearbox noise.

As reported by Sarkar *et al*., (1997), vibration analysis could be used to establish a backlash model. Disturbances, such as impacts, rolling, sliding and friction produce elastic deformations which absorb the energy during gear meshing. These elastic deformations cause elastic waves which transmit the energy from the gear to the gear housing. From the aspect of sensors mounted on the gear house, the typical propagation path is gears, shaft, bearing and housing (Ognjanović and Snežana, 2012). The elastic wave released by material deformations is the direct source of AE signals. On the other hand, a vibration sensor measures the velocity, which is the second derivation of the micro-displacement.

Gear noise and vibration are the direct source of AE signals and vibration signals. Therefore, AE and vibration are among the most effective tools for gear fault detection. AE and vibration based detection methods will be discussed next.

## 1.4 AE Introduction

AE analysis is a powerful technology that can be used in a wide range of non-destructive applications, such as: metal pressure vessels, piping systems, reactors, and the similar (Vallen, 2002). The AE generation diagram is showed in Figure 4 for illustration (Hellier, 2003).

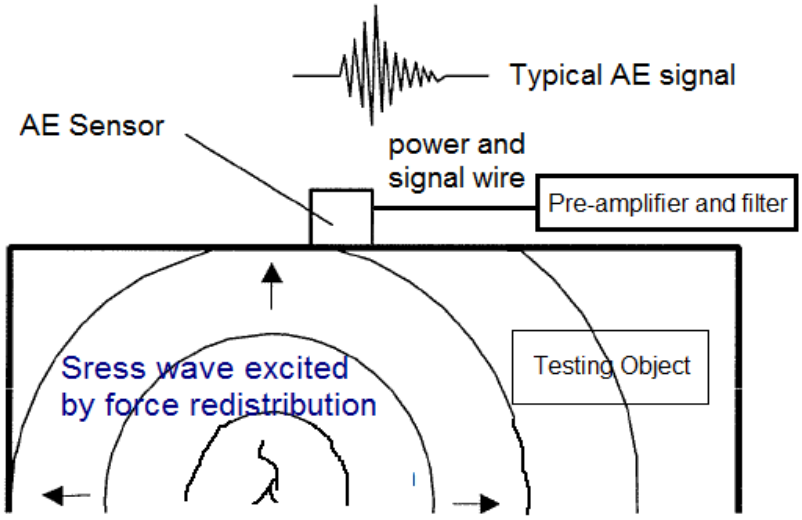


Figure 4. The source of AE

AE is commonly defined as transient elastic waves within a material, caused by the release of localized stress energy. It is produced by the sudden internal stress redistribution of material because of the changes in the internal structure of the material. All solid materials have certain elasticity. When external force is imposed on the material, the material could be strained or compressed and spring back when the force is released. Under higher force, there is higher elastic deformation, and therefore, higher elastic energy is generated. Especially, when there are cracks inside the material, the cracks will cause rapid relaxing of the elastic energy with a fast dislocation. This rapid release of elastic energy is called an AE event. The AE event then generates an elastic wave, which could be detected by AE sensors and recorded thereafter. The impact at its origin has a wide frequency range (from 10s of kHz to several MHz), while the frequency of AE testing of metallic objects is in the range of ultrasound, usually between 100 and 300 kHz (Vallen, 2002).

AE testing is a passive technique of measuring and analyzing the ultrasound pulses emitted by a defect at the moment of its occurrence. In contrast to the ultrasound technique, one does not measure the response/reflection to an artificial and repeatable acoustic excitation which is sent to

the test object. Instead, the AE signals are generated by the defects directly under certain stress. This signal is measured, recorded and then analyzed.

AE data collecting can be accomplished by portable instruments or in a stationary laboratory setting. Typically, AE testing systems contain a sensor, preamplifier, and a DAQ board. Other auxiliary components like displays, and storage equipment (for example, personal computers) can be constructed as required. AE sensors respond to dynamic motion caused by an AE event. Inside the AE sensor, a certain form of a transducer is used to convert mechanical movement into an electrical voltage signal. The transducer element in AE sensors for most of the cases is a piezoelectric crystal, which is generally made from ceramic material such as lead zirconate titanate (PZT).

In the ideal case, the AE signal collected by AE sensors will be noise free. Unfortunately, this cannot be achieved in reality. In order to reduce the noise interference, preamplifiers were designed to help restrain the background and electromagnetic noise. Most of the modern AE sensors have incorporated integrated preamplifiers. After that, the signal will be sampled at a certain frequency by the DAQ system and eventually stored on a computer for analysis.

There are two types of AE signals: burst AE signals and continuous AE signals. The differences between these two types of AE signals are their ability to convey information about transient AE events or continuous AE event sequence, and their post-processing flexibility. Traditionally, most of the research papers are focused on the analysis of the AE bursts, which are pulses or short wave packets. The rise and fall time, AE count, measured area under the rectified signal envelope (MARSE), duration and energy level are typical AE burst features of research interest, as given in Figure 5.

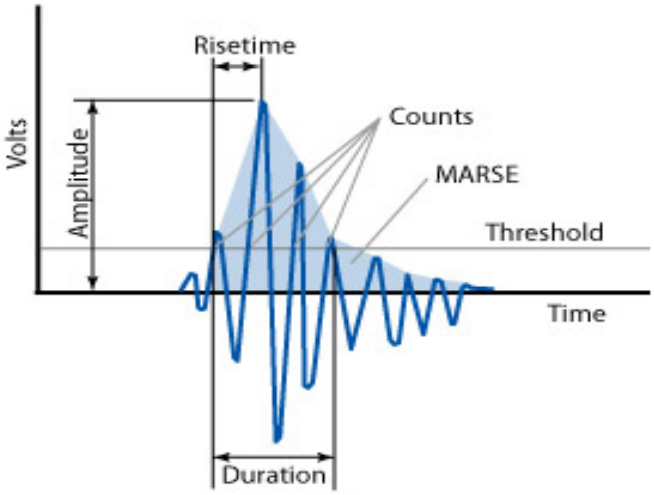


Figure 5. AE burst features

In this dissertation, continuous AE signals are collected. AE signals are collected in a similar manner as vibration signals. An example of continuous AE signal is shown in Figure 6.

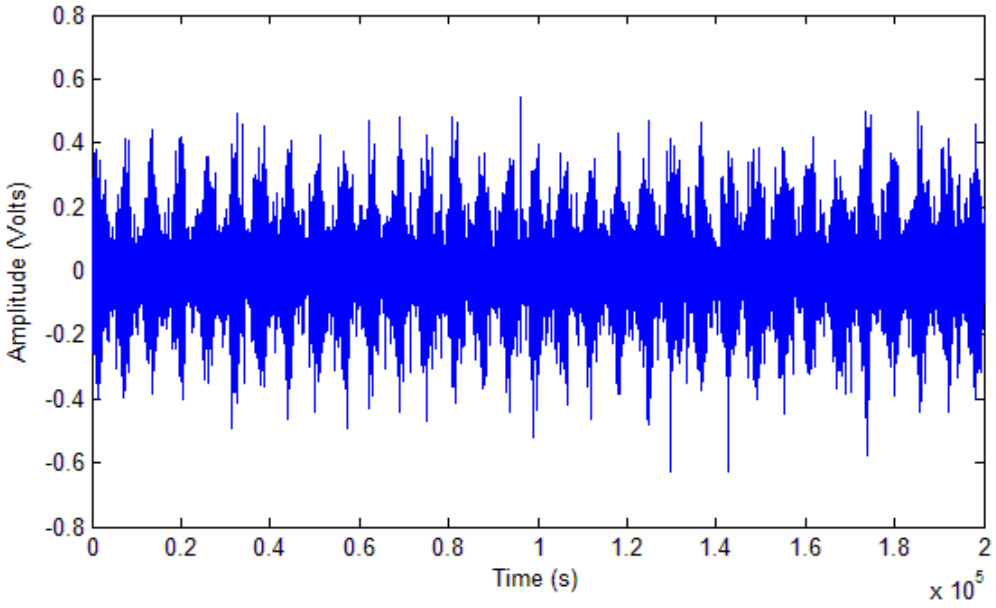


Figure 6. An example of continuous AE signal

Using continuous AE signals, the fault diagnosis process would be similar to that of vibration based methods. This potentially allow us to develop AE methods based on the well-developed vibration techniques.

There are several advantages of AE testing compared with vibration testing (Holroyd, 2000):

1) AE is insensitive to structural resonance and unaffected by typical mechanical background noises;
2) AE is more sensitive to activities of earlier faults;
3) AE provides good trending parameters;
4) AE signals are sensitive to the location of the faults.

Challenge of using AE sensor include: The output signal from AE sensor are generally high frequency, even as high as several MHz. Thus high sampling rates are required, 2 – 10 MHz. Other challenges include the high data volume and complicated features of AE signals, which make the data processing difficult.

## 1.5 The Research Challenges of AE Diagnosis

As mentioned in the last section, AE signals require a sampling rate above 2 MHz. This not only makes the AE detection more expensive but also leads to hard AE signal processing problems. The data processing of AE data brings a large computational burden even for the newest personal computer. This further restricts the application of sophisticated signal processing methods to AE signals, making the AE based fault detection less attractive within the range of current knowledge and technique.

On the other hand, traditional vibration based diagnosis is less sensitive to earlier stage faults (Balushi and Samanta, 2002; Ghamd and Mba, 2006; Loutas *et al*., 2011). A lot of industrial companies have realized AE could bring a revolutionary change to machine health monitoring. AE is considered as the next generation of vibration for condition monitor by Kittiwake (Lucas, 2012)

As a promising technology, one also needs to be aware of the tremendous difficulty of mastering the new method. Researchers by far only have limited knowledge of interpreting the AE signal and the correlation of the AE frequency components with machine faults. The challenge lies in how to efficiently extract more useful and usable information from AE signals similar to what is done with vibration signals.

## 1.6 Research Objectives

This research on AE based machinery fault detection is intended to explore the potential of future applications of AE based techniques and further establish the methods and tools that are associated with its applications. Specifically, the efficiency and effectiveness of the diagnosis methods will be considered concurrently in order to lower the cost and complexity for commercial usage.

In order to develop a set of methods and tools that can effectively and efficiently detect gear faults, a notational split torque gearbox (STG) was designed and built in the Intelligent Systems Modeling and Development Laboratory. The testing tools and data acquisition system were also built to facilitate the testing process. Simulated faults on the gears will be tested in the lab environment. Experiments were conducted on detecting different tooth faults seeded in the STG. AE data was then collected and analyzed. It is proposed that the following research objectives should be accomplished for gear fault diagnosis:

1) Hardware based frequency demodulation technique should be established and validated.
2) An effective methodology to diagnose the fault feature in the faulty AE signal should be developed.
3) Condition indicators for the diagnosis of tooth damage severity level should be developed and validated.

# CHAPTER 2
# RESEARCH BACKGROUND AND LITERATURE REVIEW

Currently, vibration is the most widely used tool in diagnosis of machine fault, like bearings, gears, etc. Common vibration sensors include accelerometers, displacement and velocity sensors. Various time and frequency domain analysis techniques have been applied to vibration signal analysis. However, vibration signals have some drawbacks when it comes to the incipient stage of the machine fault. Some early signs of fault in rotation machines might not show in vibration signals but could be caught by AE sensors (Al-Ghamd, 2006). If these faults could be caught in an early stage, significant maintenance cost could be saved. Hence, AE techniques began to attract researchers' attention to machine health monitoring and fault diagnosis.

AE is commonly defined as transient elastic waves within a material, caused by the release of localized stress energy. It is produced by the sudden internal stress redistribution of material because of the changes in the internal structure of the material. The ability to extract AE signatures can be used to give diagnostic indications of component health.

In comparison with vibration analysis, AE has the following advantages (Holroyd, 2000): 1) insensitive to structural resonance and unaffected by typical mechanical background noises; 2) more sensitive to activities of faults; 3) provide good trending parameters; and 4) AE signals are sensitive to the location of the faults. Challenge of using AE sensor includes: The output signals from AE sensors are generally high frequency, even as high as several MHz. Thus high sampling rate is required, 2 – 10 MHz. Other challenges include the high data volume and the complicated features of AE signals, which make the data processing highly difficult.

Since, most of the methodologies developed for AE signal analysis are closely related to vibration analysis, it is important to understand the fundamentals of how to extract machinery fault features using vibration analysis. This review section will include two subsections. Section 2.1 will give a literature review on vibration monitoring techniques and Section 2.2 will present the current status of AE based research and applications.

## 2.1 Vibration Analysis

### 2.1.1 General Technique Classification for Vibration Analysis

Numerous signal processing techniques and algorithms have been investigated for machine fault diagnosis and prognosis. In industrial applications, the useful algorithm varies depending on the specific situation. It also highly depends on experience and previous knowledge to choose the effective and efficient methods.

Some recent review papers have given the classification for vibration analysis. A detailed review was done by Randall (2004) for rotating machinery monitoring. A wide range of method, such as, FFT and spectrum analysis, Autoregressive (AR) model, separation of periodic and random signals using TSA and order tracking, noise cancellation, and demodulation techniques, were reviewed in the paper. Another review paper for helicopter transmission gearbox was published by Samuel and Pines (2005). Vibration-based helicopter transmission diagnostics for the development of health and usage monitoring system (HUMS) for rotorcraft gearbox and drivetrain components are the main focus of this paper. From traditionally used techniques, such as statistical measurement of the energy of the vibration signal, McFadden's amplitude and phase demodulation methods, to modern methods based on diagnosis condition indicators were given detailed discussions. Root mean squared (RMS), crest factor (CF), energy ratio (ER), kurtosis,

FM0, FM4, etc., are among the most popular and useful indicators for vibration analysis. Time-frequency analysis, wavelet analysis, neural networks and modeling methods are the other large categories of vibration methods. Relatively new emerging methods like empirical mode decomposition (EMD) and intrinsic mode functions (IMFs) were also reviewed in this paper. A more comprehensive review paper which covered both diagnosis and prognosis was given by Jardine *et al*. (2006). Regarding to fault diagnosis and health monitoring, three large categories of methods, namely, time domain analysis, frequency domain analysis and time-frequency analysis were reviewed in detail. In this paper, a similar review process based on these three classes was conducted.

### 2.1.2 Time Domain Vibration Analysis

Time domain analysis techniques aim to analyze the waveform itself. It is probably the most traditional method in literature. Under the commonly accepted assumption that the vibration level will increase as the fault increases, waveform energy level and amplitude as well as their derivative parameters are the main interests of earlier researchers. Later, Steward (1977) noticed that besides the random noise inside the vibration signal, signals at the meshing frequency and its sideband frequency are the main components of the vibration noise in gearbox. Inspired by this observation, he proposed the prototype of TSA applied on gear vibration. The theoretical basis of TSA was introduced earlier by Braun (1975) for the purpose of extracting periodic signals from the raw noisy signals. The idea of TSA is to calculate the ensemble average of the raw signal over a number of revolutions in order to synchronize the periodic signal that is associated with shaft revolution while reducing the random noise from other sources and enhancing the signal component of interest.

According to the observation of Stewart (1977), in a healthy gearbox, the amplitude of the sidebands were small. He argued that the presence of a fault would superimpose additional

modulation on the signal, and further, for different types of faults, different modulation effects would appear on the vibration signal. In the presence of major tooth faults, the peak to peak value of $x(t)$ tends to increase. However, for distributed tooth surface damage, the peak-to-peak value might not increase, while the amplitude of the mesh frequency and its harmonics would decrease due to lower level of frequency centralization. Stewart also had another crucial observation that the additional dynamics caused by the appearance of a fault tend to significantly increase the amplitude of the sidebands, especially when a local defect such as a single tooth failure is presented. This could further generate an increase of the high amplitude components in the modulation functions.

In order to amplify the abnormal changes in the amplitude of the modulation functions, especially those corresponding to the sidebands frequency, Stewart (1977) proposed to construct a difference signal which is equal to the subtraction of the gear meshing signal and its harmonic, as well the corresponding first order sidebands from the original signal. Then, the statistical properties of the difference signal can be analyzed and the health status of the gear system can be concluded. The initial purpose of this difference signal was to eliminate the entire meshing harmonic signal along with the first order sideband signal, while obtaining most of the high order sidebands signal and Gaussian noise. Later, Zakrajsek (1993) argued that the first sideband signal needs not to be removed.

Upon the extraction of residual signal, the amplitude and phase demodulation techniques could be applied on the residual signal. For normal gearbox this signal should only contain the low amplitude meshing harmonic sidebands and Gaussian noise, while for faulty gearbox, abnormal amplitude modulation behaviors could be observed. Many gear fault detection methods were developed based on the residual signal features (Wang, 2001; Siegel *et al*., 2012). As shown in

Figure 7, Lebold *et al*. (2000) gave a processing flow of the TSA based CBM feature extraction methods.

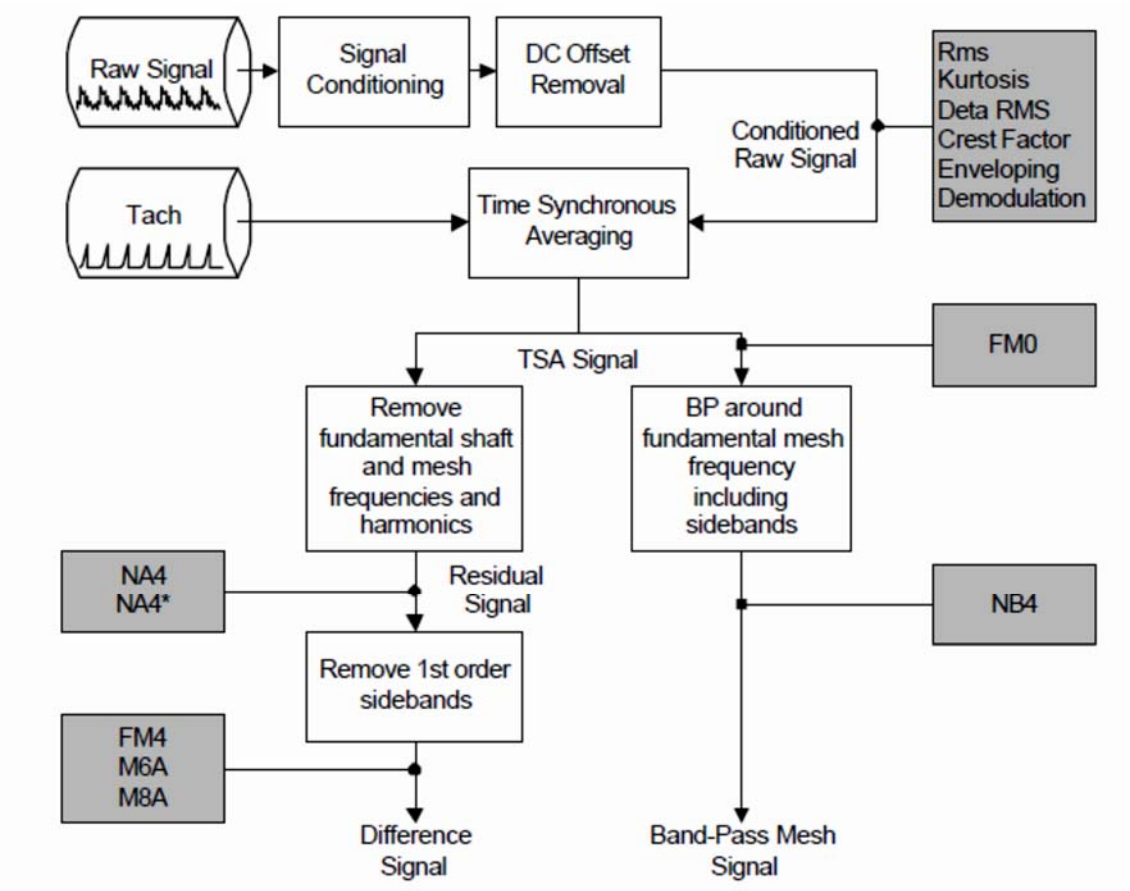


Figure 7. The processing flow of TSA based diagnosis methods

TSA was widely used in vibration analysis. Some reference details could be found in (McFadden, 1986, 1987, 1991, 2000; Braun, 2011). Review on TSA algorithm could be found in (Dalpiaz *et al*., 2000; Bechhoefer and Kingsley, 2009). Different interpolation techniques for the tachometer signal and vibration signal were compared by Bechhoefer and Kingsley (2009). The conclusion drown from this article was that different interpolation algorithms were relatively close in performance. However, they suggested Fourier domain TSA gave a better distinction in fault

detection. Also tested in their paper was tachometer less TSA technique. The performance of tachometer less TSA was comparable to that of TSA with tachometer signal.

Tachometer less TSA technique has been reported in several other papers as well. Jen Jong, *et al*. (1996) are the first who realized the important of tachometer less TSA technique. They proposed a method to extract the phase reference directly from the vibration signal and use this reference signal as the tachometer signal to perform standard TSA. The synchronous phase averaging method could transform a quasi-period signal into a period signal and ready to be used for fault detection. The proposed technique first narrow band filtered out one of the meshing harmonics. The phase variation signal was then calculated by Hilbert transform. Then, a standard periodic signal was obtained by non-uniform sampling of the original signal with reference to the phase variation signal. After that, a uniformly sampled periodic signal could be reconstructed by interpolation. Later, standard TSA was calculated and plotted. This was the first paper to show that the gear fault could be identified by discontinuity and irregularity behaviors in enhanced TSA waveforms. Bonnardot *et al.* (2005) proposed another tachometer less TSA method by angular resampling, and later this work was enhanced by Combet and Gelman (2007). They processed the shocks produced by gear tooth meshing to estimate the position of the gear against time. Then, interpolation enables the ability to reconstruct the signal in angular domain. After that, the classic TSA method can be used to calculate the TSA signal. A recent paper for bearing fault detection also employed the method of tachometer less TSA technique (Siegel *et al*., 2012). In their paper, they computed the average signal with reference to the fault frequency instead of shaft rotation frequency. Compared with envelope analysis, they obtained an enhance fault feature results which could better indicate the damage level of the bearing case.

Time series analysis is another time domain analysis method. The methodology behind time series analysis is to fit the historical vibration data to a parametric model and use this model to

test future data. AR and the autoregressive moving average (ARMA) are the most popular models used in practice. Poyhonen *et al*. (2004) used an AR model fitted to the vibration data of induction motor for condition monitoring. Baillie and Mathew (1996) compared the performance of AR model, back propagation (BP) neural network model and radial basis networks in bearing fault diagnosis. A state space based adaptive AR model was proposed by Zhan *et al*. (2003) to analyze vibration data.

Self-adaptive noise cancellation (SANC) is based on adaptive noise cancellation (ANC). ANC requires a reference signal coherent with the noise contained in a primary signal to remove the noise. The system takes two inputs, a primary input containing the corrupted signal and a reference input containing noise but not the useful signal. The noise signal is correlated in some unknown way with the primary noise. SANC used a delayed version of the primary signal itself as a reference signal, and can be used to separate discrete frequency components from random components, which have a short correlation length.

SANC is capable of attenuating any discrete frequency components masking the gear meshing frequency or gear fault frequency. This method has been investigated for the removal of masking components which reside in the same frequency region as the bearing fault components by Ho and Randall (2000). The results of this paper showed that SANC could greatly improve the signal to noise ratio (SNR). After SANC was used, the ball-pass frequency of the outer race (BPFO) could be enhanced and clearly viewable.

Some other time domain methods were also presented in current literature. In (Wang *et al*., 2001), they investigated three non-linear diagnostic methods for rotating machinery diagnosis, namely, pseudo-phase portrait, singular spectrum analysis, and correlation dimension. Wang and Lin (2003) presented a phase space reconstruction method based on singular value decomposition

technique and evaluated its effectiveness on the application of gear system condition monitoring. Baydar *et al*. (2001) developed a method based on multivariate statistical and principle component analysis (PCA) for incipient local faults at an early stage for gears.

### 2.1.3 Frequency Domain Vibration Analysis

The most simple frequency domain method is investigating the frequency spectrum by Fourier transform. The frequency domain signal can clearly display the related vibration components corresponding to different parts of the system and those frequency components directly caused by certain faults. It is easier to separate, remove or extract different vibration components. Besides the most commonly used fast Fourier transform (FFT), envelope analysis, and power spectrum are other powerful tools for spectrum inspection.

Ho and Randall (2000) investigated the application of self-adaptive noise cancellation (SANC) in conjunction with envelope analysis in order to remove discrete frequency masking signals. They proposed two ways of combining these techniques. In both methods, the original signal was band-pass filtered and frequency-shifted to reduce the number of samples to be processed by SANC. It was then proposed that the subsequent envelope analysis could be performed by Hilbert transform or band-pass rectifications. Both of the methods reduce the masking effects in the envelope spectrum by removing pseudo-sum frequencies or placing them outside the frequency range of interest. Simulated and actual vibration signals were used to illustrate the effectiveness of the methods.

Squared envelope analysis was compared with cyclostationary analysis (Randall *et al*., 2001). The conclusion of this paper was that cyclostationary analysis obtains the same result as a Fourier transform of the average squared envelope of the signal. It was argued that if envelope analysis was carried over to spectral correlation analysis, a comparable result could be acquired without

performing such complicated cyclostationary analysis. It was further claimed that there was a possibility that the full spectral correlation may still give some advantage in distinguishing modulation effects due to gear rotations and bearing inner race rotations (even at the same speed) by virtue of the different amounts of randomness associated with each.

Cepstrum analysis was tested by Dalpiaz *et al*. (2000). Ceptrum has its advantage in detecting the harmonics and sideband patterns in power spectrum. Dron *et al*. (1998) proposed an autoregressive spectrum analysis method for bearing fault analysis. Mechefske and Mathew (1992) investigated AR model based monitoring method and a nearest neighbor classification tool for fault diagnosis. An artificial neural network based classification method was employed with combination of frequency domain features by Yang *et al*. (2002). The vibration frequency features including the power spectrum, the bispectrum, the bicoherence, the bispectrum diagonal slice, the bicoherence diagonal slice, etc., were extracted from the vibration signatures and further investigated. Then an artificial neural network classifier was used to identify the bearing conditions. Quadratic phase coupling (QPC) was also tested in this paper.

Stack *et al*. (2004) developed an amplitude modulation (AM) detector to identify these interactions and detect the incipient bearing, with the pre-knowledge of the bearing characteristic fault frequencies.

Sideband structures in measured vibro-acoustic signatures of rotating machinery systems were often used for fault diagnostic application. Blankenship and Singh (1995) developed a set of dual domain periodic differential equations to show the force modulation inherent features based on the commonly held belief that simple amplitude and frequency or phase modulation processes are responsible for generating such sidebands. Parker *et al*. (2000) used a bispectral statistical change

detection algorithm for machinery health monitoring. Similar techniques were also presented in (Chow and Fei, 1995; Arthur and Penman, 1997).

### 2.1.4 Time Frequency Vibration Analysis

There are certain kinds of frequency information loss in the traditional Fourier analysis. The frequency variation with regard to time is not distinguishable in FFT. In order to better interpret the non-stationary signal in both time and frequency domain together, time-frequency analysis methods were developed. Short time Fourier transform (STFT) and Wigner-Ville distribution are two of the most useful techniques that fall into this category. Gear fault analysis with STFT was performed in (Wang and McFadden, 1993; Andrade *et al*., 1999), separately, while the latter gave a comparative study of STFT, Wigner-Ville distribution and wavelet analysis. Gear fault diagnosis using Wigner-Ville distribution was also investigated in (Pan *et al*., 1998; Naim and Andrew, 2001).

Wavelet analysis is another powerful tool applied in vibration and acoustic signal analysis. Compared with FFT, Wavelet analysis has several advantages (Jardine, 2006):

1) Wavelet could express a signal with different frequency at different time.
2) Wavelet is able to provide a high frequency resolution at low frequency end and a high time resolution at high frequency end with long duration low frequencies and short duration high frequencies.
3) Wavelet has the ability to reduce noise and extract correlated features.
4) The computational complexity is even lower than FFT.

Among numerous time-frequency techniques, WT and EMD are proven to be the most powerful tools on handling the non-stationary property in the vibration signal generated by the gear transmission system (He *et al*., 2010). An early paper using wavelet analysis to perform gear

diagnosis was reported by Wang and McFadden, (1996). It was further discussed in (Chen, 2002; Tse *et al*., 2004). Reviews about the applications of the wavelet transform in machine condition monitoring and fault diagnostics can be found in (Peng and Chu, 2004). EMD based fault diagnosis methods were introduced in (Li *et al*., 2007; Bassiuny *et al*., 2007; Shen and Huang; 2008; Wang and Heyns; 2011; Li and He 2012). Paper review on EMD based diagnosis of rotating machinery was published by Lei (2012). Hilbert Huang Transform (HHT) was first developed by Huang *et al*., (1998). HHT was the combination of EMD method with Hilbert transform. It was later revisited again by Huang *et al*., (2003). HHT was widely used in rotational machine health diagnosis (Liu *et al*., 2006; Yan and Gao, 2006).

## 2.2 AE Analysis

AE has been studied as a potential information source for machine fault diagnosis for a long time. The feasibility of the detection of fault is well established. However, AE sensors have not yet been applied widely in industrial applications for machine fault diagnosis because of the high cost and difficulties in AE data analysis. Firstly, in comparison with other sensors such as vibration, AE sensors require much higher sampling rate. The characteristic frequency of AE signals generally falls into the range of 100 kHz to several MHz, which requires a sampling system with at least 2 MHz sampling rate. Secondly, the storage and computational burden for large volume of AE data is tremendous. Thirdly, AE signal generally contains lots of complicated frequency components which make traditional frequency analysis less effective and efficient.

### 2.2.1 Current Industrial Applications and Standards for AE

AE sensing is a long established technique but it is only applied in limited industrial areas, for example, the testing of pressure vessels, bridge structural testing and other structural testing. Two ISO standards were made to regulate the calibration of transducers (ISO 12713, 1998a;

1998b). However, for the application of monitoring rotating machinery, AE still remains in the research stage, even though trial results on gear and bearing applications have been published intensively in recent years. A draft ISO standard for the condition monitoring and diagnostics of machines by AE was completed in 1996 (ISO 22096, 1996). The establishment of ISO standard showed the potential applications of AE for machinery fault diagnostics and health monitoring in the future.

### 2.2.2 Overview of AE in Machinery Diagnosis

AE is defined as transient elastic waves within a material caused by deformation and the release of localized stress energy (Mathews, 1983). Even though AE has been studied as a potential tool for machine fault diagnosis for a long time, the source and characteristics of AE signals, especially in machine fault detection, still cannot be fully understood. Initially, burst type AE signals were used for fault detection in structural health monitoring. The AE bursts were believed to be fault related. While this might hold a ground truth for static structural fault detection, it has never been proved for rotating machines. For bearings, it has been reported that asperity contact was the primary sources of AE signals (Al-Ghamd and Mba, 2006). For gears, similar studies have not been performed systematically yet. The relationship between AE signals and asperity contact under elastohydrodynamic lubrication regime has been studied, which is synonymous with gears (Tan and Mba, 2006). They identified asperity contact as a significant source of AE signals but did not investigate other sources in detail, such as the gear dynamics, backlash and so on. It is generally accepted that an increase in meshing stress would generate larger amplitude AE responses (Miller and McIntire, 1987). Based on this assumption, AE signals are postulated to be mostly related to the interaction and impact of teeth during tooth meshing. The impact on the surface of the tooth causes material deformation and is followed by the stress energy release, which will then generate transient elastic waves. The exact AE sources during gear meshing are still open to further research.

AE signals are not relatively affected by structural resonance and can be more sensitive to early fault activities (Holroyd, 2010). When an unknown fault starts to form in the machinery, energy loss actions such as impacts, friction, and crushing generate sound wave activity that spans a broad range of frequencies (Loutas *et al*,. 2011). AE sensors can catch frequencies that are much higher than those in vibration signals, and therefore, their use enables the technicians to detect inchoate faults before any damage occurs. Also, by quantitative methods, one could monitor the fault evolution process from the beginning. Compared with vibration analysis, AE signals have the potential to detect small abnormal friction, initial cracking and so on. It was found by Mba (2003) that AE signals excited from bearing defects generally lied in 100 kHz to 1 MHz frequency range, while vibration signals excited from defects such as imbalance, looseness, misalignment, and shaft bending components lied in a much lower frequency range. The similar frequency range was also found for gears that typical frequencies associated with AE activity range from 20 kHz to 1 MHz (Mba, 2005).

In an early study that applied an AE technique to the analysis of fatigue crack growth in a carburized gear tooth by Tomoya *et al*. (1994), the AE energy rate of increase was found to be proportional to the stress intensity factor and crack growth rate. Baydar and Ball (2001) used the smoothed pseudo-Wigner–Ville distribution to compare the results from acoustic and vibration signals. They simulated three types of progressing local faults: broken tooth, gear crack and localized wear. Their results suggested that acoustic signals are more effective for the early detection of faults and may provide a powerful tool to indicate the various types of progressing faults in gearboxes. However, the acoustic signal presented in their paper was collected by a microphone, which was not exactly AE. AE signal is the elastic stress wave generated inside a solid material, typically metal, due to energy release. An acoustic signal refers to the sound signal which reaches the air and can be collected by a microphone. An acoustic signal is

different from an AE signal in the way that acoustic signals are generally contained in the audible range (20 Hz ~ 20 kHz), while AE frequencies remain in the high frequency range (1 kHz ~ 1 MHz).

Traditionally, only the time domain features, like peak, total energy, standard deviation, median, AE counts, root mean square (RMS) voltage and duration have been extracted in condition monitoring (Shiroishi, 1997; Mba, 2003; Elmaleeh, 2008). However, these are all related to the absolute energy levels of the measured signal. Since the absolute energy can vary from one machine to another or in different locations on the same machine, these kinds of criteria can be inaccurate. Consequently, these parameters are not ideal for AE based fault detection purposes. Stochastic model based analysis methods were proposed by Melton (1982) and later by Hall and Mba (2004). In these methods, the feature of multiple AE burst must be extracted first, and then statistical model and clustering criteria were employed to do classification. Inevitably for these methods, a large volume of data needs to be processed and baseline criteria need to be established, which makes the methods less attractive. Gao *et al.* (2010) proposed a wavelet transform based method to analyze AE signals, which could act as a supplement redundant method for vibration test. He and Li (2011) developed a data mining based method to classify the condition indicators derived from different AE data to detect fault. Later, Li and he (2012) introduced an EMD-based AE feature quantification method. In their work, successful detection of gear fault was achieved on AE data sampled at as low as 500 kHz. Artificial neural networks (ANN) have also been adopted for AE signal classification (Wang *et al*., 2001; Kwak and Ha, 2004).

A number of recent studies on the AE monitoring of bearings and gearboxes have been reported. Discrete and continuous wavelet transform were considered in (Feng *et al*., 2006; Bains and Kumar, 2009), respectively. The Wigner-Ville distribution was also tested on AE signals (Loutas *et al*., 2011). Additionally, AE based wind turbine diagnosis results were reported by Sheng *et al*.

(2009). However, in this paper, a clear conclusion on how the AE signal features change with different operating condition was not given.

Noise cancellation applied to AE signal analysis was conducted by Chiementin *et al*. (2010). Three different methods were tested in the paper, namely, SANC, spectrum subtraction and wavelet de-noising. This paper investigated the application of temporal statistical indicators for AE detection of bearing defects. It assessed the effectiveness of various de-noising techniques in improving sensitivity to early defect detection. It was concluded in this paper that de-noising methods offer significant improvements in identifying defects with AE, especially the self-adaptive noise cancellation method. It was also concluded that kurtosis was the most sensitive temporal indicator. Possible reasons were concluded that kurtosis was sensitive to the impulses which are more obvious after de-noising.

Kilundu *et al*. (2011) presented an experimental study that characterized the cyclostationary aspect of AE signals recorded from a defective bearing. Comparison between the cyclic spectral correlation, a tool dedicated to evidence the presence of cyclostationarity, and traditional envelope spectrum showed that the cyclic spectral correlation was most efficient for small defect identification on outer race defects. However, the success was not mirrored on inner race defects. It was concluded that cyclostationary could offer better sensitivity to the continuous monitoring of defects compared to the use of traditional temporal indicators, such as RMS, kurtosis, and crest factor.

A review paper on AE was published by Sikorska and Mba (2008). Detailed applications on multiple purposes and their limitations were discussed. Used as a ground reference, reliable AE signals of healthy cases have been considered by many researchers as an important pre-requisite for the success of AE based fault detection (Choudry and Tandon, 2003). In a recent study on

wind turbine condition based monitoring, a design of a new continuous condition monitoring system with automated warnings based on a combination of vibrational and AE analysis was reported in (Soua *et al*., 2013). The authors tried to determine a ground reference for the healthy turbine. The vibration and AE signatures for a healthy wind turbine gearbox and generator were obtained as a function of wind speed and turbine power. They listed a number of limitations in the current state of AE based research on rolling elements diagnostics. First, the measurement was mostly performed in laboratory test rigs rather than field service conditions. Second, the signal to noise ratio was low due to short term data collection. Third, classification algorithms such as pattern recognition could possibly cancel the coherent elements of the noise, but not the random or quasi random components. Thus, they proposed that in order to address the above limitations, future work was needed for AE using much longer monitoring times and repeated measurements on actual defective rolling elements in service to compensate the random noise and instrument performance error.

Some of the other published papers involved the combined use of AE with vibration data (Tandon and Nakra, 1992; Loutas *et al*., 2009, 2011). Some papers compared the performance of vibration analysis and AE analysis (He *et al*., 2010; Elforjani *et al*, 2012). The common conclusion drawn from those papers was that AE was more effective and sensitive in early fault detection. Possible reasons were presented to account for the conclusion. The first is that the AE emitted by small defects occur in frequency ranges that are higher than the operational range of accelerometer sensors. Therefore, AE could catch the fault signals out of vibration sensor's measurement range. The second explanation is that when there is only a small crack or fault in the machine which is not severe enough to change the structural vibration, the vibration signal measured on the outside part of the mechanical system may still remain the same, and thus unable to detect the incipient fault.

### 2.2.3 AE for Gear Diagnosis

Typical sources of AE waveforms in the gearbox related machinery include Plastic deformation, Micro-fracture, Wear, Bubble, Friction, and impacts (Li, 2002; Abdullah and Mba, 2006). In (Eftekharnejad and Mba, 2009), seeded defects on helical gear teeth were studied. Surface defects in the form of thin rectangular notches, were seeded to simulate the effect of gear teeth wear. In their experiment, the result showed that, the AE signal would have a clear amplitude spike when there was a fault tooth involved. Also, by comparing the RMS of the healthy gear and fault gear, they were able to classify the faults. However, as the first reported result of its kind, it is open to further validation. Similar results tested on worm gears were published in (Elforjani *et al*., 2012). It was concluded that the applicability of AE technology in detecting defects on worm gears whilst in operation was successful. Observations of continuous monitoring of gear tests revealed that AE parameters such as RMS and energy were more reliable, robust and sensitive to the detection of defects in worm gears than the corresponding parameters in vibration, as reported by the authors.

In another gear diagnosis paper by Al-Balushi and Samanta (2002), energy-based features were introduced for monitoring and diagnosis for various machine operating conditions with speed and load variations. A feature called energy index (EI) was proposed to measure the statistical relative energy levels of segments in a time domain signal over a cycle. The proposed technique was validated by comparison with some of the existing methods using the same AE data for early fault detection. The proposed method was also tested with vibration data. When applied to AE signal analysis, it was able to effectively detect the early fault. However, in their research, AE signals were sampled at a high rate of 1 MHz, which hindered them from doing TSA due to the large data volume. They used an alternative method of plotting the result of each revolution together to get a visual data graph of the results. Also, their work only aimed to evaluate AE and vibration for fault detection purpose other than fault level diagnostics.

### 2.2.4 Overview of the Effect of Shaft Speed and Loading on AE

As known, vibrational signals of a rotating element increase strongly with shaft rotation frequency under almost all conditions. Some papers tried to find the correlation of the AE signal amplitude and frequency feature under different shaft speeds and loading conditions. The correlation between AE activity and load, speed, and asperity contact for spur gears were investigated by Tan and Mba (2005). The following conclusions were provided in the paper:

1) Load had insignificant influence on AE RMS levels under other fixed conditions.
2) Speed had a significant influence on AE RMS levels under other fixed conditions.
3) Sliding contact was responsible for generating continuous type AE waveform, while rolling contact generated AE transient bursts at the gear mesh frequency.
4) The proportion of sliding and rolling contributed to the generation of AE depended on the rotational speed of the gears and specific film thickness. The overall levels of AE RMS had a strong dependence on the sliding and rolling regime.

It was the first time in literature that one clarified the opinion that AE bursts were not all fault related. At least, as in gear meshing, the healthy gear will also generate burst signals. It was also proposed in this paper that the AE technique has the potential for real time assessing the level of asperity contact under different operation conditions, such as, speed, surface roughness and lubricant temperature, etc.

Similarly, reports on the effect of loading on bearing AE signals showed almost the same kind of correlation for loading condition and speed. For a constant rotation speed, it was reported that AE count was not sensitive to load variations by He *et al.*, (2009). However, AE count was sensitive to the speed variation. Observation also showed that AE count was not sensitive to small defect and incipient defect. The condition indicator for the size of the defect was not as

good as expected. This made the traditional AE burst based methods less attractive and further research on continuously collected AE signals would be required.

### 2.2.5 Comments on AE for Machinery Fault Diagnosis

Many recent AE studies of rotating components for machinery health monitoring have been conducted. The feasibility of the detection of fault was well established. However, nearly all of the present papers were based on a black box type of reasoning. The collected AE signals were poorly understood. The physical structure and characteristics of the testing systems were often neglected. Besides that, most of those algorithms were either based on classification or pattern recognition which can effectively cancel the coherent elements of the noise but not the random noise. A substantial random noise component will always accompany the useful signal at least from friction sources. As for AE signal, the signal itself is highly modulated with high frequency components. The AE sensor itself also tends to randomize the AE signature even in the healthy signal and aids in the discrimination between faulty and healthy components more difficult.

In summary, there are a number of limitations in the reported work as follows:

1) Most of the reported methods are based on poorly understood statistical features using blind reasoning algorithms. Transient burst type AE signals are still the main type of collected AE signals. Continuous type of AE signals collected over long term are not widely used.
2) High sampling rates are required for AE data acquisition, resulting in high costs.
3) Most of the classification or pattern recognition methods, or so called data driven methods, require large amount of training data, which is cumbersome to store and process in the real applications.

4) The features of the collected AE signals were poorly understood. The lack of interpretation between AE features and physical structure greatly limited the diagnostic ability.

In order to address the above limitations, it is needed for future work to collect continuous AE data over longer time. To date, only some repeated measurements on defect signatures were used to increase the detection probability. However, this unavoidably suffers from long term temperature and voltage drift in ambient conditions. Due to the high data volume associated with time and high sampling rates, the ability to collect AE data under a lower sampling rate is needed. Some useful time domain methods like TSA have never been applied on AE data because of the high data volume and computational resource restriction. TSA and residual analysis, other than wavelet and EMD based methods, will greatly help the AE data processing.

# CHAPTER 3
# METHODOLOGY

There are some common short comings in the currently existing methodology. All of the current AE based data collection require high data sampling rates, typically around 2 MHz. Most of these papers considered the AE signal as a separate energy burst, not a consecutive wave form just like any vibration signal. The time domain features extracted from the AE signal are transient time based. These features are often compared with other healthy case references blindly. They do not give much interpretation of overall AE signal dynamics along the time axis. For example, when a small portion of the gear is damaged or only one tooth has a crack on it, most of energy related AE bursts are normal, only the burst signal generated when the faulty tooth is meshing may have certain abnormal time domain feature. By the above reviewed statistical analysis, the faulty AE features are not enhanced but weakened, which makes these methods difficult to make the conclusion of fault detection. A more effective and efficient AE signal processing technique is required. Actually, some information about the testing object is pre-known, for example, the structure of a gearbox, the approximate rotation speed of the shaft, etc. In this dissertation, the author aims to develop a method which could utilize these kinds of useful information using the proposed heterodyne and TSA based method.

Frist, the heterodyne technique for frequency reduction is introduced and explained. Then, TSA methods are introduced to AE signal analysis. In order to conclude the fault, different methods are proposed to further distinguish the faulty signals.

### 3.1 AE Sampling Rate Reduction using Heterodyne

Current AE signal processing steps are given in Figure 8.


Figure 8. Traditional AE signal acquisition and preprocessing procedure

In a traditional AE signal processing procedure, all of the data is collected and stored to computer without any signal processing. There are two disadvantages associated with this procedure. First, it increases the data acquisition cost. Second, it heavily relies on the computer to process the resulting large data set.

For rotating machinery, a periodic displacement (which may only cause a small acceleration) can be indicative of a fault. The displacement will cause a dislocation associated with the AE signature. The information contained in the AE signature is not related to the AE signature itself, but the modulation rate of the signature. This load information is recovered through a demodulation process. The demodulation process is similar to information retrieval in an amplitude/phase modulated radio frequency signal. The carrier signal of a typical AM radio signal is several MHz, while the information modulated onto that signal is audio signal of a couple of kHz. After demodulating the carrier using an analog signal conditioning circuit, the acquisition system can then be sampled at audio frequency (10s of kHz). The signal processing can then be performed at a lower cost with an analog circuit other than a high speed analog to digital converter. Moreover, the associated computation power required to process the large data set resulting from the high sample rate is reduced.

The AE signal demodulation technique proposed in this dissertation is called heterodyne. Heterodyne is defined as the process of combining a radio-frequency wave with a locally generated wave of different frequency in order to produce a new frequency equal to the sum or difference of the two. Two different frequencies are combined to produce two new frequencies, the sum and difference of the original frequencies, either of which may be used in the next step by proper filtering.

Mathematically, Heterodyning is based on the trigonometric identity:

$$sin\,\theta sin\varphi = \frac{1}{2}cos(\theta - \varphi) - \frac{1}{2}cos(\theta + \varphi) \tag{1}$$

Further, for two signals with frequency $f_1$ and $f_2$ , respectively, it could be written as

$$sin(2\pi * f_1 * t) * sin(2\pi * f_2 * t) = \frac{1}{2}\cos[2\pi(f_1 - f_2)] - \frac{1}{2}cos[2\pi(f_1 + f_2)] \tag{2}$$

where, $f_1$ is the carrier frequency, $f_2$ is the demodulator's reference input signal frequency. This process could be explained with a simple example.

Let $f_1 = 4$ Hz and $f_2 = 5$ Hz, note $y_1 = sin(2\pi * 4 * t)$ and $y_2 = sin(2\pi * 5 * t)$. Take their multiplication as $Y = y_1 .* y_2$. Their plots are shown below in Figure 9.

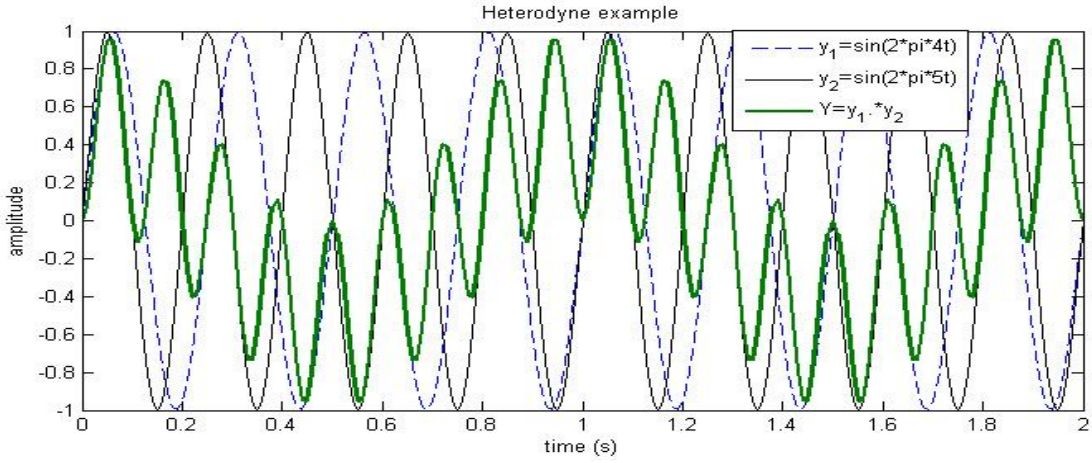


Figure 9. The multiplication of two sinusoid signals

Then this multiplication signal could be low pass filtered. The high frequency image at frequency $(f_1 + f_2)$ will be removed prior to sampling. This is shown in Figure 10.

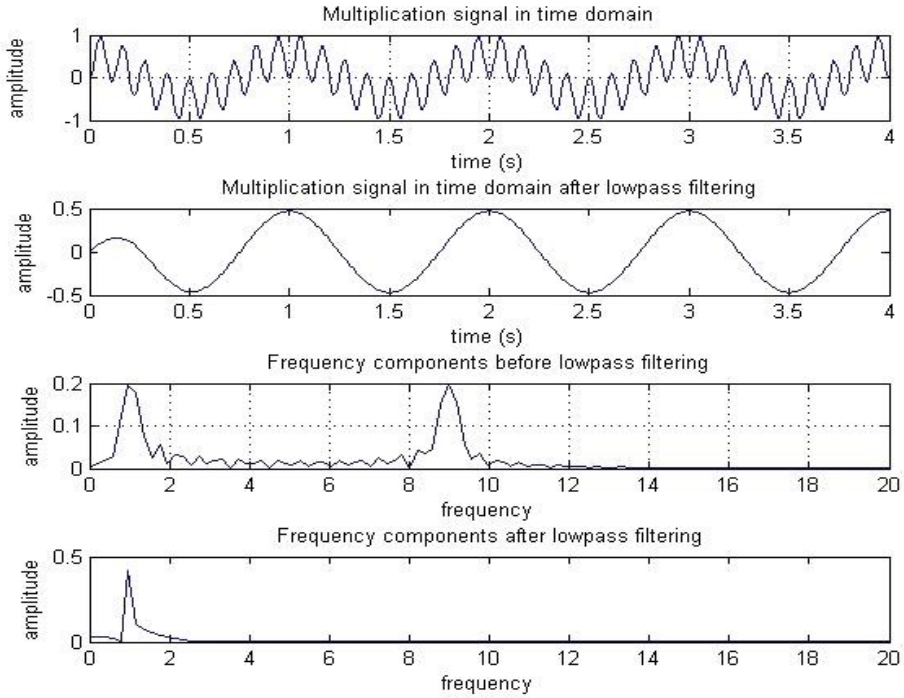


Figure 10. Heterodyne process

In order to successfully shift the signal to a new frequency range, two conditions must be satisfied: 1) certain nonlinear operations, typically multiplication, must be presented in the heterodyne devices. 2) The frequency components contained in two source signals must be different. Otherwise, only the high frequency signal is left after heterodyning.

Next, a detailed discussion of the heterodyne technique applied on the raw AE signal is given. Since the AE sensor is a complicated modulation device. It is unconfirmed which type of modulation could exist in AE signal excitation. The principle of amplitude modulation (AM) and frequency modulation (FM) is showed in Figure 11.

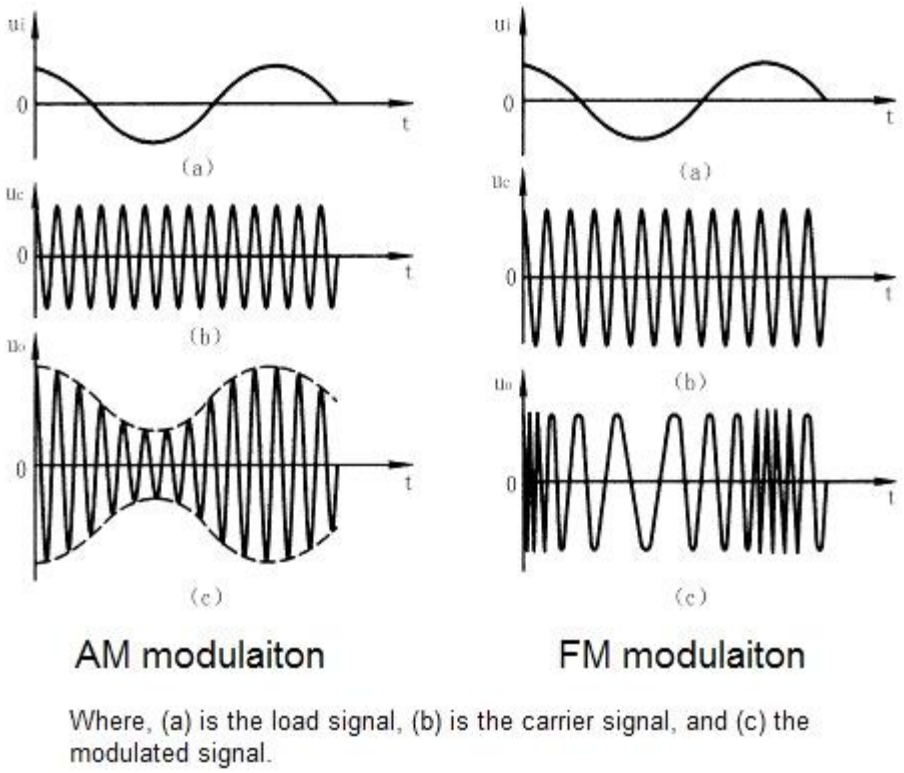


Figure 11. The principles of AM signal and FM signal

There are limited papers that investigate the correlation between frequency variation and load or speed. Reported results about the correlation between loading and AE showed that loading changes did not have much effect on AE count (related to AE signal frequency) (He *et al*., 2009). This means that when the amplitude of the stress energy increases, the AE frequency does not increase accordingly, which contradicts the principle of frequency modulation. This serves as an indirect proof that frequency modulation for AE signal is not significant. On the other hand, the speed change of machine had an approximately proportional effect on AE RMS (Tan and Mba, 2005). This phenomenon is consistent with amplitude modulation effect. Therefore, it is concluded that amplitude is the major modulation effect in AE signature while frequency modulation is insignificant. However, this conclusion is open to future validation. Nonetheless, the focus of this work will be amplitude modulation information other than the frequency or

phase modulation. Frequency and phase modulation will be considered negligible. Therefore, only the amplitude modulation will be considered in the following part.

A detailed discussion of the heterodyne technique applied on the raw AE signal is given in the following. In general, amplitude modulation is the major modulation form for AE signal. Although, frequency modulation and phase modulation could be present in the AE signal potentially, they are considered trivial and will not be discussed here. The amplitude modulation function is given in Eq. (3).

$$U_a = (U_m + mx)co\,s\,\omega_c t \tag{3}$$

where, $U_m$ is the carrier signal amplitude, $\omega_c$ is the carrier signal frequency, $m$ is the modulation coefficient. $x$ is the modulated signal, note as

$$x = X_m cos\Omega t \tag{4}$$

Then, with heterodyne technique, the modulated signal will be multiplied with a unit amplitude reference signal $\cos(\omega_c t)$. The result is given in the following.

For the amplitude modulation signal,

$$U_o = (U_m + mx)\,cos\,\omega_c t\,cos\,\omega_c t = (U_m + mx)\left[\frac{1}{2} + \frac{1}{2}cos(2\omega_c t)\right] \tag{5}$$

Then substitute Eq. (4) into Eq. (5), it gives:

$$\begin{aligned} U_o = {} & \frac{1}{2}U_m + \frac{1}{2}X_m cos\Omega t + \frac{1}{2}U_m cos(2\omega_c t) \\ & + \frac{1}{4}mX_m[cos(2\omega_c + \Omega)t + cos(2\omega_c - \Omega) \end{aligned} \tag{6}$$

Since $U_m$ does not contain any useful information related with the modulated signal, it could be set as 0, or removed by detrending. From Eq. (6), it can be seen that only the modulated signal will be left after low pass filtering, where the high frequency components around frequency $2\omega_c$ will be removed.

The diagram of the proposed down sampling system using heterodyne is shown in Figure 12.

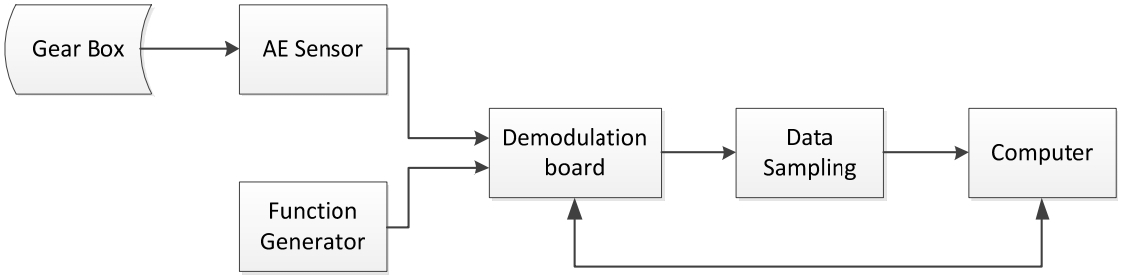


Figure 12. Proposed AE signal processing diagram

By adding a demodulation step, it could achieve the purpose of reducing the signal frequency to 10s of kHz. This is close to the frequency range of general vibration signals. Any data acquisition board with a low sampling rate could be able to sample the pre-processed AE data.

In order to get the best demodulation effect, an optimization procedure is developed to search for the optimal frequency of the reference signal using a linear chirp function as the demodulation input. In a linear chirp, the instantaneous frequency $f(t)$ varies linearly with time. A linear chirp function could be described as:

$$f(t) = f_0 + k \cdot t \tag{7}$$

where, $f_0$ is the initial frequency, $k$ is the chirp rate, $f(t)$ is the instantaneous frequency at time $t$.

In searching for the optimal reference frequency, normally a frequency range is pre-selected, for example, 50 kHz - 1050 kHz. The chirp function will start with an initial frequency of $f_0$ and chirp with a constant rate of $k$ Hz per second. Before the presentation of the algorithm, the following terms are defined:

$f_{min} = lowest\ reference\ frequency$

$f_{max} = highest\ reference\ frequency$

$\Delta f = frequency\ increment$

$n = \frac{f_{max} - f_{min}}{\Delta f}, the\ total\ number\ of\ frequency\ segments$

$N_i = number\ of\ digitized\ data\ samples\ in\ each\ segment\ i, i = 1, \dots, n$

$X(j) = digitized\ modulated\ signal\ of\ x(t), where\ x(t) = \frac{1}{2}\cos[2\pi(f_1 - f_2)t]$ ,as described in Eq. (2)

$f^* =$ *the optimal demodulation reference frequency*

The optimization process is to search for the best frequency such that the RMS of the demodulated signal is maximized. It is defined by the following algorithm.

---

Algorithm: Optimal AE reference frequency searching procedure

---

Step 1. Set the initial frequency $f_0 = f_{min}$

Step 2. For $i$ = 1 to $n$

$$RMS_i = \sqrt{\sum_{j=1}^{N_i} \frac{X(j)^2}{N_i}}$$

End For

$$i^* = \underset{1 \le i \le n}{arg\ max}\ RMS_i$$

Step 3. Compute optimal reference frequency of demodulation as:

$$f^* = f_0 + i^* \times \Delta f$$

---

### 3.2 AE Signal Processing using TSA

TSA is a useful technique for analyzing vibration data. However, TSA has never been applied to analyze AE signals in the literature. The complicated features and huge data volume of AE

signals make TSA algorithm unrealistic to be performed directly on these data. In this dissertation, the author first explores the application of TSA to AE signal analysis.

Basically, two types of TSA algorithm are available in the literature, i.e., TSA with tachometer, and tachometer less TSA. For TSA with tachometer method, a tachometer needs to record the shaft speed and the real time angle. But in most applications, the installation of tachometer might be expensive or even impossible. For tachometer less TSA algorithm, although an angular reference signal is still required, it can be derived directly from the tested signal, which is generally a vibration signal. Thus, no external tachometer is required. Both types of TSA will be discussed next.

### 3.2.1 Traditional TSA Methods

TSA has been widely used in the processing of vibration signals (McFadden and Toozhy, 2000; Combet and Gelman, 2007). The concept of TSA is to compute the ensemble average of the raw signal over a number of revolutions in order to get an enhanced signal of interest with less noise from other sources. For a function $x(t)$, digitized at a sampling interval $nT$, resulting in sampling in samples $x(nT)$. Denoting the averaged period by $mT$, TSA was given as (Braun, 1975):

$$y(nT) = \frac{1}{N}\sum_{r=0}^{N-1} x(nT - rmT) \tag{8}$$

If the signal $x(t)$ is written as

$$x(t) = f(t) + noise(t) \tag{9}$$

Then after N summation, the uncorrelated noise will be reduced by a factor of $\sqrt{N}$ , the averaged signal could be written as (Braun, 1975)

$$\bar{x}(t) = f(t) + \sqrt{N} \cdot noise(t) \tag{10}$$

Therefore, the signal to noise ratio is enhanced by $\sqrt{N}$ after averaging over $N$ revolutions. More details about TSA could be found in (McFadden, 1987).

### 3.2.2 Tachometer-less TSA Methods

The feasibility of extracting a phase reference signal directly from the vibration signal by phase demodulation has been studied in previous papers. Jong *et al.* (1996) proposed a synchronous phase averaging method which could transform a quasi-period signal into a period signal and then perform TSA. The proposed method first narrow band filtered out one of the meshing harmonics. Then, the phase variation signal could be calculated by Hilbert transform. After that, a standard periodic signal was obtained by the non-uniform sampling of the original signal with reference to the phase variation signal. Next, a uniformly sampled periodic signal could be reconstructed by interpolation. Last, the standard TSA can be calculated and plotted. This was the first known paper showing that the gear fault could be identified by discontinuity and irregularity in enhanced TSA waveform. A similar method for AE TSA is developed and presented next.

AE signal after heterodyne could be expressed same as gear vibration signal (McFadden, 1987):

$$x(t) = \sum_{m=0}^{M} X_m cos(2\pi m N f_s t + \emptyset_m) + e(t) \tag{11}$$

where, $X_m$ is the $m^{\text{th}}$ order harmonics, $N$ tooth number, $f$ shaft frequency, $\emptyset_m$ the initial phase angle.

Assume the signal is amplitude and phase modulated by the function $a_m(t)$ and $b_m(t)$, respectively. An important point need to be mentioned is that, any fault in the gear will impose extra modulation effect on the signal. For the simplicity of notation, it is included in $a_m(t)$ and $b_m(t)$. Then the amplitude and phase modulated signal could then be expressed as:

$$y(t) = \sum_{m=0}^{M} X_m[1 + a_m(t)]\cos[2\pi mNft + \emptyset_m + b_m(t)] + e(t) \quad (12)$$

If the signal average is ideally band pass filtered out one of the meshing harmonics $m$ with a narrow bandwidth $W$, then the filtered signal could be written by:

$$z_m(t) \cong X_m[1 + a_m(t)]\cos[2\pi mNft + \emptyset_m + b_m(t)] \quad (13)$$

In this equation $z_m(t)$ could be viewed as the real part of a complex function $\epsilon_m(t)$ (McFadden, 1986), known as the analytic signal and defined by

$$\epsilon_m(t) = z_m(t) - jH[z_m(t)] \quad (14)$$

where, $H(z_m(t))$ is the Hilbert transform of $z_m(t)$.

Then the instantaneous phase could be calculated as

$$\psi(t) = arctan(H[z_m(t)]/z_m(t)) \quad (15)$$

The instantaneous frequency (IF) is defined as the first derivative of the instantaneous phase as a function of time

$$\omega(t) = \dot{\psi}(t) \quad (16)$$

There are several ways to calculate the instantaneous frequency. In this work, the derivative of the unwrapped phase signal is taken. The zero crossing time is then computed from the instantaneous frequency. A more detailed explanation of extract phase reference was provided in (Feldman, 2011).

### 3.2.3 Residual Signal and Difference Signal

Based on the TSA signals, sometimes it is hard to distinguish the faulty signal and healthy signal because it is dominated by the meshing frequency and shaft frequency. In many cases, it is

suggested to take a look at the residual signal with the shaft and meshing frequency as well as their harmonics removed. The TSA residual signal is defined as

$$r = x(t) - y_r(t) \tag{17}$$

where, $x(t)$ is the original time synchronous signal, $y_r(t)$ is the meshing frequencies and their harmonics. Generally, the residual signal could be obtained by zeroing the meshing frequency and their harmonics and then perform an inverse Fourier transform.

## 3.3 Fault Feature Extraction and CI Computation

### 3.3.1 Narrow Band Filtered TSA

According to Jong *et al*. (1996), a periodic signal can be reconstructed from the original signal by non-uniform sampling and TSA. However, this is infeasible for raw AE signals because AE signals contain a lot of complicated frequency components. Hence, instead of performing TSA on the raw AE data, a narrow band filtering is proposed to filter out the meshing harmonics and the filtered AE data will be used to perform TSA. In this paper, a zero-phase filter with a bandwidth of only 2Hz is designed. Then, through classic TSA technique, an enhanced periodic signal of a single meshing harmonic frequency could be calculated. The procedure of the modified TSA algorithm for processing AE data is given below:

1) Calculate the power spectrum density and identify the base meshing frequency and the harmonics frequency.
2) Construct the analytic signal based on the meshing frequency and the raw AE data. Narrow band filter the analytic signal and take the unwrapped version of the phase, and then the angular position of the shaft could be extracted as proposed in (Loutas *et al*., 2011).

3) Narrow band filter the original data. Notice that zero-phase filtering is required in order to prevent phase shifting of the signal.
4) Perform TSA algorithm on the filtered data.
5) Inspect the waveform of the TSA signal for any irregular behavior to identify gear fault.

This modified TSA algorithm is performed on a zero-phase filtered harmonic signal instead of on the original signal. It enables us to inspect a single harmonic to detect the hidden fault. The reason why the demodulated AE signal need to be narrow band filtered is explained as follows: The demodulation process could only demodulate the AE signal modulated on a specific carrier frequency. The signal modulated on other frequency bands will be shifted down to a frequency band around their base bands and will act as noise. In order to enhance the signal to noise ratio, the narrow band pass filter is proposed. If sufficient averages are taken, the time domain averaged signal should approach a standard periodic signal. For healthy gears, the enhanced TSA signal should display a fully or near fully periodic characteristic. While for the faulty gear, it is assumed there will be some abnormal behavior in the TSA signal. Validation results of this method will be shown in the Section 4.

### 3.3.2 Spectral Kurtosis

It is proposed before doing TSA and calculate condition indicators, band pass filter is need to filter the signal to extract faulty features. Spectral kurtosis (SK) provides a solution to design an optimal band pass filter.

SK was proposed by Dwyer (1983), as a statistical tool that can be used to identify the non-Gaussian components in a signal as well as their location in the frequency domain. The SK was given a more formal definition in (Capdevielle, 1996) from the perspective of higher-order

statistics. By Capdevielle's definition, SK is the normalized fourth-order cumulant of the Fourier transform and can be used as a measure of distance of a process from Gaussianity. Therefore, it can act as a measure of the peakiness of the probability density function of the process at a frequency of $f$. However, SK did not draw much attention from the researchers until it was revisited and further developed by Antoni (2006). The SK of a signal $x(t)$ is defined as the energy-normalized fourth-order spectral cumulant as:

$$K_x(f) = \frac{S_{4x}(f)}{S_{2x}^2(f)} - 2 \tag{18}$$

where, $S_{nx}(f) = \langle |X(t,f)|^n \rangle$, $\langle \cdot \rangle$ stands for the time averaging operator, $X(t,f)$ is the complex envelope of signal $x(t)$.

$X(t,f)$ can be estimated by any time-frequency analysis methods, such as: short time Fourier transform (STFT), the filter bank method, Wigner-Ville distribution, and wavelet package, and so on.

Take STFT for example, the STFT of signal $x(t)$ discretely sampled as $X(n)$ is defined as:

$$X_w(kP,f) = \sum_{n=-\infty}^{\infty} X(n)w(n-kP)e^{-j2\pi nf} \tag{19}$$

where, $w(n)$ is a positive analysis window, $P$ is a given temporal step.

As noted, the SK is suitable for identifying the peakiness of a signal with regard to frequency. It is able to extract non-stationary event in the signal. In general, the vibration signals measured from rotating machinery is considered as stationary. However, an AE signal is considered non-stationary. Gear signals can be classified as cyclostationary processes. As indicated in (Antoni, 2006), the signals from rotating machinery can be resynchronized with a phase reference and then

form a non-stationary signal with a periodic statistical structure. It is therefore conditionally non-stationary, which is suitable to use SK for fault detection.

In order to estimate SK, the kurtogram was proposed by Antoni and Randall (2006). A kurtogram is a three dimension graph which gives the kurtosis value for different frequency and different window size. Window size $N_w$ is an important parameter because it directly affects the spectral resolution of the SK. A short $N_w$ will yield high SK value, but too short a $N_w$ will also lose some details and reduce the frequency resolution. Therefore, both the frequency and $N_w$ should be optimized to maximize SK. Since a kurtogram can identify the optimal frequency range and optimal window size where the signal displays the maximum peakiness, it is useful for filter design. When the frequency line where the maximum SK is obtained, several filter methods could be applied to extract an enhanced SNR signal, such as Wiener filter, matched filter and band pass filter (Antoni and Randall, 2006).

For optimal band pass filtering, the objective is to find: 1) the central frequency $f_c$ and 2) the bandwidth $B_f$ of the filter which maximizes peakiness on the filtered signal. For a fault detection problem, in order to recover the impulse associated with a faulty signature, a band pass filter which is used to maximize the kurtosis of the envelope of the filtered signal. As demonstrated in (Antoni and Randall, 2006), this problem is strictly equivalent to finding the frequency $f$ and the window length $N_w$ that maximises the STFT-based SK over all possible combinations. The optimal central frequency $f_c$ and bandwidth $B_f$ of the band pass filter are determined as those values which jointly maximize the kurtogram. Therefore, both the center frequency $f_c$ and window length $N_w$ could be identified by using kurtogram. By doing this, the best compromise between maintaining the highest possible signal to noise ratio and extracting the impulse like signature of the fault is achieved.

### 3.3.3 AE Condition Indicators

There are many condition indicators available in literature. Most of the condition indicators deal with the data distribution, such as peakiness, amplitude level, deviation from the mean and so on. A major difference between these condition indicators lies in the signal from which they are calculated. Generally four types of signal are used for computation, i.e., raw signal, TSA signal, residual signal and difference signal (Večeř *et al*., 2005; Lebold *et al*., 2000). A residual signal is generally defined as a synchronous averaged signal with the shaft, gear mesh, and their associated harmonic frequencies removed (Zakrajsek, 1993). The difference signal is defined by further removing the first order sidebands from the residual signal (e.g. the distinction between the residual and difference signals is the first order sidebands). For this filtering process, the spectrum values corresponding to these features are set to zero and the inverse Fourier transform is performed to convert it back to the time domain. However, these definitions are not strict. Also in practice, different filtering methods of performing the above mentioned process will give different results.

Other operations on the TSA include:

**Teager's Energy Operator**: Teager's energy operator or energy operator (EO) is a type of residual of the autocorrelation function (Kaiser, 1990; Teager, 1992). For a nominal gear, the predominant vibration is gear mesh. Surface disturbances, scuffing, and etc., generate small higher frequency values which are not removed by autocorrelation. The CIs of the EO are the standard statistics of the EO vector. The $i^{th}$ element in EO vector is computed as:

$$\psi[x_i] = x_i^2 - x_{i-1} \cdot x_{i+1} \tag{20}$$

where, $x_i$ is the $i^{th}$ data point of signal $x$.

Condition indicators are statistical features performed on these analysis, which include:

**RMS**: The root mean square (RMS) for a discretized sampled signal is defined as:

$$x_{rms} = \sqrt{\frac{1}{N}\sum_{i=1}^{N}(x_i{}^2)} \tag{21}$$

where, $x_{rms}$ is the root mean square value of data set $x$, $x_i$ is the $i^{\text{th}}$ element of $x$, $N$ is the length of data set $x$.

From the definition of RMS, it is easy to understand that the RMS may not increase greatly with isolated peaks in the signal, and consequently it is not sensitive to incipient tooth crack or initial failure. Its value will increase as the speed and load increase.

**P2P:** Peak to peak amplitude is the change between peak (highest amplitude value) and trough (lowest amplitude value, which can be negative).

**Crest factor:** Before crest factor could be defined, peak value must be understood. Peak value generally refers to the maximum value in the collected data. The crest factor then could be given in Eq. (22)

$$CF = \frac{|x|_{peak}}{x_{rms}} \tag{22}$$

where, $CF$ is the crest factor, $|x|_{peak}$ is the peak amplitude in data $x$, $x_{rms}$ is the RMS.

Crest factor is more sensitive to initial gear fault, such as one tooth crack. Since the RMS will not change in incipient fault, but the crest factor should see an increase.

**Kurtosis:** kurtosis describe how peaky or how smooth of the amplitude of data set $x$. If a signal contains sharp peaks with high values generated by a fault in the gearbox, it is expected that its

distribution function will be sharper. Thus, the kurtosis of the fault signal should be higher than that of the healthy signal. The function of kurtosis is given below,

$$Kurt = \frac{N\sum_{i=1}^{N}(x_i - \bar{x})^4}{[\sum_{i=1}^{N}(x_i - \bar{x})^2]^2} \tag{23}$$

where, *Kurt* is the kurtosis of data set $x$, $x_i$ is the $i^{\text{th}}$ element of $x$, $N$ is the length of data set $x$.

It is worth to mention that for any normal distribution, the kurtosis value is 3. This could be easily verified by the moment generating function.

Some other gear fault algorithms are functions of operations, such as:

**FM4:** The FM4 parameter is simply the kurtosis of the difference signal. It is assumed that a healthy gearbox difference signal should display a Gaussian amplitude distribution, while a damaged gearbox will produce some high peak value which does not conform to Gaussian distribution.

$$FM\,4 = \frac{N\sum_{i=1}^{N}(d_i - \bar{d})^4}{[\sum_{i=1}^{N}(d_i - \bar{d})^2]^2} \tag{24}$$

where, $d_i$ is the $i^{\text{th}}$ element of the difference signal, $N$ is the length of difference signal.

**NA4:** NA4 is an improved version of FM4. NA4 is based on the argument that sideband signal contains the fault related information. So, the NA is calculated based on the residual signal which keeps the sideband while removing other meshing components. Also, NA4 takes an average value of the variance. The NA4 formula is given as:

$$NA4 = \frac{N\sum_{i=1}^{N}(r_i - \bar{r})^4}{[\frac{1}{M}\sum_{j=1}^{M}\sum_{i=1}^{N}(r_{ij} - \bar{r}_j)^2]^2} \tag{25}$$

where, $r_i$ is the $i^{th}$ data point in the residual signal, $r_{ij}$ is the $i^{th}$ data point of the $j^{th}$ group of residual signal, $M$ is number of the data group of TSA residual signal, $N$ is the number of data point in one TSA residual signal.

To sum it up, the overall procedure of calculating condition indicators can be presented in Figure 13.

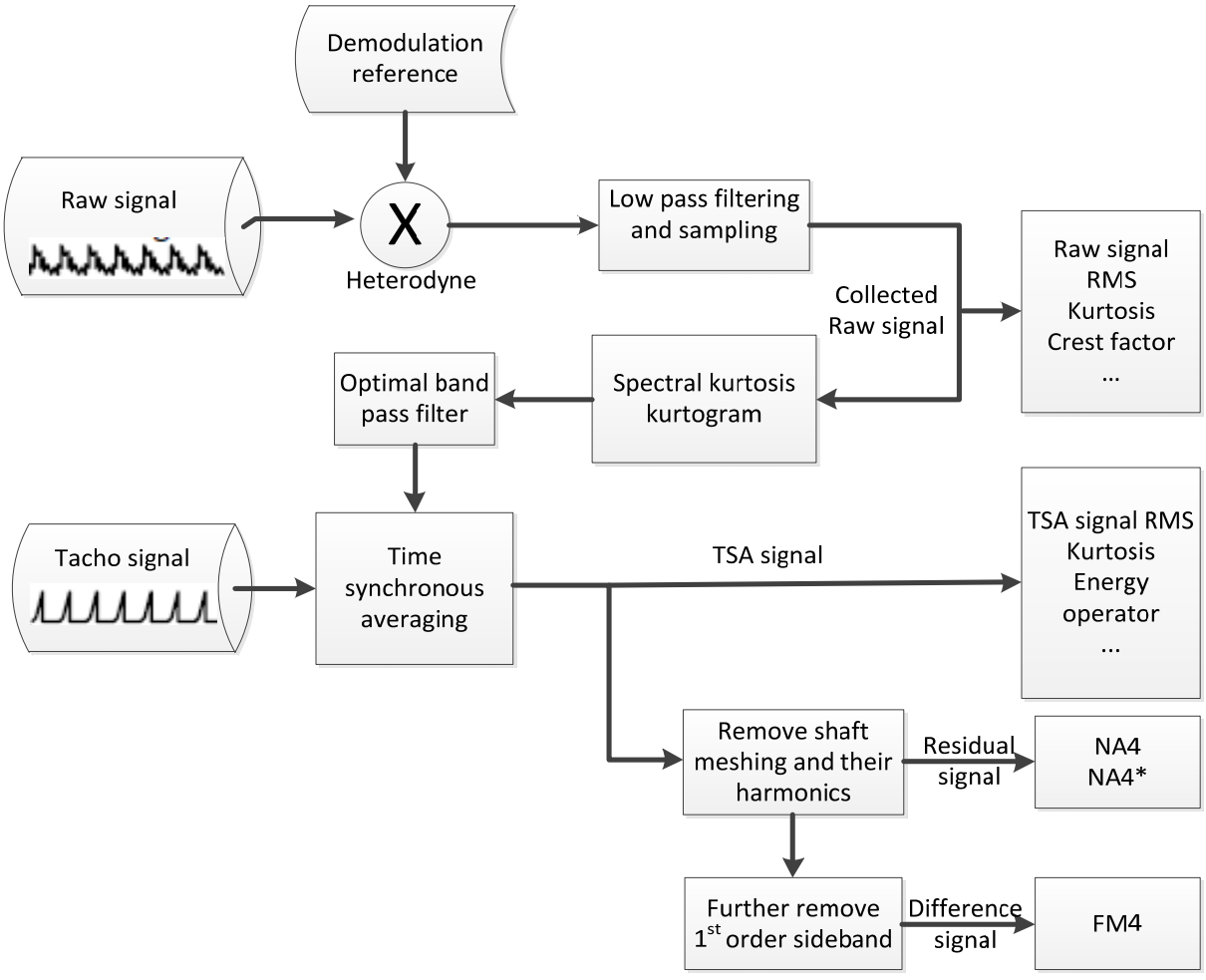


Figure 13. The overall process of computing the condition indicators

The evaluation and validation of these condition indicators on AE signals will be shown in Section 4.

# CHAPTER 4
# VALIDATION OF AE BASED FAULT DIAGNOSIS METHODS

The methods proposed in Section 3 were validated with a laboratory test rig. Different types of fault cases were tested to evaluate these methods. In Section 4.1, the experimental setup, such as the test rig information and DAQ system, will be introduced. Then, the validation tests for the methodology will be described in Section 4.2. Also, the results and discussion will be provided. Lastly, conclusions will be drawn in Section 4.3.

## 4.1 Experimental Setup

### 4.1.1 Test Rig Setup

In order to validate the proposed methodology, seeded gear tooth fault tests were conducted on a notational two stage split torque gearbox (STG). A brief review on split torque gearboxes will be given first in order to understand the characteristics of a STG. Invented in the 1970s (White, 1974, 1983, 1989, 1993, 1998), the STG was used to solve the problem of high rate reduction and large output torque for helicopters. Some corporations have filed patents for split torque transmission systems on helicopters, such as the Sikorsky Aircraft Corporation and McDonnell Douglas Helicopters (Craig *et al.*, 1998; Gmirya and Kish, 2003; Gmirya, 2005). The design of large torque with high transmission ratio has been presented in (Kish, 1992, 1993a, 1993b; Krantz, 1992, 1994, 1996; Krantz and Delgado, 1996). Compared with traditional planetary gearboxes, the STG has the following advantages (Robleda *et al.*, 2012):

1) In the final transmission stage where the greatest torque is needed, if given equal torque and stress levels in the teeth, the STG could achieve a larger torque/weight ratio when compared to planetary gear systems.

2) In the final transmission stage, the STG could achieve higher transmission ratios. Therefore, it is possible to use a smaller number of gear stages, resulting in lighter gear systems.
3) The STG has higher transmission efficiency and lower energy loss because the STG needs fewer gears and bearings than planetary gearboxes.
4) The STG has higher reliability than planetary gearboxes because it has multiple paths. Thus, even if one path fails, operation is still valid through other paths.

A possible disadvantage for the STG is that the uneven torque split between different paths in the gearbox could possibly result in extra vibration or damage to the rest of the system. Nonetheless, there are several available solutions to ensure correct torque split (Robleda *et al*., 2012).

Since the application of the STG is still in the beginning stages, most of the current research is focused on the modeling and building of the transmission systems. The dynamics of the STG system was analyzed by Krantz (1994). Moreover, configurations to increase power density in STG were reported by Vilán *et al*. (2009). Recently, the diagnosis of the STG has been reported in (He *et al*., 2010; Li and He, 2011; Li *et al*., 2012). He *et al*. (2010) are among the first who tried to simulate gear faults in the STG and they developed several detection methods based on vibration and AE analysis. In general, there is limited research on the detection of gear faults for the STG.

The notational STG used in this work uses a parallel shaft layout for both the input side and output side. All of the gears inside are spur gears. On the input side, the input driving gear is a 40 tooth gear which drives three input driving gears, each containing 72 teeth. On the output side, three output driving gears with 48 teeth drive a 64 tooth output gear. A 3HP three phase induction AC motor with a maximum speed of 3600 rpm is used to drive the notational gearbox.

To accommodate for shaft misalignment and reduce the vibration transmission, a disc type coupling is utilized to transmit the torque from the motor to the driving shaft. A magnetic loading system is controlled by a power supply and the load can be adjusted by changing the output current of the power supply. Figure 14 shows the structure of the notational STG. The test rig and sensor locations are shown in Figure 15.

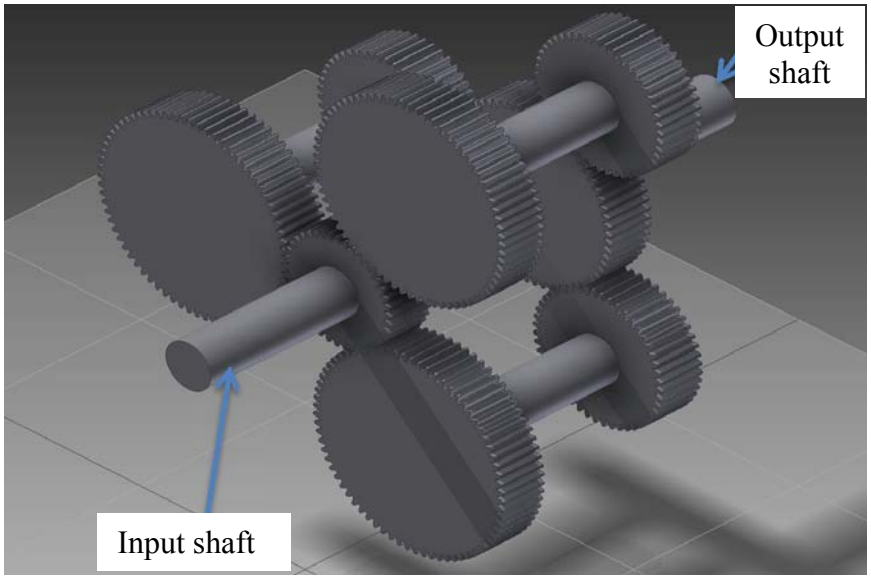

Figure 14. The gear structure of the notational STG

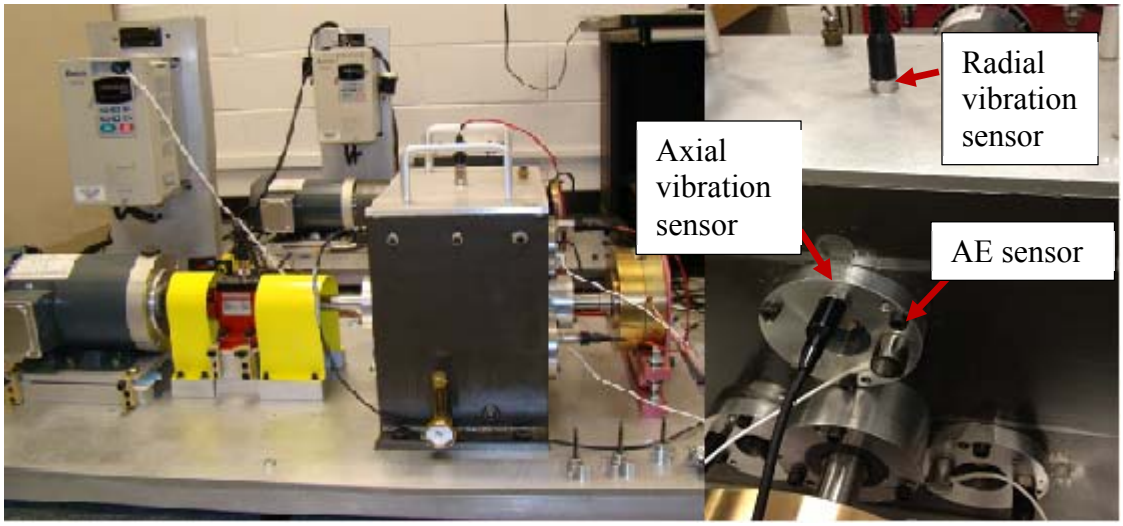

Figure 15. The notational STG and sensor locations

As a speed reduction gearbox, the input side and the output side have a 2.4 times speed reduction ratio. In Table 2, the output shaft speed and the interested shaft (faulty gear shaft) speed are given under the tested speeds.

Table 2. Output shaft speed corresponding to input shaft speed

| Input shaft speed (Hz) | 10 | 20 | 30 | 40 | 50 | 60 |
|---|---|---|---|---|---|---|
| Faulty gear shaft speed | 5.56 | 11.1 | 16.7 | 22.2 | 27.8 | 33.3 |
| Output shaft speed | 4.17 | 8.33 | 12.5 | 16.7 | 20.8 | 25 |

### 4.1.2 Data Acquisition Systems Setup

In this section, the experiment to verify the proposed AE signal processing method is presented. In Figure 16, the demodulation board from Analog Devices -- AD8339 and sampling devices from National Instrument -- NI-DAQ 6211 are shown. The demodulation board performed the multiplication of sensor signals and reference signals. It is an analog device and much more affordable than a high rate sampling board. It takes two inputs, one from the AE sensor, and another from a function generator as reference signal. The basic principle of AD8339 could be explained by Gilbert cell mixers. In electronics, the Gilbert cell is commonly used as an analog multiplier and frequency mixer. This circuit's output current is an accurate multiplication of the base currents of both inputs. Therefore, according to Eq. (2) it could convert the signal to baseband and twice the carrier frequency. The output of the demodulation board goes to the sampling board and the high frequency component is filtered out. NI-DAQ 6211 is a low frequency data acquisition device, with a sample frequency up to 250 kHz.

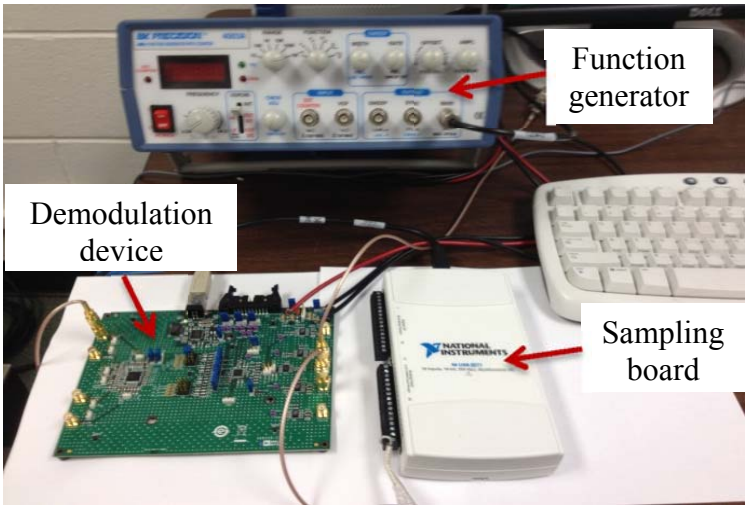

Figure 16. Demodulation device and data sampling board

Before data acquisition, one needs first to determine the frequency of the reference signal for demodulation. The purpose is to down shift the AE signal frequency as low as possible. Based on Eq. (2), in order to remove the carrier frequency, the reference signal frequency needs to be as close to the AE carrier frequency as possible. Thus, the next step is to identify the AE sensor response frequency.

Each AE sensor has its specific frequency response range, which further depends on the testing system it is mounted on. The same sensor attached to different machines will have different frequency response. With reference to the AE sensor user manual, a coarse range of the sensor response frequency is given. In order to identify a more accurate AE sensor response frequency, an optimization process was conducted as introduced in section 3.1. The frequency of reference signal was obtained as 400 kHz by the proposed optimization algorithm. In searching for the optimized reference frequency, a chirp function with a range of 50 kHz - 1050 kHz was selected to cover the whole sensor response range. The chirp function started with an initial frequency of 50 kHz and chirped up at a rate of 139.89 kHz/s. The output of the demodulation board goes to the sampling board and the high frequency component was filtered out.

The AE sensor used in this work is a true differential wideband sensor with high sensitivity. It has good frequency response over the range of 100 – 900 kHz. Differential sensors offer a lower noise output from a pre-amplifier. The accelerometers used for vibration data collection are ICP accelerometers, model IMI 608-A11. The frequency response of the accelerometers was from 0.5 Hz– 10 kHz.

## 4.2 Validation Results

In this section, the validation result of the proposed methods in Section 3.3 will be presented and discussed.

### 4.2.1 50% Tooth Cut Fault Detection Results using Waveform Deformation

The fault tested in this case study was 50% tooth cut in one of the intermediate gears. The gearbox was running at 10 Hz – 60 Hz. 25% loading was applied to the output shaft. The gear with 50% tooth cut is shown in Figure 17. The location of the gear with the tooth cut in the gearbox is shown in Figure 18.

Figure 17. 50% tooth cut gear

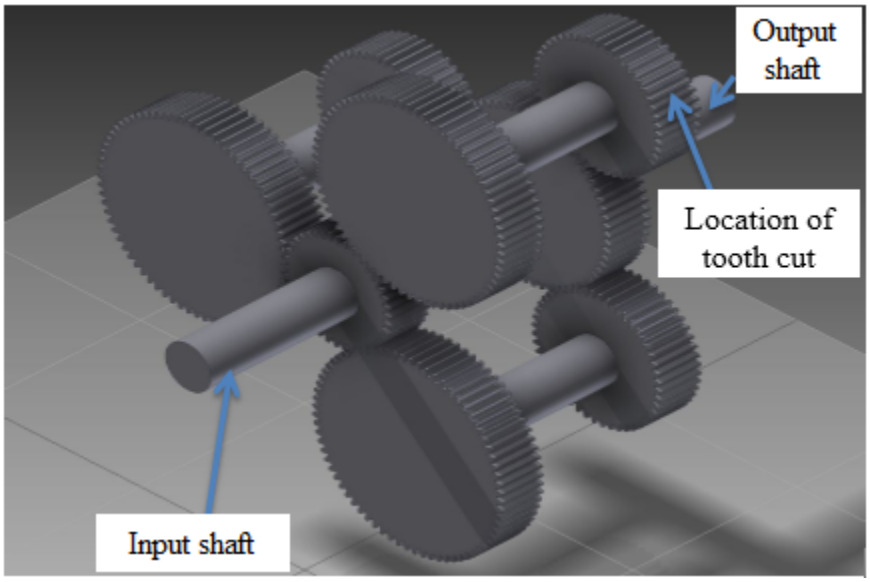


Figure 18. Location of the gear with seeded tooth faults

The recorded signals after heterodyne, one faulty signal and one healthy signal, are shown in Figure 19.

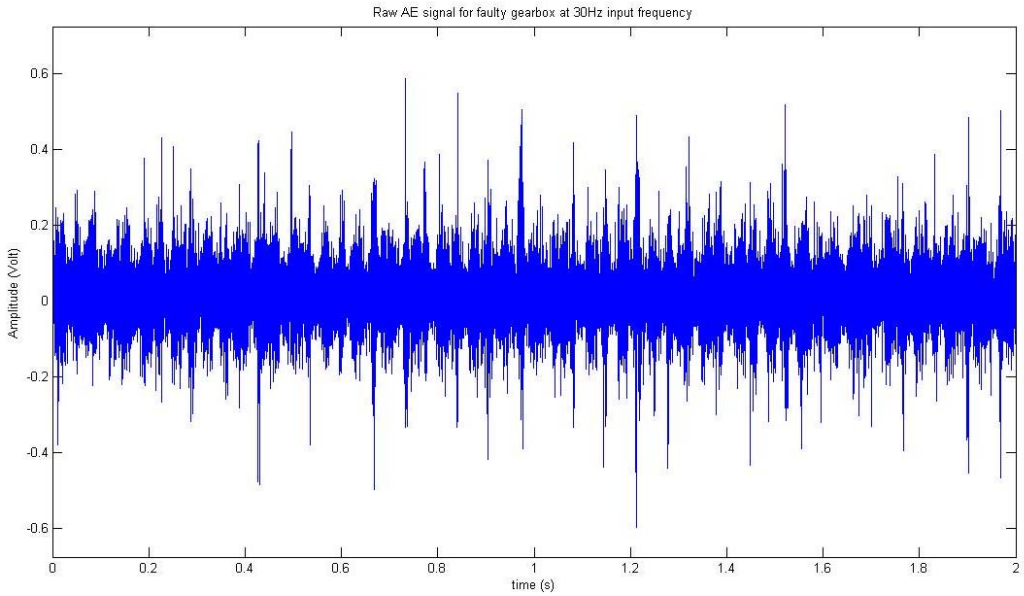

(a) Faulty AE signal at 30Hz input shaft speed

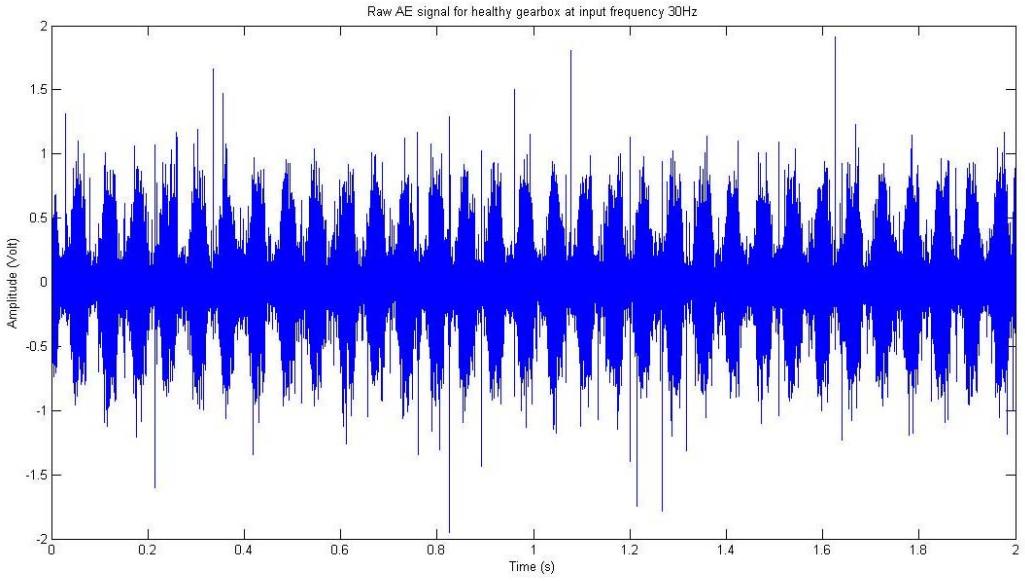


(a) Healthy AE signal at 30 Hz input shaft speed

Figure 19. Raw AE signal of faulty and healthy gear

The corresponding frequency components are given in Figure 20.

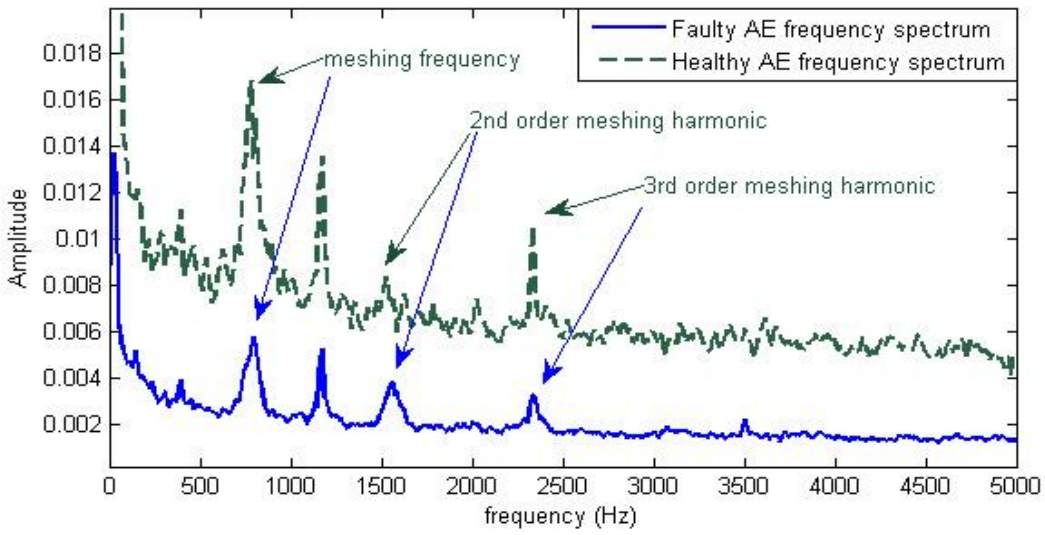


Figure 20. The frequency component of the raw AE signal

As shown in Figure 20, the meshing frequency and meshing harmonic could be easily identified. This validates the demodulation technique. However, the frequency components of the healthy

and faulty gearbox are almost the same and the frequency component in healthy gearbox has larger amplitude. This could be due to the assembly error, such as the pad tightness, gear and gear friction, etc. So the proposed method was further applied to the data, as will be shown next.

The base band meshing signal was chosen to do TSA for all of the following result to keep consistency. But the method works as well with the meshing harmonics.

Results show that all 10 Hz - 60 Hz faulty TSA signals show an obvious wave defect. When there is a faulty feature involved, the corresponding teeth will generate some anomaly during gear meshing. This will affect the meshing signal wave shape in these cycles as well the overall dynamic of the shaft. Therefore, the faulty signal will have some underdeveloped or defect cycles. Next, the analysis results of the experiments on the test-rig are presented in Figure 21 through Figure 26.

Figure 21 gives the TSA results comparison for input shaft speed at 10 Hz.

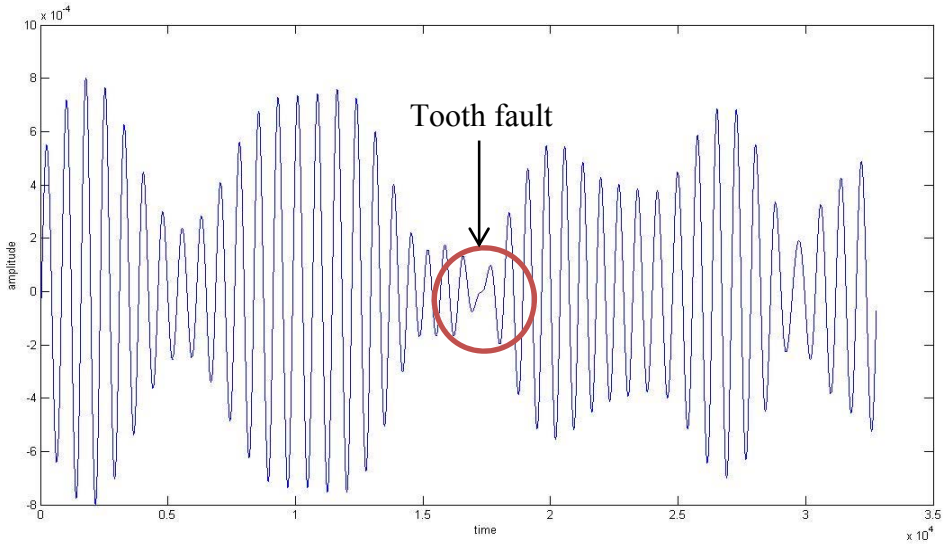


(a) Faulty signal TSA

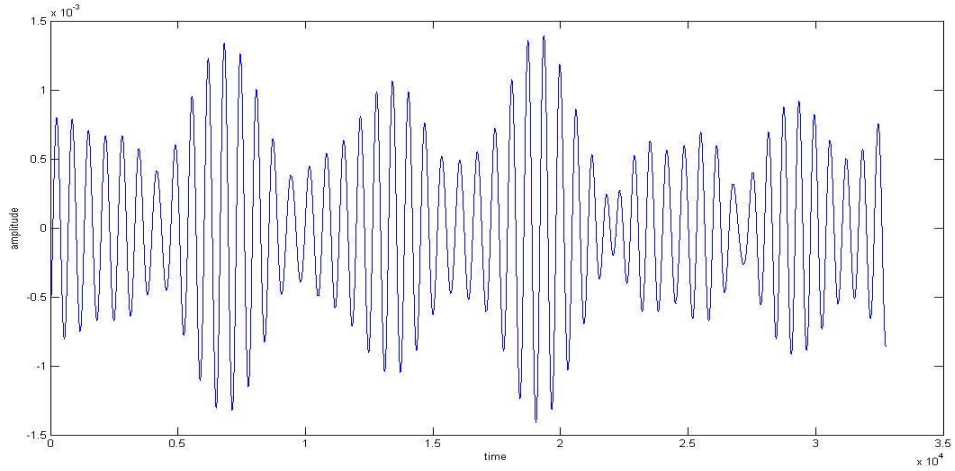


(b) Healthy signal TSA

Figure 21. Faulty and healthy gear TSA under 10 Hz input shaft speed

A clear indicator of fault could be identified from the signal as pointed by a circle and arrow. On the other side, the healthy gear signal displayed a normal periodic characteristic.

Figure 22 gives the TSA results comparison for input shaft speed at 20 Hz. Again, the waveform defect is readily observed in faulty TSA signal.

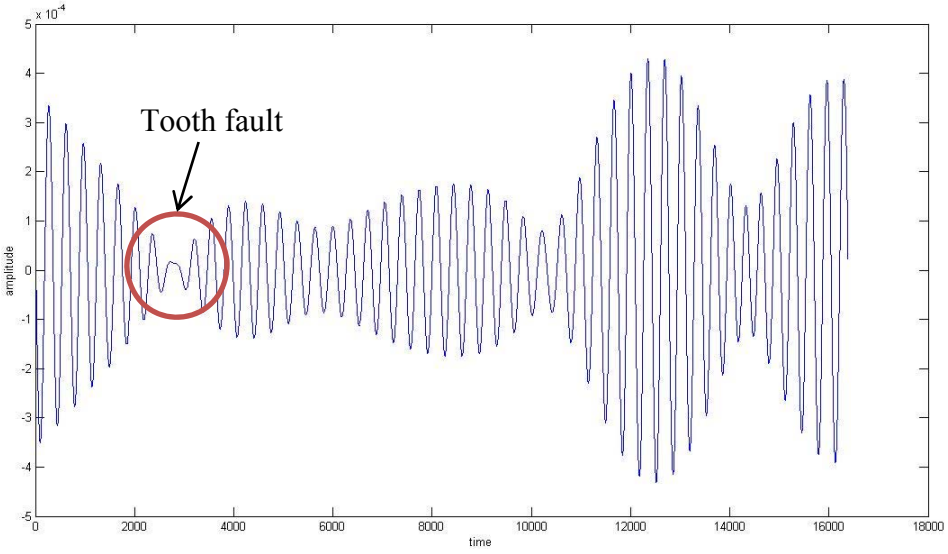


(a) Faulty signal TSA

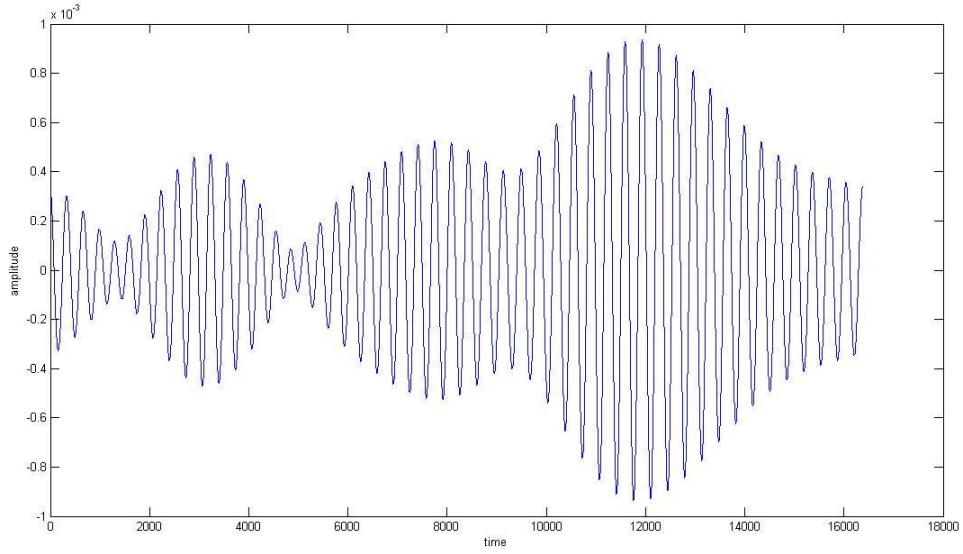


(b) Healthy signal TSA

Figure 22. Faulty and healthy gear TSA under 20 Hz input shaft speed

Figure 23 gives the TSA results comparison for input shaft speed at 30 Hz. The tooth fault can be identified as well.

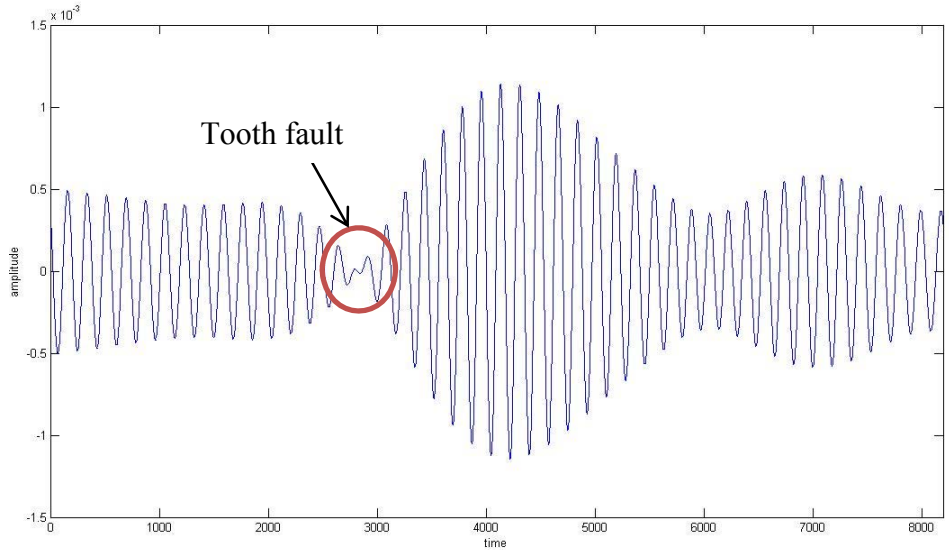


(a) Faulty signal TSA

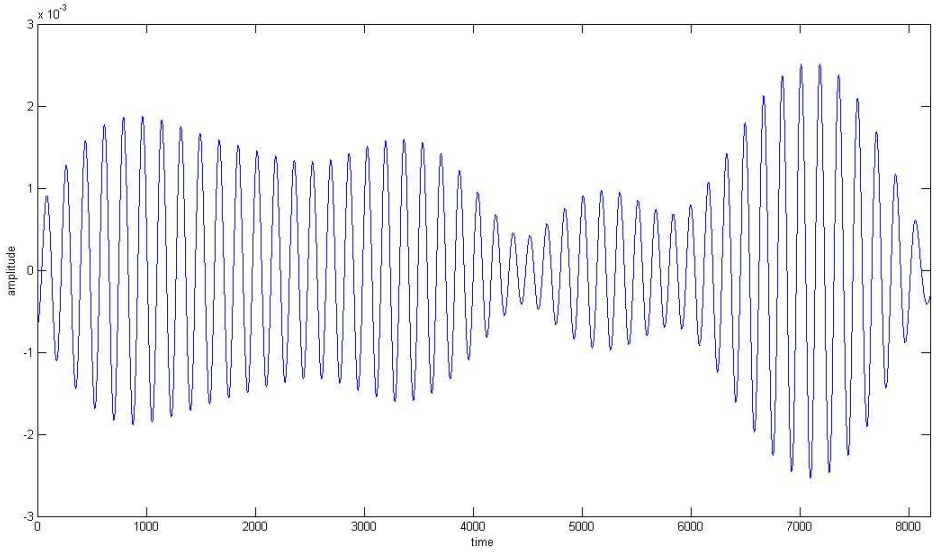


(b) Healthy signal TSA

Figure 23. Faulty and healthy gear TSA under 30 Hz input shaft speed

Figure 24 gives the TSA results comparison for input shaft speed at 40 Hz. The waveform defect is readily observed in the faulty TSA signal.

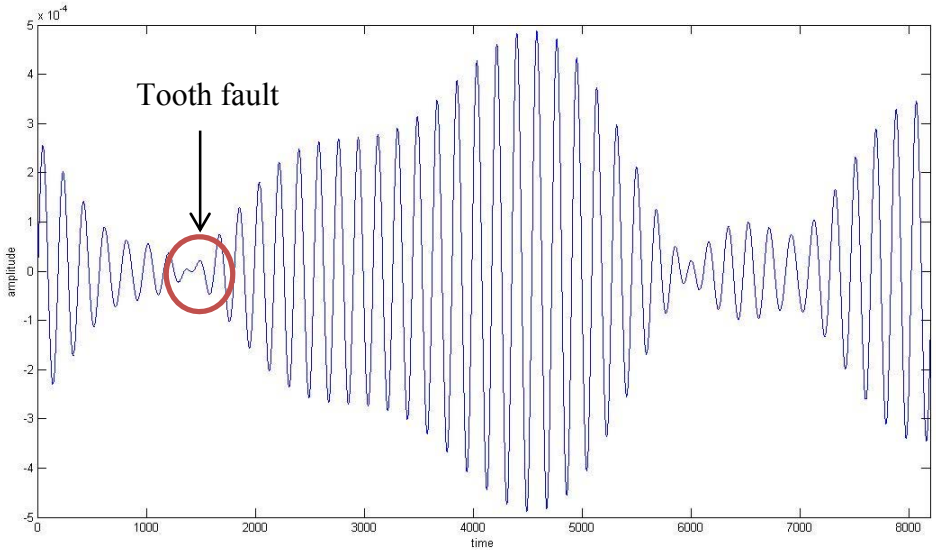


(a) Faulty signal TSA

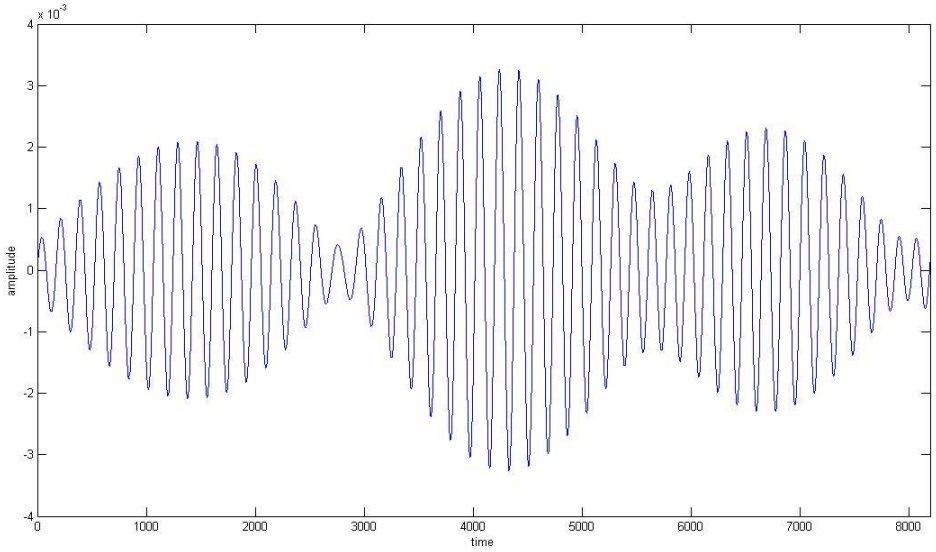


(b) Healthy signal TSA

Figure 24. Faulty and healthy gear TSA under 40 Hz input shaft speed

Figure 25 gives the TSA results comparison for input shaft speed at 50 Hz.

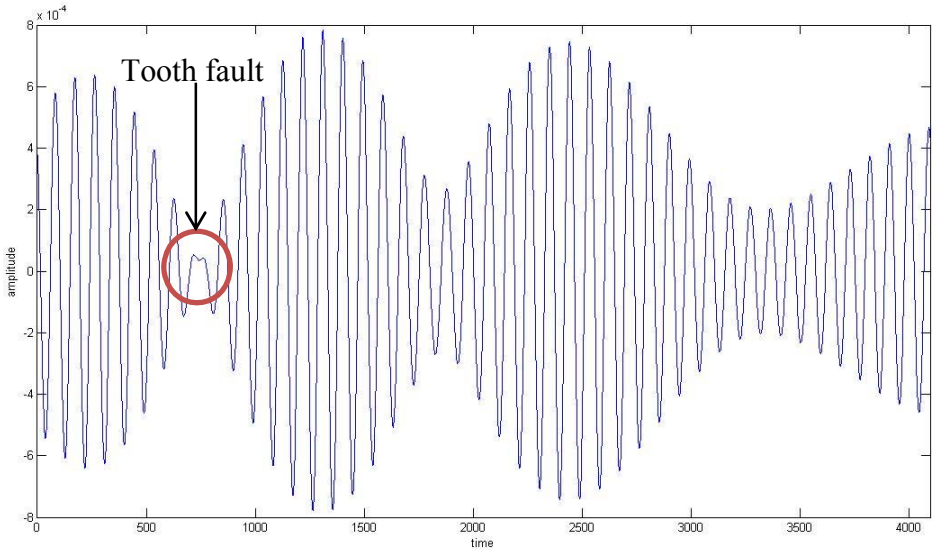


(a) Faulty signal TSA

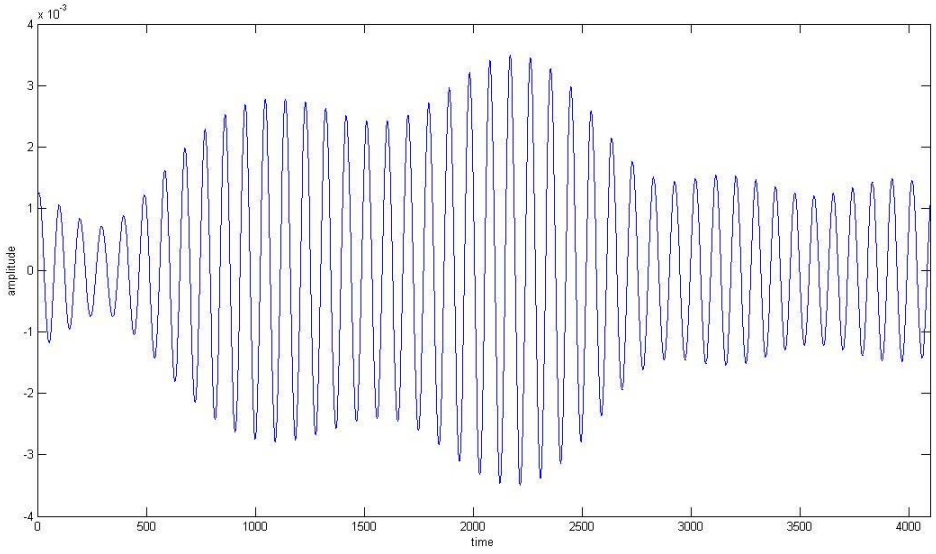


(b) Healthy signal TSA

Figure 25. Faulty and healthy gear TSA under 50 Hz input shaft speed

Figure 26 gives the TSA results comparison for input shaft speed at 60 Hz.

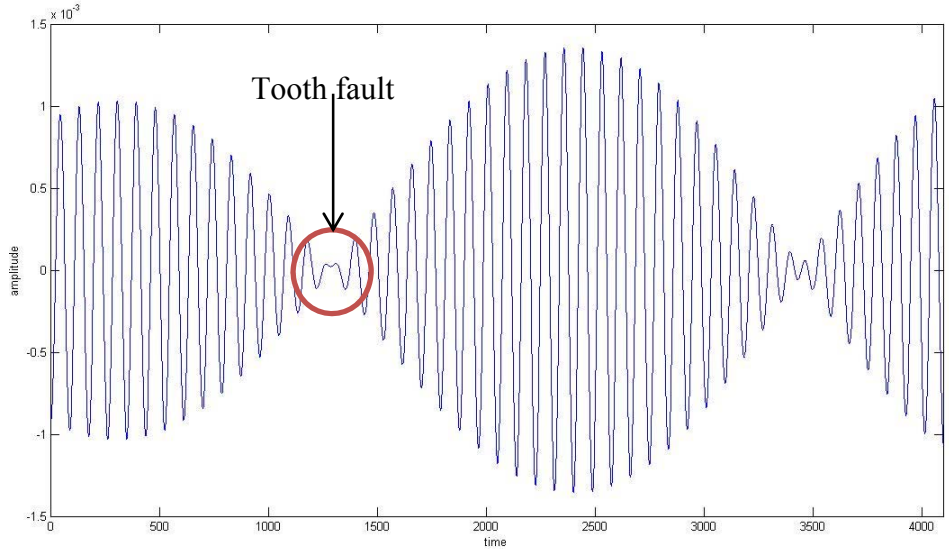


(a) Faulty signal TSA

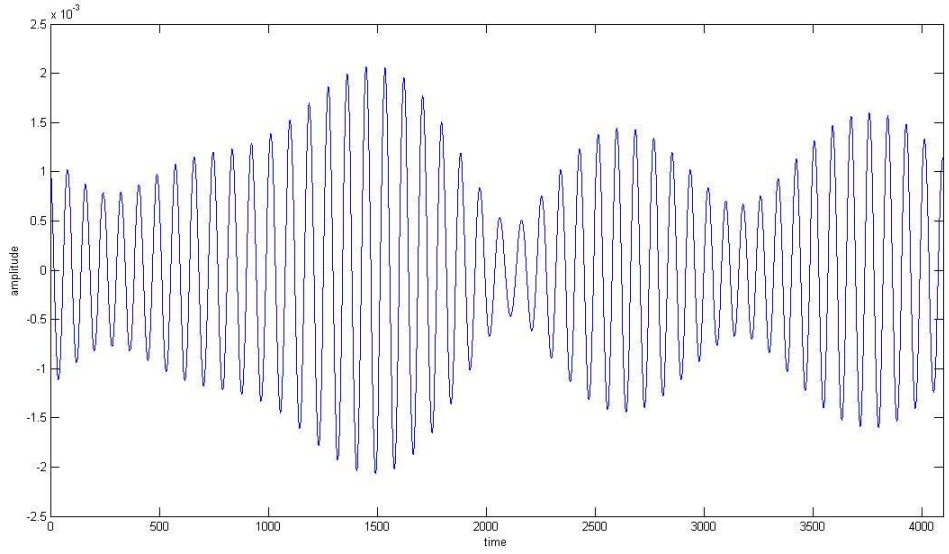


(b) Healthy signal TSA

Figure 26. Faulty and healthy gear TSA under 60 Hz input shaft speed

From the results shown above, it is possible to detect the tooth fault by inspecting the enhanced TSA signals in all of the tested data. Generally, since there was a 50% tooth cut, the faulty tooth was not meshing normally like other teeth on the same gear. From the perspective of AE signals, the meshing impact corresponding to that periodic cycle is corrupted. Thus, in the faulty gear TSA signals, some underdeveloped cycles were generated. While in the healthy case, the waveform of the TSA signal is periodic (with limited amplitude fluctuation) and each cycle is fully developed.

In order to evaluate the effectiveness of the proposed methods, a repeated experimental test was performed. Five sets of data were collected at each speed from 10 Hz to 60 Hz for both healthy gear and faulty gear. The detailed detection results are given in Table 3 to Table 5.

Table 3. Detection results on faulty data

| Faulty Gear | Waveform defect? YES | NO |
|---|---|---|
| 10Hz | 3 | 2 |
| 20Hz | 4 | 1 |
| 30Hz | 3 | 2 |
| 40Hz | 3 | 2 |
| 50Hz | 3 | 2 |
| 60Hz | 2 | 3 |
| Total | 18 | 12 |

Table 4. Detection results on healthy data

| Healthy Gear | Waveform defect? YES | NO |
|---|---|---|
| 10Hz | 0 | 5 |
| 20Hz | 0 | 5 |
| 30Hz | 0 | 5 |
| 40Hz | 0 | 5 |
| 50Hz | 0 | 5 |
| 60Hz | 0 | 5 |
| Total | 0 | 30 |

Table 5. Confusion matrix

| Predicted / Actual | Healthy | Faulty | Total |
|---|---|---|---|
| Healthy | 30 | 0 | 30 |
| Faulty | 12 | 18 | 30 |
| Total | 42 | 18 | 60 |

Overall detection accuracy = $(30 + 18)/60 = 80\%$.

False alarm for healthy gears = 0/30 =0%.

Faulty detection rate = 18/30 = 60%.

In summary, a novel methodology of gear diagnosis by processing an AE signal has been tested and validated. Compared with traditional AE signal processing techniques, this technique gives a deeper interpretation of the internal physical characteristics of the testing system and AE signals themselves. Previously, researchers treated AE signal as separate energy bursts, focusing mainly on the characteristic within the burst, but ignored the time continuous features, which is closely related to the testing system. Also, the fact that raw AE signals are a carrier signal of the load information is always overlooked. By inspecting the signal features along the time axis, abnormal behavior occurred repeatedly in a rotating machine can be extracted and detected. A waveform defect can be found on the enhanced TSA signal when tooth fault is presented.

Although this method achieved initial success in detecting the tooth fault, there are still some drawbacks:

1) As an intuitive method, the fault detection is made by visual inspection, which makes it hard to automatically detection fault and trigger fault alarms.
2) The detection rate is relatively low for practical purpose, as the fault detection rate is around 60%.

In order to develop a robust method based on reliable parameters, a condition indicator based method has been introduced in Section 3.3. The validation results will be shown next.

### 4.2.2 Tooth Crack and Tooth Cut Fault Detection Results using Condition Indicators

The previous shown methods did not give specifically parametric based fault criteria, which would be important in industrial application for decision making. In this section, the condition indicator based fault detection method will be tested and the results will be shown.

Two kinds of faults are used to validate the condition indicator based methods, tooth crack fault and tooth cut fault. The tooth crack fault is considered as an incipient fault which is hard to detect in practice. Therefore, it suffices to validate the effectiveness of the method if it could detect the tooth crack fault. The tooth cut fault are used to further test the sensitivity of the method to the level of tooth fault by comparing both results.

The first gear fault tested in this section is tooth crack. Specifically, one of the intermediate gears with 48 teeth was damaged by cutting the root of a gear tooth with a depth equal to half width of the gear tooth by EDM (electric discharge machining) with a wire of 0.5 mm diameter, to simulate the root crack damage in real applications. The seeded tooth crack is shown in Figure 27.

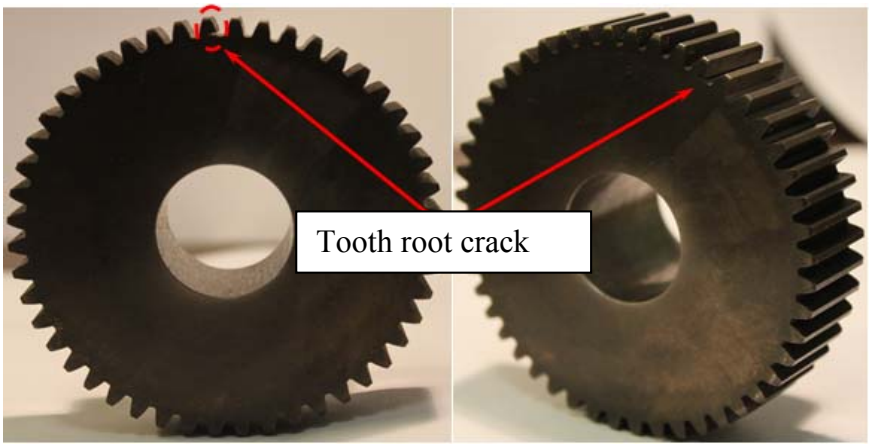

Figure 27. Seeded tooth root crack

The gearbox input shaft speed range is from 10 Hz – 60 Hz with 10 Hz interval. For each speed, 5 data sets were collected. There was no torque load during the test. It should be noted that with a load, the faulty gear feature will be amplified due to increased impact on the gear. In zero loading experiments, the identification of gear fault is more challenging than loaded cases.

The raw AE data after heterodyning are shown in Figure 28.

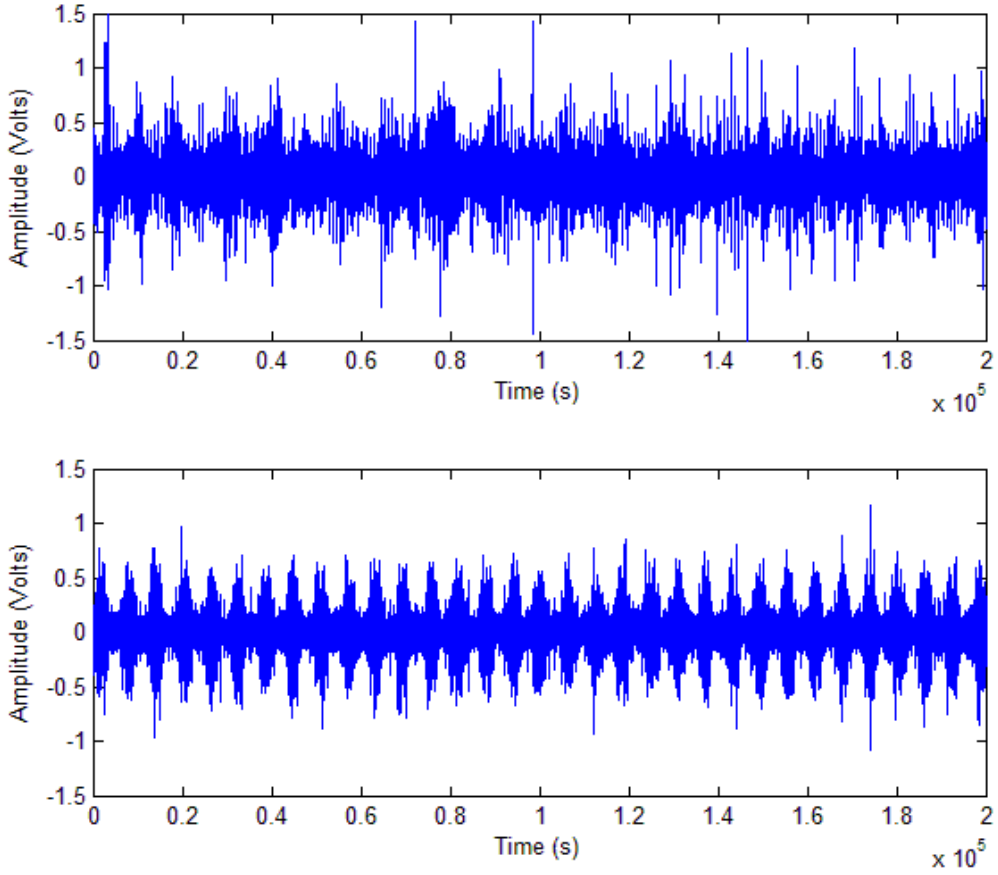


Figure 28. Healthy (upper) and faulty AE signals (lower) collected with heterodyne

Before performing TSA, the data was first analyzed using kurtogram. Figure 29 shows the kurtogram for a faulty signal at 30 Hz. The center frequency identified from this kurtogram is 37500 Hz, with a band width of 25000 Hz. Based on the kurtogram, the center frequency and bandwidth where the SK is maximized could be identified. An optimal band pass filter was designed to filter the signal with regard to the corresponding frequency range.

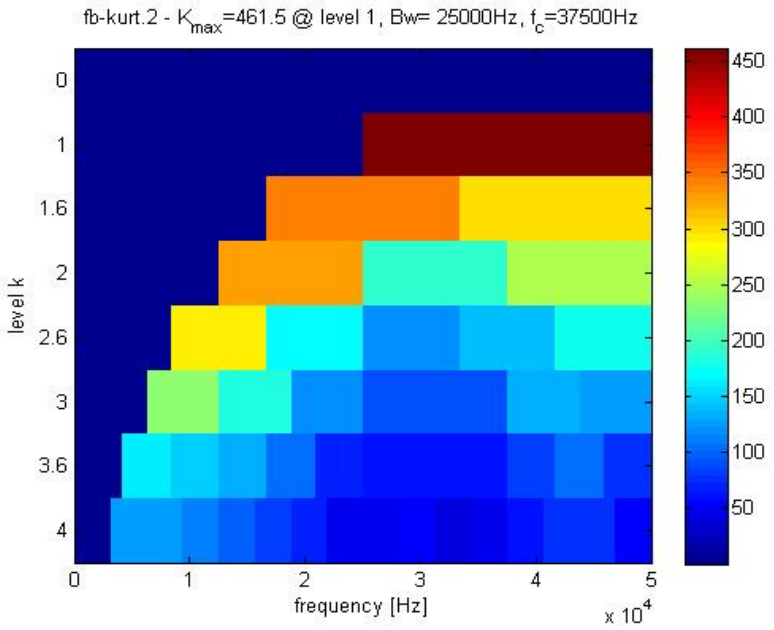

Figure 29. The kurtogram for a faulty signal at 30 Hz input shaft speed

After the band pass filtering, the TSA was computed using the filtered data. Since the raw signal was filtered before TSA, to maintain the phase unchanged, a zero-phase filter was used. About 260 averages were taken for each group of data. The TSA signal at 30Hz is shown in Figure 30.

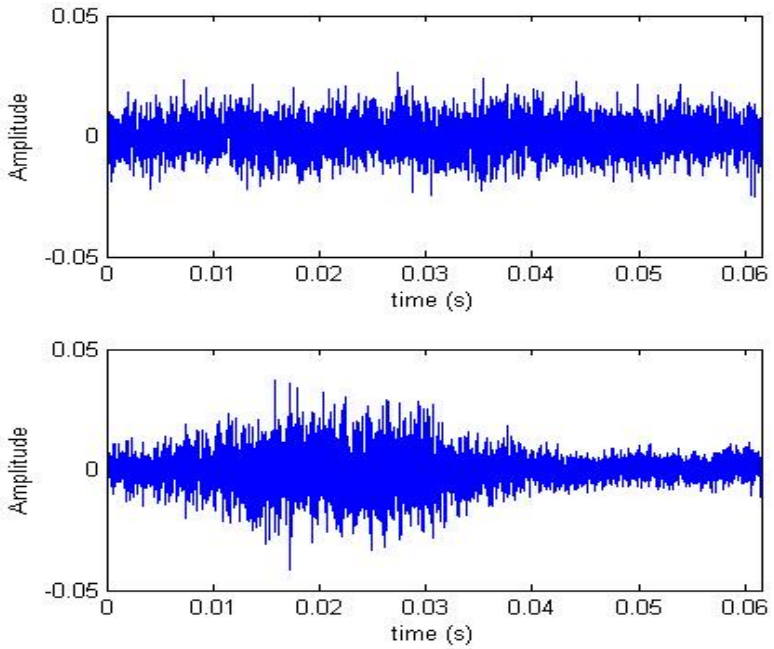

Figure 30. Healthy signal TSA (upper) and faulty signal TSA (lower)

In order to test the effectiveness and sensitivity of different condition indicators, the following groups of condition indicators are compared:

1) RMS, P2P, kurtosis and crest factor of the raw data.
2) RMS, P2P, kurtosis and crest factor of the TSA data.
3) In addition, condition indicator FM4 and NA4 are also tested on the TSA data. RMS, P2P, kurtosis and crest factor for the EO signals of the TSA.

The condition indicators calculated on the raw data without band pass filter and TSA are shown in Figure 31 through Figure 34. Note that in the experiment, 5 sets of data were collected for each input shaft speed: a total of 30 data samples were collected. Each 5 data set at the same speed will then be averaged to get a mean value. The mean values are aligned from low speed to high speed. It can be seen from Figure 31 that the raw RMS cannot separate the faulty gear from the healthy one. As the speed of the gearbox increases, the RMS increase gradually. From Figure 32, one can see that health signals have slightly larger P2P values than the faulty signals. This could be caused by random noise, either from the misalignment of the gearbox or from the sensors. In Figure 33, it shows that the healthy signals have larger kurtosis values than the faulty signals. Based on the raw kurtosis, it is possible to separate the faulty signals from the healthy ones when the input speed is lower than 40 Hz. However at a speed higher than 40 Hz, it is difficult to distinguish healthy signals from faulty signals. Similarly in Figure 34, the healthy crest factors have larger amplitude than faulty ones.

Based on the raw data condition indicators, it is impossible to separate the health signals from faulty ones. Also, the fact that the condition indicators of raw healthy signals have larger amplitude than the faulty condition indicators makes it impractical to set fault alarm threshold in real application.

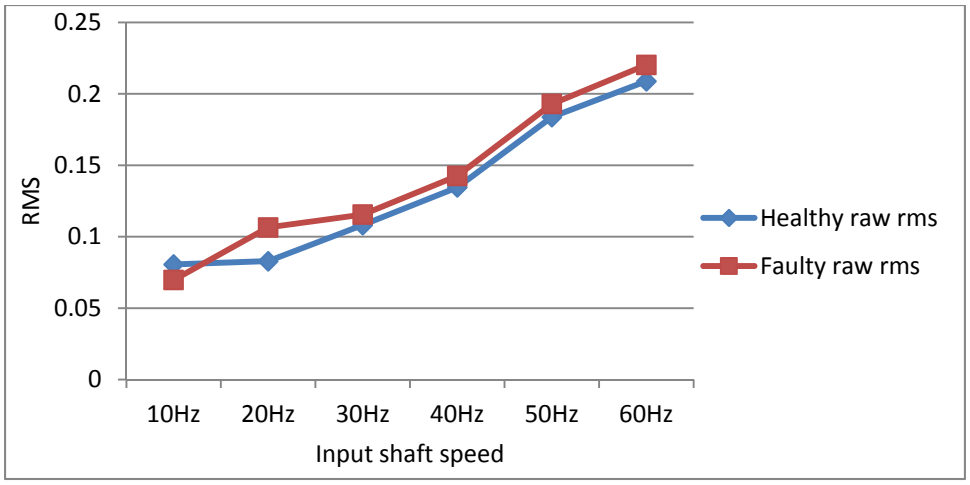


Figure 31. Raw data RMS

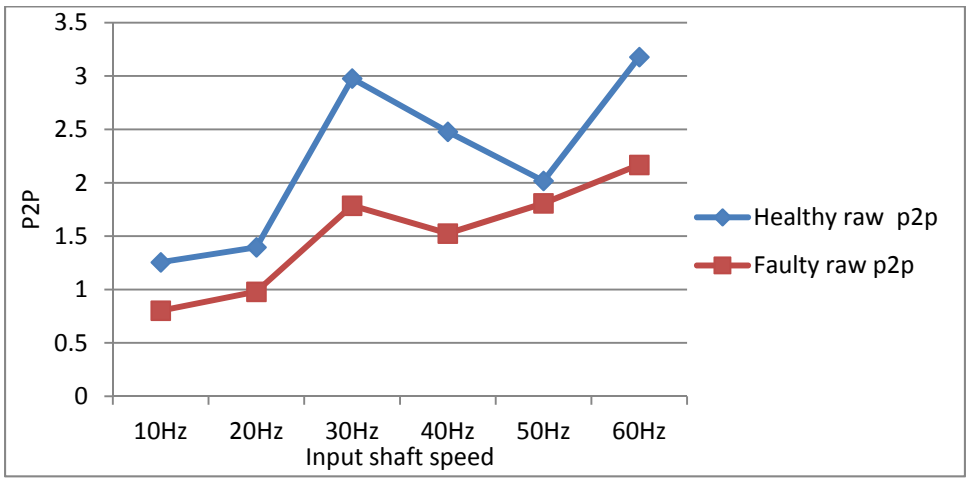


Figure 32. Raw data P2P

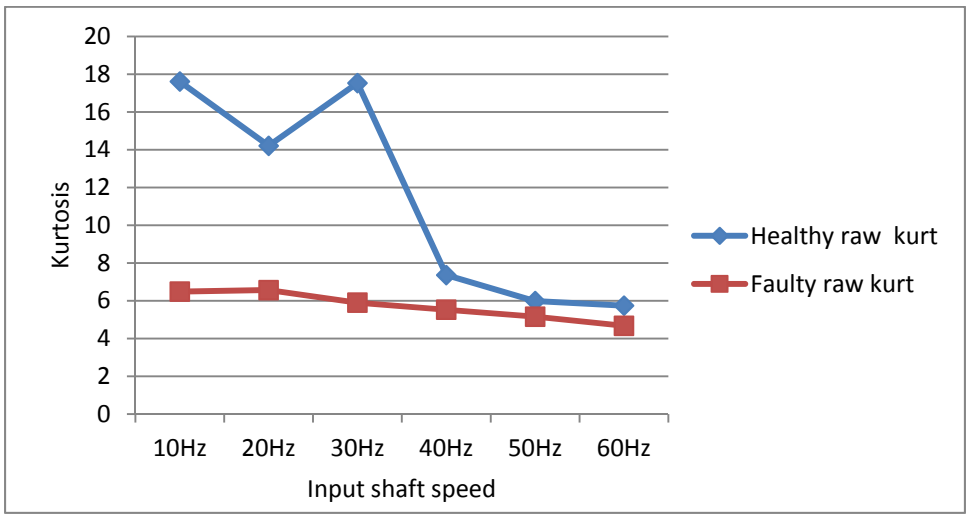


Figure 33. Raw data kurtosis

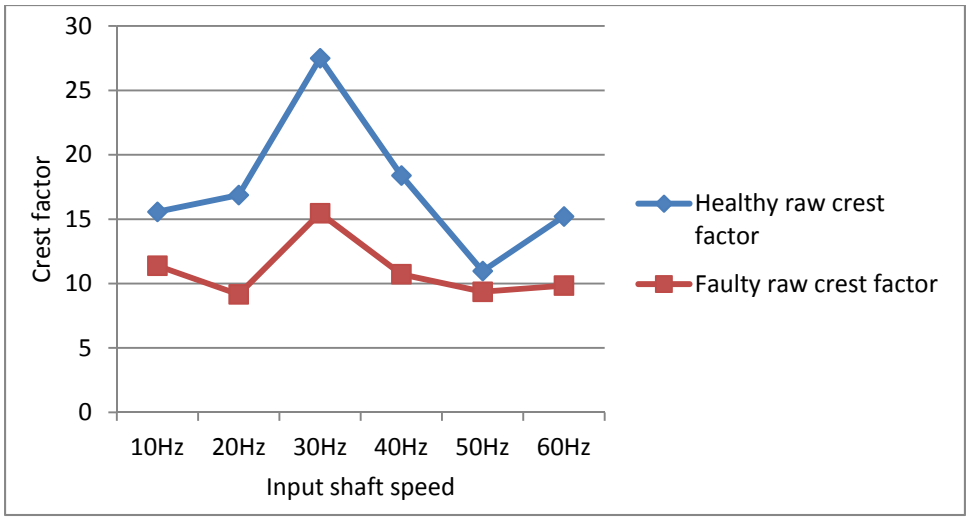


Figure 34. Raw data crest factor

In order to minimize the random noise and enhance the faulty feature hidden in the raw signal. SK based filter followed by TSA is performed on the raw data.

The plots of the condition indicators computed using TSA are provided in Figure 35 to Figure 44.

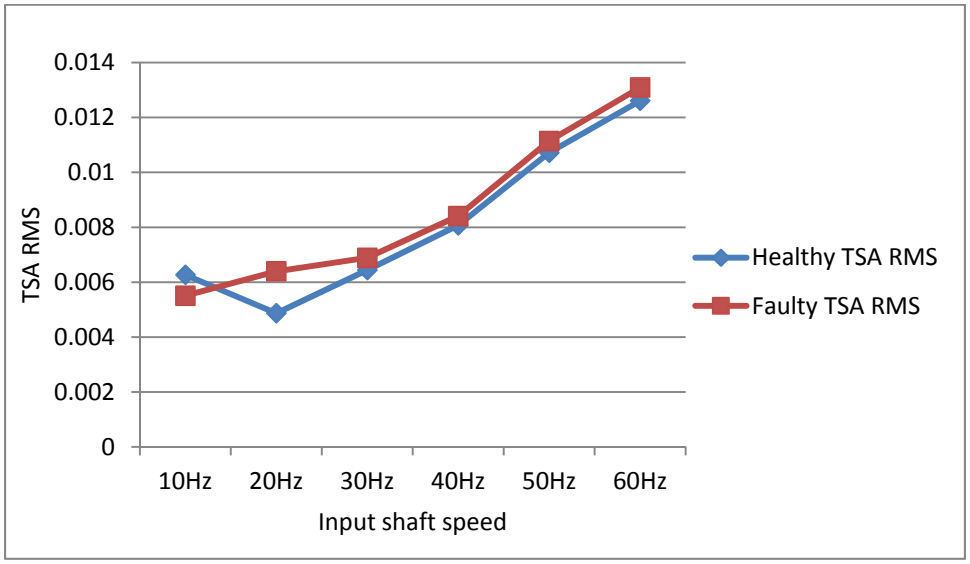


Figure 35. TSA RMS of the healthy data and faulty data

From Figure 35, one can see that the behavior of the TSA RMS is similar to that of the raw RMS in Figure 31. As the input shaft speed increases, the RMS increases for both health and faulty

gears. Since both the RMS of the health signals and the RMS of the faulty signals overlap over the entire testing conditions, it is impossible to separate the gear fault using TSA RMS.

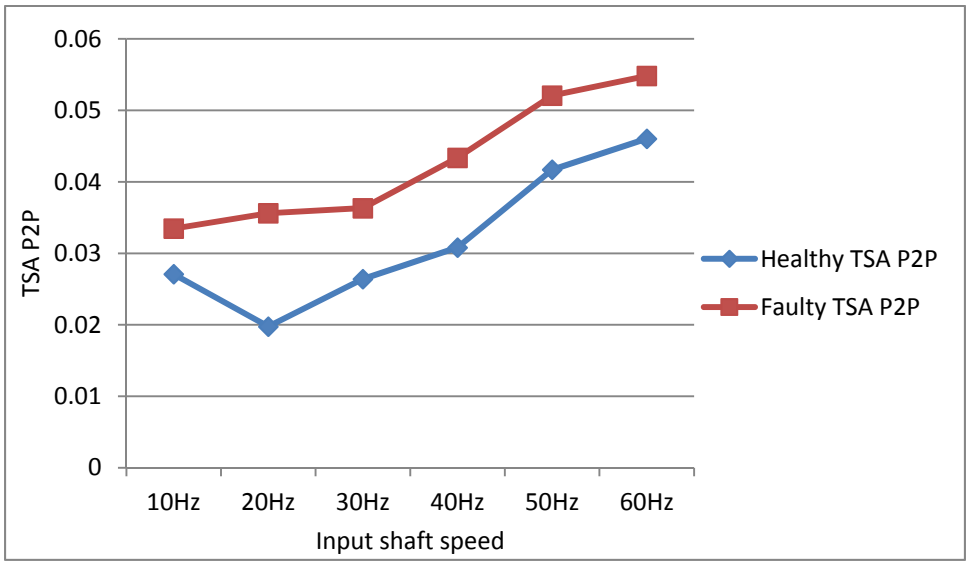


Figure 36. TSA P2P of the healthy data and faulty data

Compared with P2P of the raw signal, one can find that the P2P of the faulty TSA signals are all larger than that of the healthy TSA signals under each individual input shaft speed, as shown in Figure 36. This verified that the random noise is removed by TSA while the faulty features in the tooth crack condition are largely enhanced.

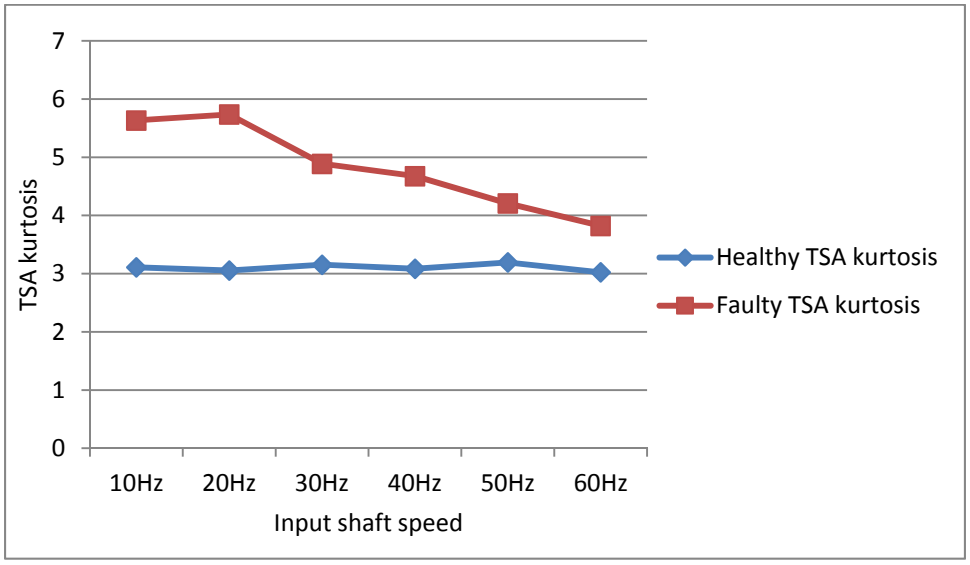


Figure 37. TSA kurtosis of the health data and tooth crack data

From Figure 37, it can be seen that the TSA kurtosis values of the health data remain almost constant around 3. As mentioned before, for any Gaussian distribution, the kurtosis is exactly calculated as 3. This concludes that the health gear TSA satisfied the Gaussian distribution. It means the amplitude of the AE impact waves generated by each tooth meshing complies with Gaussian distribution as expected. On the other hand, the TSA kurtosis of the faulty data is all above 3.6. This simply illustrates behavior of the faulty signal patterns.

Since kurtosis is non-quantitative value, it does not depend on the absolute amplitude. Kurtosis can serve as a reliable condition indicator for gearbox fault detection under variable load and speed.

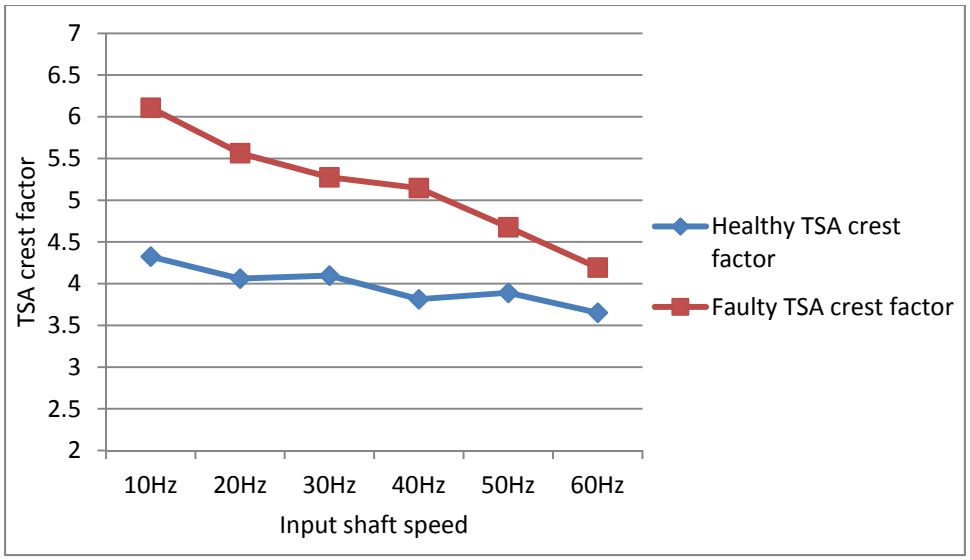


Figure 38. TSA crest factor of the healthy data and faulty data

The crest factor shows the statistics of the peak and the mean amplitude ratio. As show in Figure 38, all of the faulty TSA crest factors are larger than their health counterparts. The TSA crest factor still can be used as an effective condition indicator for detecting the gear fault.

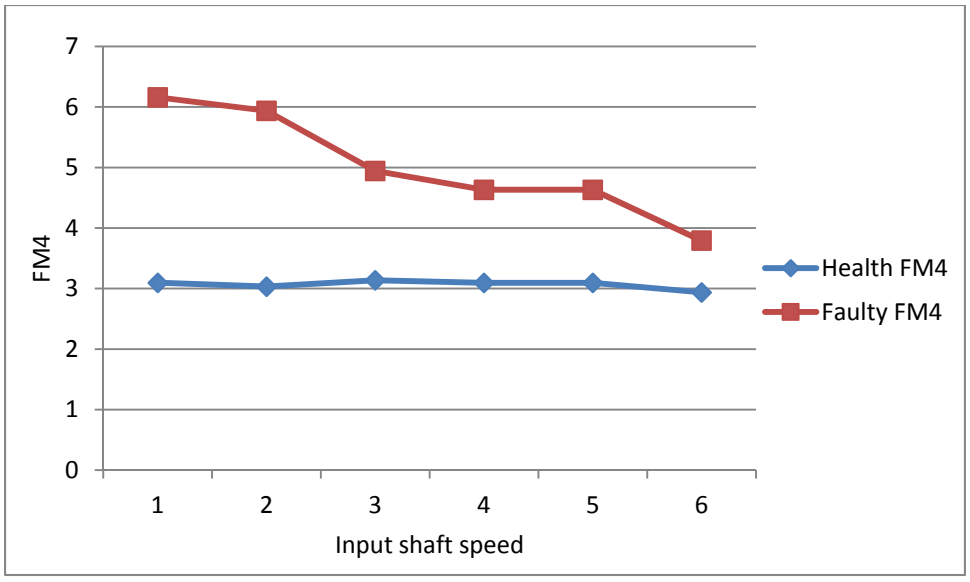

Figure 39. TSA FM4 of the health data and tooth crack data

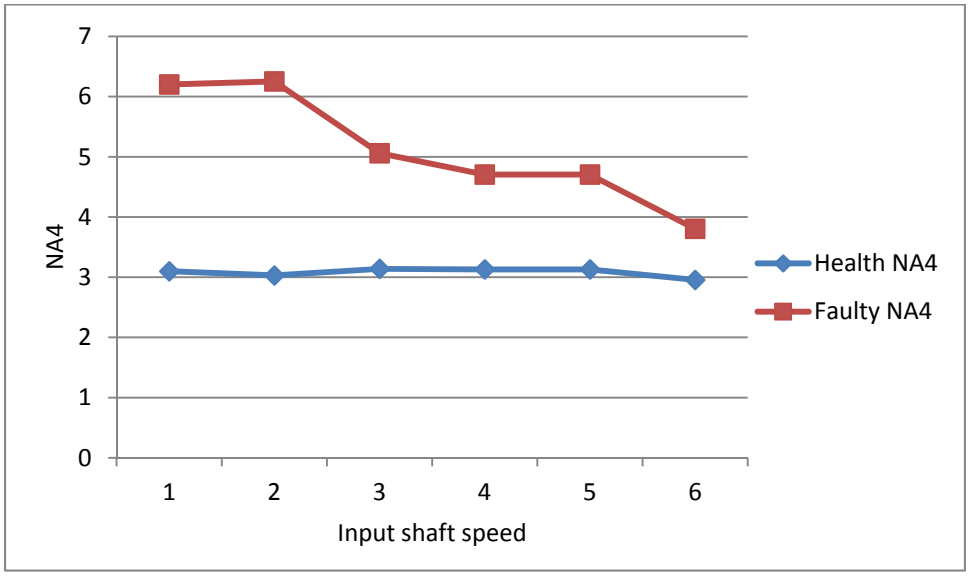

Figure 40. TSA NA4 of health and tooth crack data

Figure 39 and Figure 40 show the plots of the FM4 and NA4 condition indicators, respectively. FM4 is the difference signal kurtosis while NA4 is the residual signal kurtosis. From Figure 39, the healthy data FM4 identified itself as near Gaussian distribution. The faulty FM4 is larger which indicates fault feature. For NA4 in Figure 40, it behaves similarly with FM4 with healthy NA4 at 3 and healthy NA4 at a much high value. NA4 is also able to separate the healthy signals from the faulty ones.

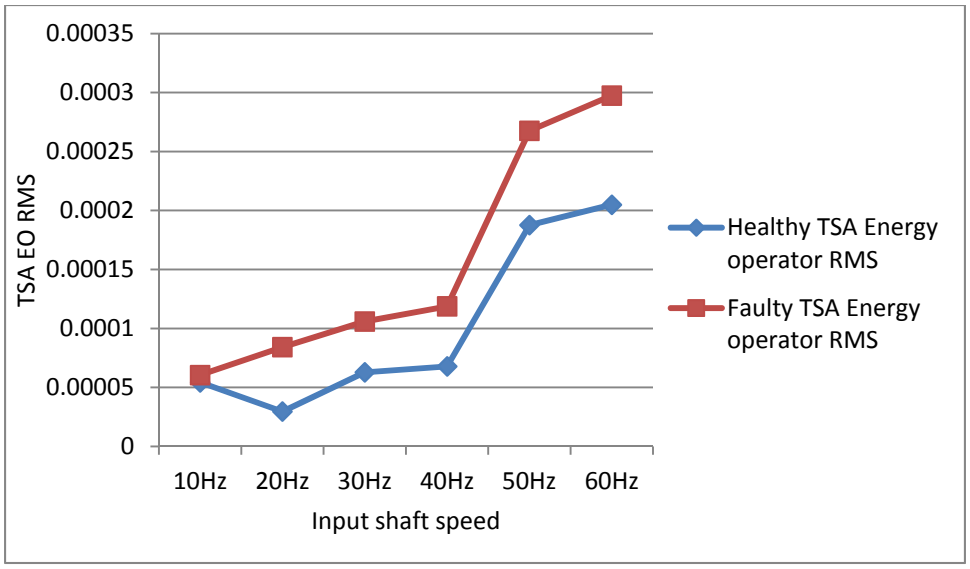


Figure 41. EO RMS of healthy and tooth crack TSA data

From previous shown results of the condition indicators computed on the raw signal and TSA signal, RMS cannot separate the healthy signals and faulty signals. Surprisingly, when taking the EO, one could actually see that faulty signal RMS values clearly separate themselves from the healthy signal RMS values as the speed increases, as shown in Figure 41.

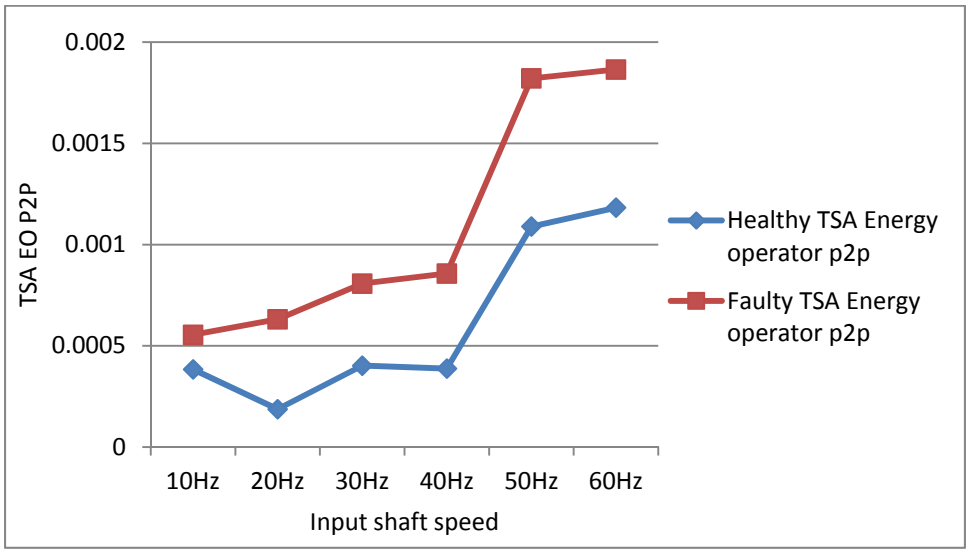


Figure 42. EO P2P of healthy and tooth crack TSA data

Figure 42 shows the P2P values of the TSA EO signals. The P2P condition indicator could roughly separate the faulty signals from the healthy signals.

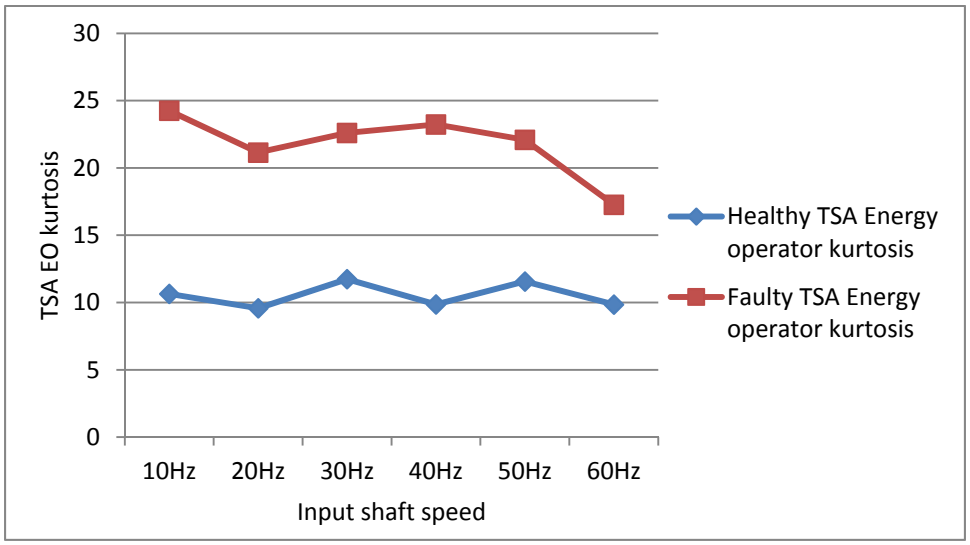


Figure 43. EO kurtosis of healthy and tooth crack TSA data

Figure 43 shows the EO kurtosis for both cases. EO kurtosis is another kurtosis based condition indicator. From the plot, it is easy to see that EO kurtosis can clearly separate the healthy gear from the faulty gear.

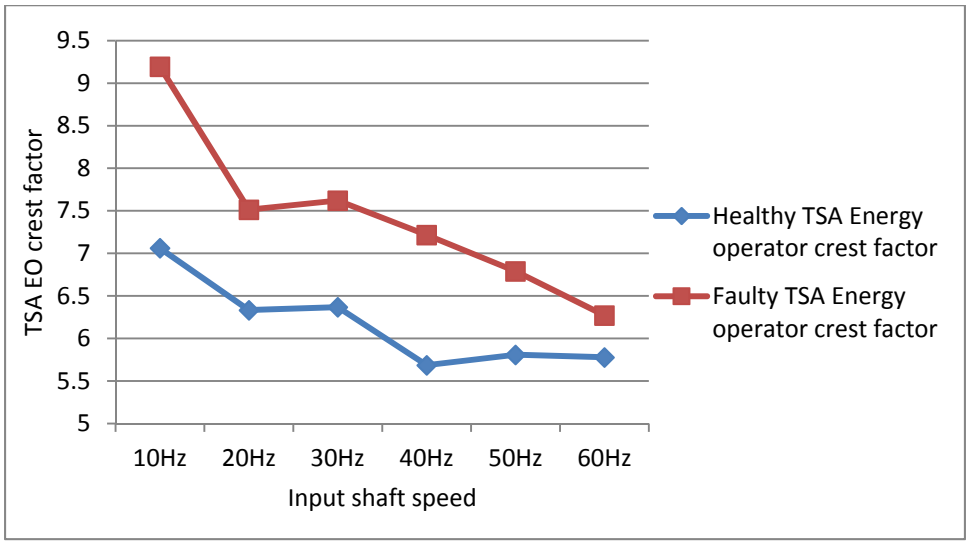


Figure 44. EO crest factor of healthy and tooth crack TSA data

Figure 44 plots the TSA EO crest factor. It could be seen from the plot that the faulty signal crest factors are roughly larger than the healthy ones. Based on the experiment results, crest factors are less reliable than kurtosis in term of tooth crack detection.

It was observed that as the gearbox speed increase, the kurtosis based condition indicators generally decrease. Two reasons might count for these behaviors. The first reason is that when the gearbox input shaft speed increases, the variance value in the denominator of Eq. (23) – Eq. (25) increases rapidly, which results in a decrease of the kurtosis based condition indicators. The second reason is that when an incipient fault is presented, the fault features are relatively small. When the gearbox is operating at a high speed, the normal gear meshing has similar impact amplitude as the fault feature, which overwhelms the fault feature. The AE signals during high speed operations tend to display more Gaussian like characteristics than low speed cases. For gear fault detection using AEs, this might be a shortcoming at high shaft rates because AE signal amplitude increases significantly with speed. The high amplitude of the normal gear meshing impact signals might overwhelm the incipient fault features.

Conversely, in the high shaft rate conditions, the RMS and P2P of the EO give clear indication for the faulty signal. The EO RMS and P2P of the fault signals increase much faster than healthy signals, so it is possible to use these condition indicators to compensate for the performance degradation of kurtosis based condition indicators.

One solution to this problem is to substitute the denominator with the variance of a gearbox in good condition, which then leads to the condition indicator NA4*, reported by Lebold *et al*. (2000). NA4* is more suitable for continuous monitoring. In the case of naturally grown fault, it is convenient to use the variance when the gearbox is new and under good condition. The evolution of the fault growth will be easily observed. On the other hand, while this phenomenon

is not exactly as desired in a high speed operational condition (1000 RPM or higher), it may benefit the detection of gear fault operated at lower speed (under 1000 RPM), such as the input side of wind turbine gearboxes.

Further, the tooth crack result are compared with 100% tooth cut fault result to evaluate whether the condition indicator is sensitive to the fault level. The 100% tooth cut fault is shown in Figure 45.

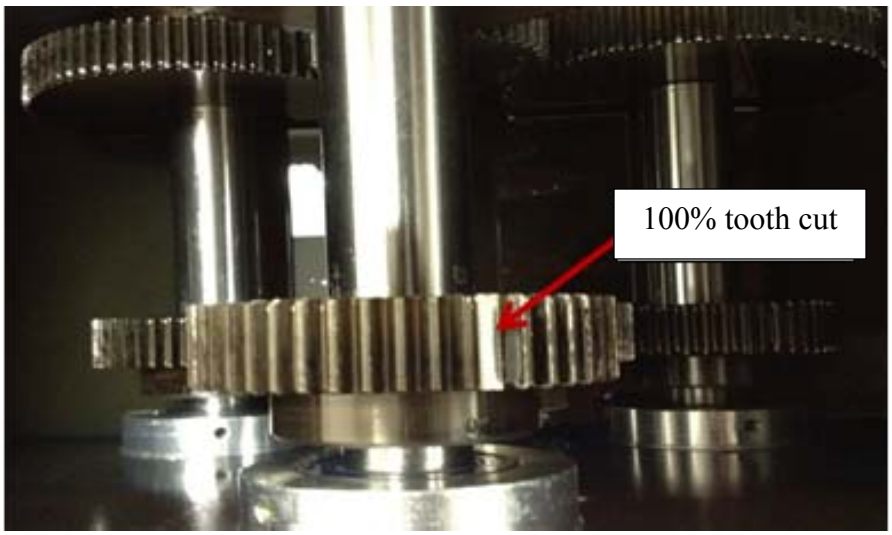


Figure 45. Seeded 100% tooth cut fault

Followed the procedure of condition indicator calculation, the results of the condition indicators for healthy gear, tooth crack and 100% tooth cut are plotted together and are shown in Figure 46 through 51.

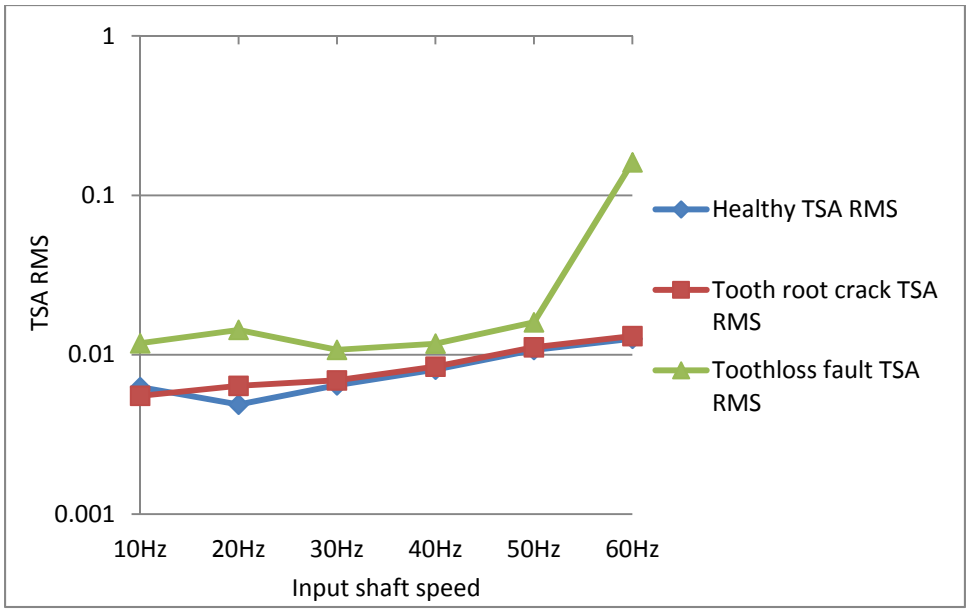


Figure 46. RMS of the TSA signals (*Y* axis: logarithmic scale)

Figure 46 shows that the RMS of the TSA signals of the tooth crack fault and healthy condition closely follow each other, which means RMS is not sensitive for incipient fault. However, all of the RMS values of the tooth loss fault are significantly larger than the healthy one. As the gearbox shaft speed increases, the RMS values for all conditions increase gradually. For the tooth loss fault, the RMS increases substantially at 60Hz shaft speed. Note that the vertical *Y* axis is in logarithmic scale.

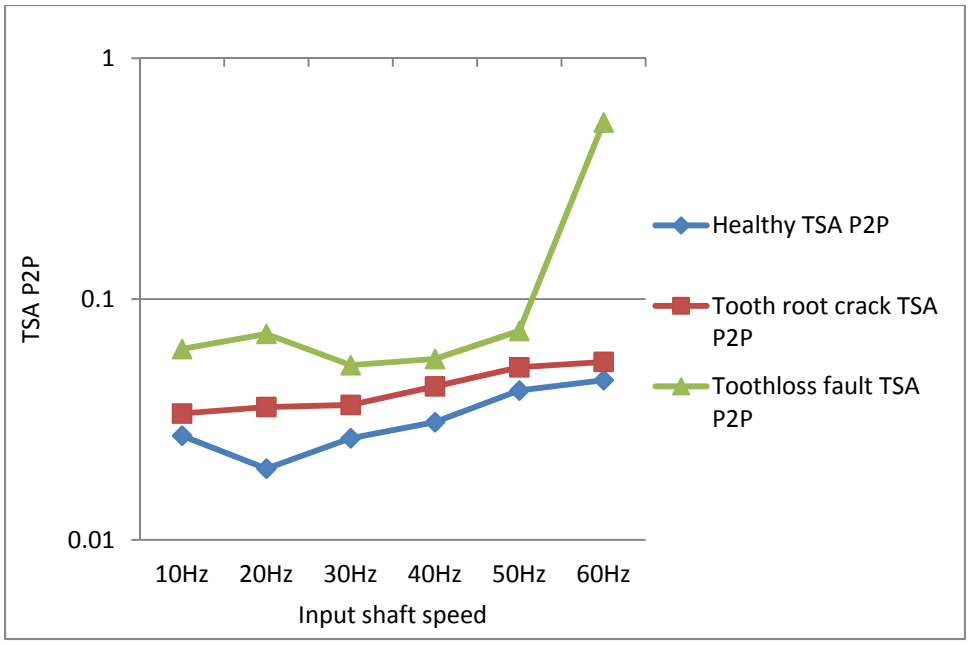


Figure 47. P2P of the TSA signals (*Y* axis: logarithmic scale)

From Figure 47, one can see that like RMS, the P2P values of all of the TSA signals increase with the increase of the shaft speed. Based on P2P, all the three gear conditions can be separated from each other. Unlike RMS, the P2P could better detect the tooth loss fault as the tooth loss P2P is significantly larger than the healthy condition.

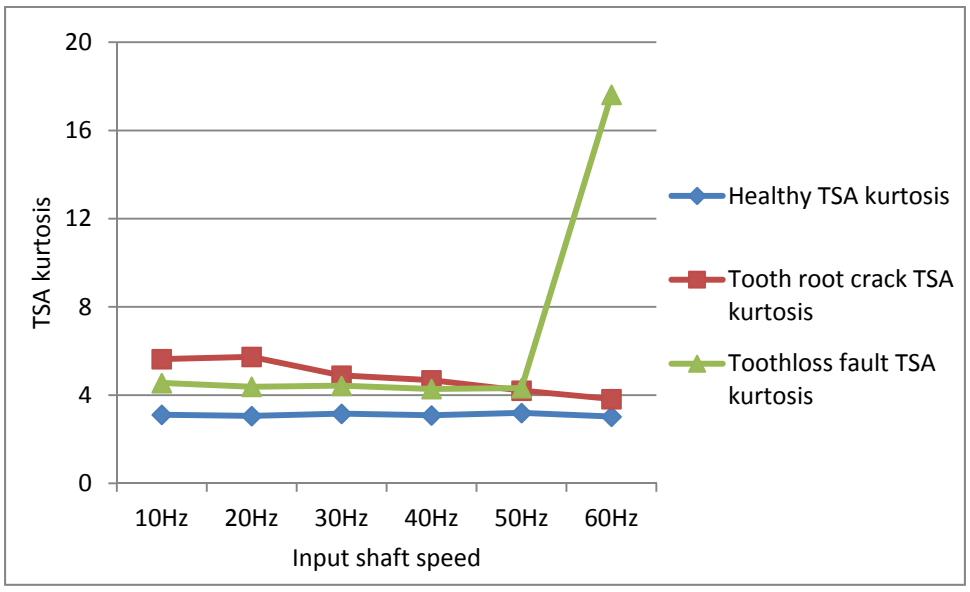


Figure 48. Kurtosis of the TSA signals

Kurtosis values of the three gear condition are given in Figure 48. It can be seen that kurtosis is more sensitive to tooth crack fault than tooth loss fault except at around 60 Hz shaft speed. By looking at the kurtosis, the tooth crack faults can be detected under all speed. Note that the kurtosis of the tooth crack fault is greater than the tooth loss fault. This result confirmed with the report that kurtosis based condition indicator was less sensitive to severe gear fault (Večeř *et al.*, 2005). However, the reason why the kurtosis increases suddenly at 60 Hz is not fully understood.

Besides, it can be seen that the TSA kurtosis values of the health data remain almost constant around 3. For any Gaussian distribution, the kurtosis is exactly calculated as 3. This concludes that the health gear TSA satisfied the Gaussian distribution. It means the amplitude of the AE impact waves generated by each tooth meshing complies with Gaussian distribution as expected. On the other hand, the TSA kurtosis of the faulty data is all above 3.6.

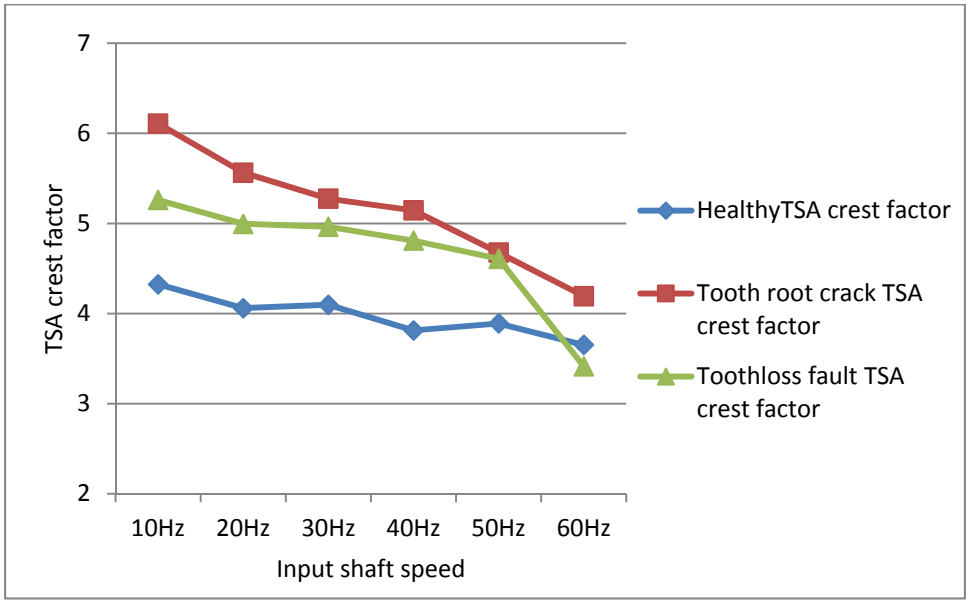


Figure 49. Crest factor of the TSA signals

Figure 49 shows the crest factor for all the three gear conditions. Crest factor can roughly detect the two gear faults with the shaft speed lower than 60 Hz. When the shaft speed reaches 60 Hz, the crest factor could not detect the tooth loss fault. Even though the differences of the crest factors between the healthy and faulty signals shown in Figure 49 are not as significant as those of kurtosis, the TSA crest factor still can be used as an supportive condition indicator for detecting the gear fault.

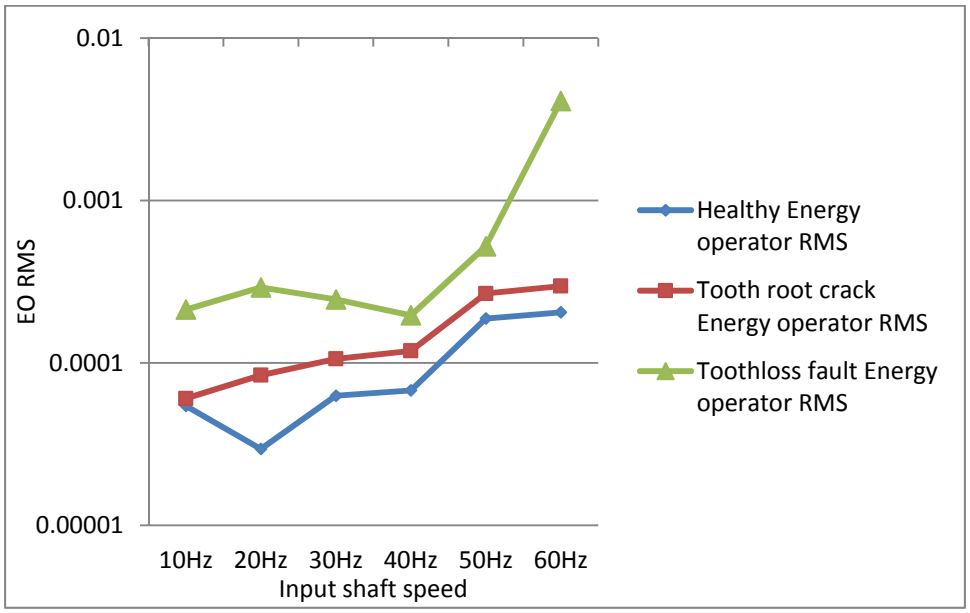


Figure 50. EO RMS of the TSA signals (*Y* axis: logarithmic scale)

From Figure 50, one can see that EO RMS is another condition indicator which can separate all the three gear conditions. EO RMS is more sensitive to tooth loss than tooth crack as shown in Figure 50.

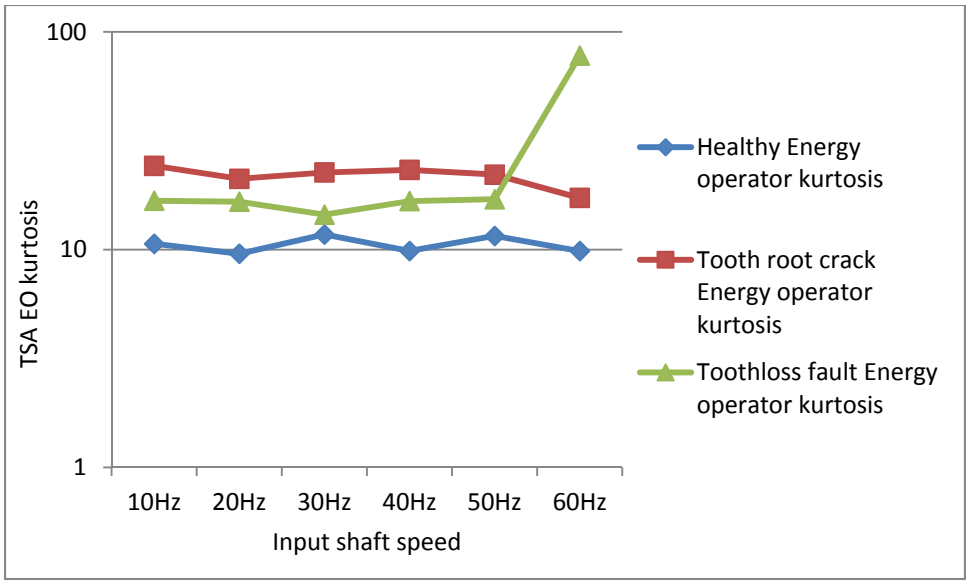


Figure 51. EO kurtosis of the TSA signals (*Y* axis: logarithmic scale)

From Figure 51, one can see that unlike the RMS, the kurtosis of the Teager's energy operator is not effective in separating the three gear conditions. However, it can separate the tooth crack fault and tooth cut from the healthy condition. Nonetheless, it works for fault detection purpose.

Based on the results, it can be seen that the TSA could be used as an effective AE signal processing technique to compute the condition indicators for gear fault detection. Among all TSA based AE condition indicators tested, RMS and P2P are more sensitive to tooth loss fault, while kurtosis is better for incipient fault detection such as root crack. Also, the TSA P2P and EO RMS can be used to separate the tooth crack fault from the tooth cut fault. The results prove that the condition indicators are sensitive to the fault as well as the fault level.

It was shown that the condition indicators on the raw AE data did not convey much useful information for fault detection. The SK filter and TSA greatly enhanced the fault features. Most of the condition indicators on the TSA could clearly separate the faulty condition signals and healthy signals: the TSA kurtosis and FM4 works the best in this tooth crack fault detection

experiment. Furthermore, the EO based condition indicators could successfully separate the faulty signals from the nominal gear, too. EO has significant improvement on the RMS condition indicator. In addition, EO increased the level of separation between healthy TSA kurtosis and faulty TSA kurtosis.

In summary, the condition indicator approach presented in Section 3.3.3 was validated using seeded gear tooth crack fault tests on a notational STG. Condition indicators, such as RMS, P2P, kurtosis, and crest factor are computed from the raw signals, TSA signals, and EO signals, separately. The results show that the condition indicators computed on the TSA signals and EO signals can effectively separate the faulty signals from the healthy signals. Among all the condition indicators tested, kurtosis related condition indicators, like TSA kurtosis, FM4, and EO kurtosis, have shown the best performance of detecting the gear tooth crack for all the testing conditions. TSA P2P and EO RMS can be used to separate the tooth crack fault from the tooth cut fault.

## 4.3 Conclusions

In this section, the test rig and DAQ systems were introduced. Experimental conditions were specified and presented. The methodology proposed in Section 3.3 were tested and validated by case studies.

Specifically, an intuitive waveform deformation method was first tested. The results show that the heterodyne demodulation technique could effectively demodulate the AE signals and shift down the frequency. From narrow band filtered TSA, a discontinuity associated with fault tooth meshing can be observed, which indicates the presence of the fault. However, the fault detection is made by visual inspection which makes it hard to automatically detect fault and trigger fault alarms. Additionally, the fault detection rate is relatively low for practical purposes.

Then, a condition indicator based method using SK and an optimal band pass filter was validated to test the tooth cut fault. It can be seen that by using SK, the fault feature can be extracted from the heterodyned signals. The proposed AE condition indicators, such as RMS, P2P, kurtosis, FM4, and NA4 were tested for tooth crack detection. As shown in the results, using kurtosis and FM4, all of the faults signals can be separated from the healthy signals and a 100% detection rate is achieved. Thus, it can be concluded that the condition indicator based method is more effective for gear fault detection. Moreover, based on the comparison results of tooth crack, 100% tooth cut, and healthy gears, it can be seen that the condition indicators, such as P2P and EO RMS, are also sensitive to severity of the tooth damage.

# CHAPTER 5

# COMPARATIVE STUDY ON GEAR FAULT LEVEL DIAGNOSTICS USING VIBRATION AND AE SIGNALS

In Section 4, it has been shown that AE signal could be sampled at 100 kHz and remains effective for fault diagnosis. However, it is questionable if an AE based technique would give a better or at least the same performance as the vibration analysis based techniques using the same sampling rate. To answer the question, this section presents a comparative study for gearbox tooth damage level diagnosis using AE and vibration measurements, the first known attempt to compare the gearbox fault diagnostic performance of AE and vibration analysis based approaches using the same sampling rate. Partial tooth cut faults are seeded in a gearbox test rig and experimentally tested.

## 5.1 Experiment Setup

In order to compare the gearbox fault diagnostic performance of the AE and vibration sensors, tests with gear tooth cut seeded faults were conducted on a STG. Different tooth cut level was created to test the sensitivity of AE and vibration sensor to tooth damage level. Specifically, 25%, 50%, 100% tooth cut gears and healthy gear were tested, as shown in Figure 52.


Figure 52. Seeded tooth cut faults

In order to understand the actual influence of the varying tooth conditions on the gear meshing activity, it is important to take a brief look at the gear profile before and after the tooth cut. The schematic of two gears meshing is shown in Figure 53.

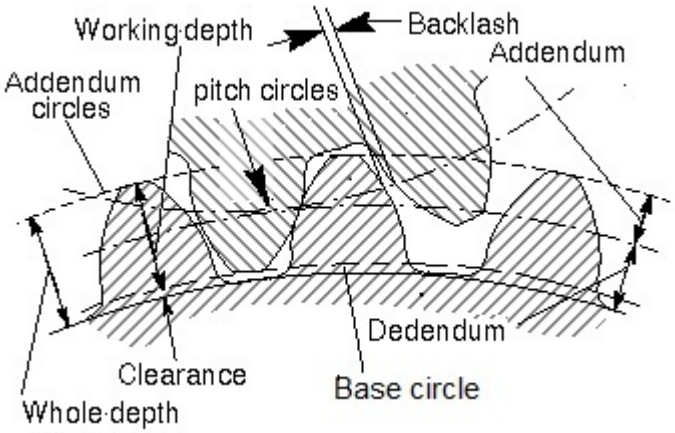


Figure 53. Schematic diagram of two gears meshing

The terminologies shown in Figure 53 are defined as follows:

1) Pitch circle: The circle through the pitch point having its center at the axis of the gear. The pitch circle of a gear is an imaginary circle which passes through the point where the teeth touch when one gear meshes with another.
2) Base circle: The circle from which an involute tooth curve is generated or developed.
3) Addendum: The radial distance between the pitch circle and the outside diameter or the height of the tooth above the pitch.
4) Dedendum: The radial distance from the pitch circle to the bottom of the tooth space.

Contact ratio is defined as the number of angular pitches through which a tooth surface rotates from the beginning to the end of contact. In a simple way, it can be defined as a measure of the average number of pairs of teeth in contact during the period in which a tooth comes and goes out of contact with the mating gear. It can be calculated as:

$$Contact\ ratio = \frac{\sqrt{r_{a1}^2 - r_{b1}^2} + \sqrt{r_{a2}^2 - r_{b2}^2} - Csin\emptyset}{P_c cos\emptyset} \tag{29}$$

where, $r_{a1}$ and $r_{b1}$ are addendum radius (distance from the tops of the teeth of a gear to the gear center) and base radius (distance from the base circle to the gear center) for the pinion gear center, and $r_{a2}$ and $r_{b2}$ are addendum radius and base radius from the pairing gear center, respectively; C is the gear axis center distance; $\emptyset$ is the angel of the pressure line; $P_c$ is the circular pitch of the pinion gear. Circular pitch is length of the arc of the pitch circle between the centers or other corresponding points of adjacent teeth. For more detail of the concept and calculation, refer to (Budynas and Nisbett, 2011).

From Eq. (29), it can be inferred that as the tooth cut gets deeper, the term $r_{a1}^2 - r_{b1}^2$ keeps decreasing until it becomes 0 when the tooth cut reaches the base circle. In this experiment study, we can draw the conclusion that due to the tooth cut, the local contact ratio of the gear keeps decreasing in the order of healthy, 25%, 50% and 100%. As the contact ratio decreases, the amount of meshing looseness increased, which is expected to generate large gear noise.

Based on the diametral pitch system, addendum $a$ and dedendum $b$ can be calculated as:

$$a = \frac{1}{P_d} \tag{30}$$

$$b = \frac{1.157}{P_d} \tag{31}$$

where, $P_d$ is the diameter pitch; $a$ is the addendum and $b$ is the dedendum as shown in Figure 54.

From Eq. (30) and Eq. (31), it is clear to see that in the case of 50% tooth cut, the depth of tooth cut would be greater than the addendum depth. In other words, the remaining tooth depth is somewhere between the pitch circle to base circle. For a gear with a 50% tooth cut, when the gear mates with another, the tooth would lose the initial contact point until the point on the pitch circle and a little over, which will cause a larger backlash than normal condition. But the remaining tooth is still above the base circle, which would make the tooth able to provide support in the next mating cycle. Based the above analysis, it can be inferred that the gear with 50% tooth cut will have a larger contact ratio and smaller backlash compared to 100% tooth cut. Similarly, 50% tooth cut will have a larger backlash and smaller contact ratio compared with 25% tooth cut. For a comparison between a gear with 25% tooth cut and a healthy gear, the 25% tooth cut gear will have smaller contact ratio because it loses the tooth tip which is essential for contact ratio. Thus, one would expect that a 25% tooth cut gear will have larger backlash than healthy gear.

In summary, it is shown that the contact ratio decreases in the order of healthy, 25% tooth cut, 50% tooth cut, and 100% tooth cut. An increasing backlash is also likely to be associated, at least presented in 25%, 50% and 100% tooth cut. For the interest of backlash analysis, more details can be found in (Sarkar *et al*., 1997).

One AE sensor and two accelerometers were mounted on the gearbox. The AE sensor was attached to the gear housing using adhesives as shown in Figure 15. One accelerometer was mounted on the gearbox housing in the axial direction and the other one was mounted on top of gearbox housing in the radial direction (see Figure 15). The signals from all of the three sensors were collected simultaneously during the test runs. In addition, tachometer signals were collected along with vibration and AE signals.

Next, the diagnostic results of the gear seeded cut fault tests using both AE and vibration sensors are provided and discussed. Comparison will be made between AE and vibration.

## 5.2 Results of AE signal analysis

After heterodyning, TSA was performed on the signals first to get the TSA signals using tachometer signal as the phase reference. Then the AE signal condition indicators were calculated on the TSA signals. Three condition indicators as introduced in Section 3.3.3, were computed using the AE TSA signals: RMS, P2P and kurtosis. In addition, RMS values of the residual signals were also computed for comparison.

Note that within each speed, the data sets are not correlated. Hence, point by point comparison may not justify the overall detection ability. In order to evaluate the diagnostic ability of the proposed methods, every 5 data sets collected at each speed are further averaged to give a clearer result.

Figure 54 shows the RMS plot of AE TSA signals. The data set numbers were arranged from 10 Hz – 60 Hz. The value at each speed is averaged over 5 data sets. Other plots in the following context are arranged in the same manner. It can be seen from Figure 54 that the RMS provided a good trend for the energy level when speed increase. For different level of tooth cut, it offers clear separation. This indicators that AE signal are sensitive to the gear meshing impact due to both speed and level of severity of tooth fault.

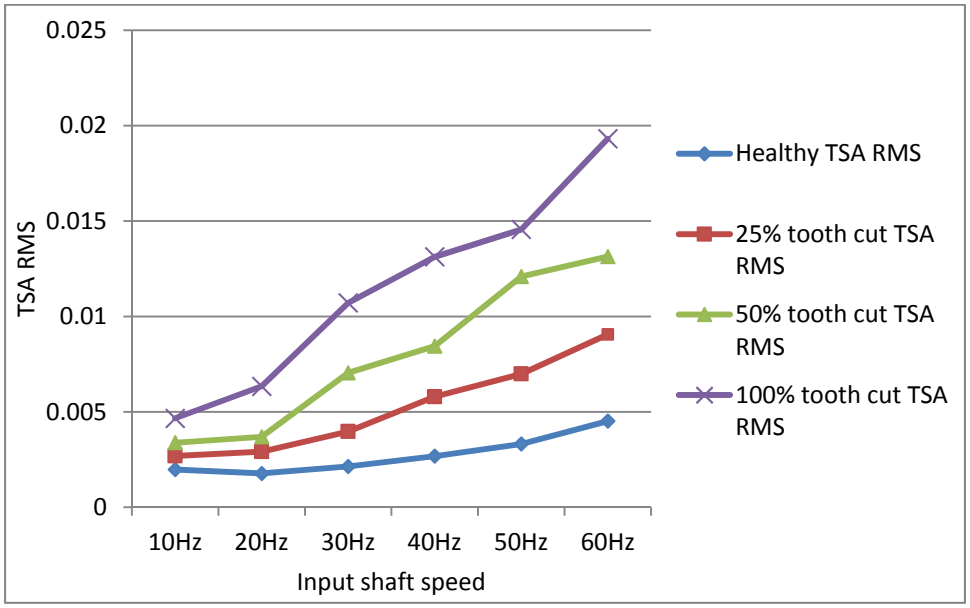


Figure 54. RMS of AE TSA signals

Figure 55 shows the plot for residual RMS of AE TSA signals. Residual RMS provides similar separation as the TSA RMS but reduces the degree of fluctuation. It also increases the fault detectability between healthy and 25% tooth cut case since the separation between the two is

clearer. As residual signals normally contain the fault features except gear meshing and harmonics, it could be more effective than the TSA signal itself.

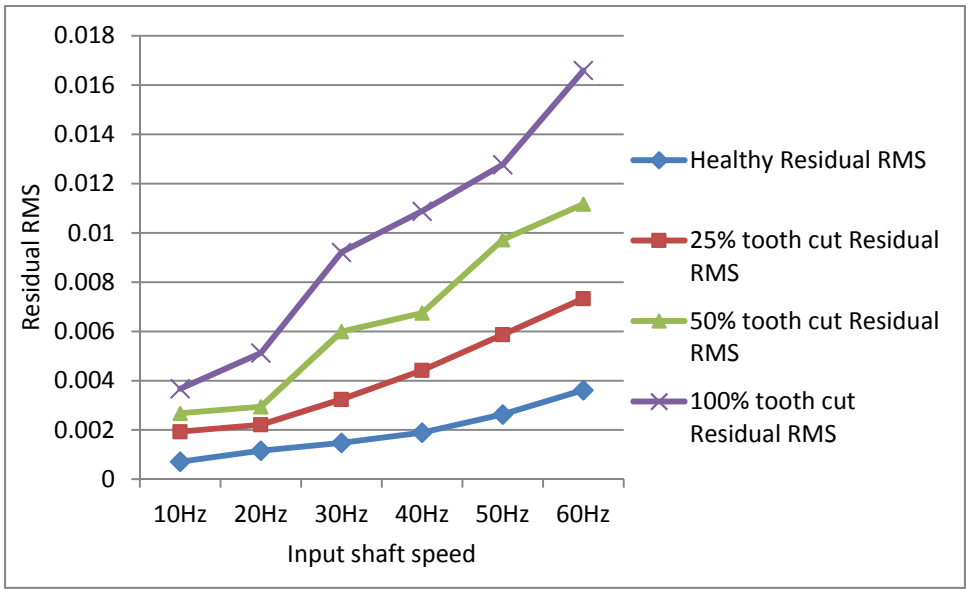


Figure 55. RMS of AE TSA residual signals

Figure 56 shows the plot for P2P of AE TSA signals. As can be seen from here, P2P generally follows the trends, but it contains some more fluctuation for 50% tooth cut compared with RMS.

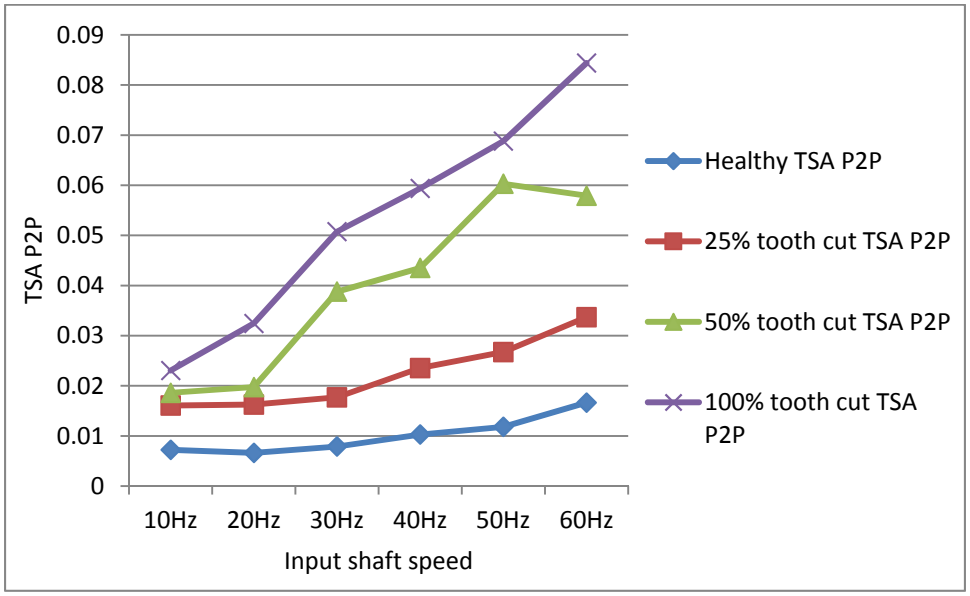


Figure 56. P2P of AE TSA signals

Figure 57 shows the plot for kurtosis of AE TSA signals. Although kurtosis is not able to distinguish fault levels, it acts as a good condition indicator for fault detection. Kurtosis measures the peakiness of the signals. It is a non-quantitative parameter, which means it is independent of the magnitude of the signal. For any Gaussian distribution, the value of kurtosis is calculated as 3. Since kurtosis is not affected by the speed, it is useful for making fault detection decisions.

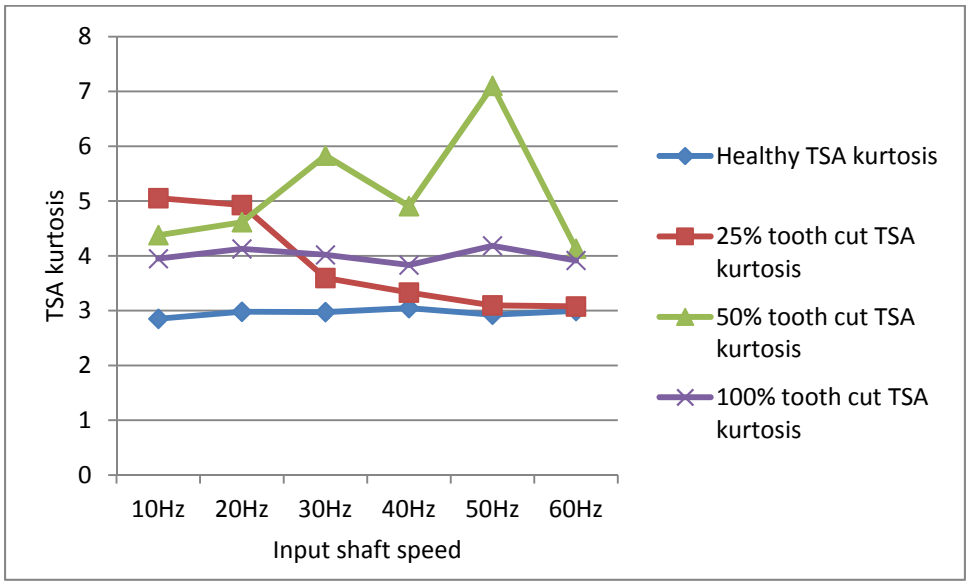


Figure 57. Kurtosis of AE TSA signals

## 5.3 Results of Vibration Signal Analysis

Vibration sensors, typically accelerometers, measure the velocity, which is the second derivation of displacement. The frequency response range of vibration signals is much lower than that of AE signals. Therefore a vibration signal has the advantage of representing the mechanically behaviors more closely. But it also has the disadvantage of being easily effected by mechanical resonance. Similar to AE signal processing, TSA was performed on raw vibration signals first, then the condition indicators were computed. A total of 4 condition indicators: RMS, P2P, FM0 and SLF were computed for vibration signals. FM0 and SLF will be introduced in the following.

**FM0**: FM0 is the zero-order figure of merit. It is a global indicator that will react to changes in the whole frequency range of the average and identifies major abnormal behaviors with regard to meshing pattern. FM0 is defined as the ratio of peak to peak amplitude (PPA) of the TSA signal to the sum of amplitudes of gear mesh frequency and its harmonics. An increase in peak to peak level is generally observed in case of major tooth faults, such as tooth breakage without significant change in the mesh frequency, which will results in increase of FM0 value (Nooli P. K., 2011). FM0 will increase if a periodic signal contains a local increase in amplitude. Mathematically, it is expressed as following:

$$FM0 = \frac{P2P_{TSA}}{\sum_{i=1}^{n} A(f_i)} \tag{32}$$

where, *FM0* is the zero-order figure of merit; $P2P_{TSA}$ is the peak to peak value of the vibration signal of TSA in the time domain; $A(f_i)$ is the amplitude of the ith harmonic of the gear meshing frequency.

**SLF**: SLF stands for the sideband level factor. It is the sum of the first order sideband amplitudes of the fundamental gear meshing frequency normalized by the RMS of the synchronous time average (Antolick L. J. *et al*., 2010). SLF is a good indicator of single tooth damage or gear shaft damage. The formula for SLF calculated is given as,

$$SLF = \frac{R_{I,-1}(x) + R_{I,+1}(x)}{RMS(x)} \tag{33}$$

where, $x$ is the vibration signal TSA, $R_{I,-1}(x)$ is the amplitude of the first order left-hand side sideband, $R_{I,+1}(x)$ is the amplitude of first order of right-hand side sideband. $RMS(x)$ is the RMS of $x$.

During the experiments, both axial and radial direction vibration signals were collected and analyzed. Figure 58 to Figure 62 show the results from the axial direction vibration sensor. Figure 63 to Figure 65 give the results from the radial vibration.

Figure 58 shows the RMS plots of the vibration TSA signals. It can be seen that in the low speed range below 30 Hz, the vibration RMS does not give any indication of the fault. In the high speed range above 30 Hz, vibration RMS with tooth faults increases significantly and provides good indication for fault detection. However, vibration RMS is not sensitivity to the level of tooth cut as the vibration RMS for 100% cut is lower than that of 50% and 25% tooth cut.

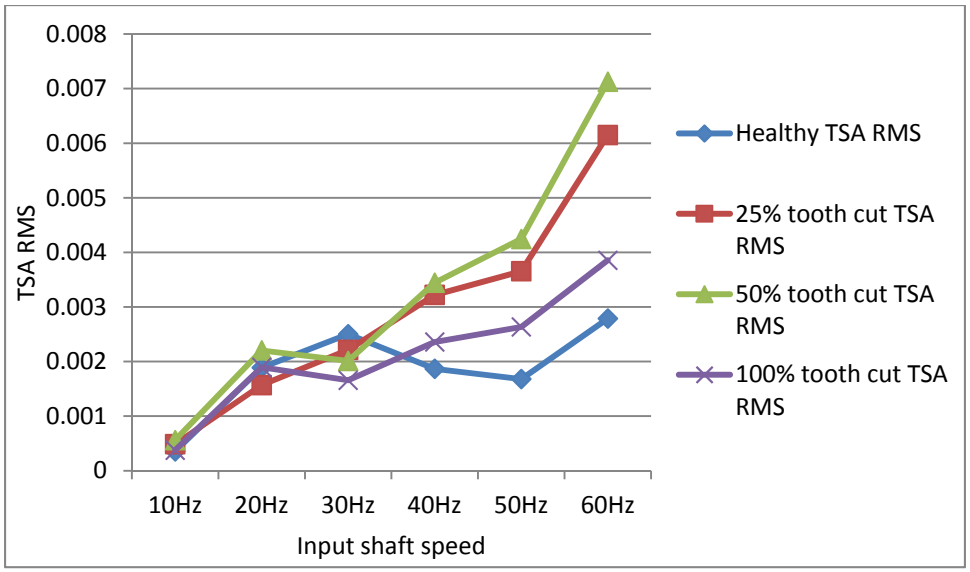

Figure 58. RMS of axial vibration TSA signals

Figure 59 gives the P2P plots of vibration TSA. P2P values of the faulty signals are mostly higher than the healthy counterpart except at 10 Hz input shaft speed. Similar to RMS, P2P shows potential capability for fault detection but not for fault level diagnostics.

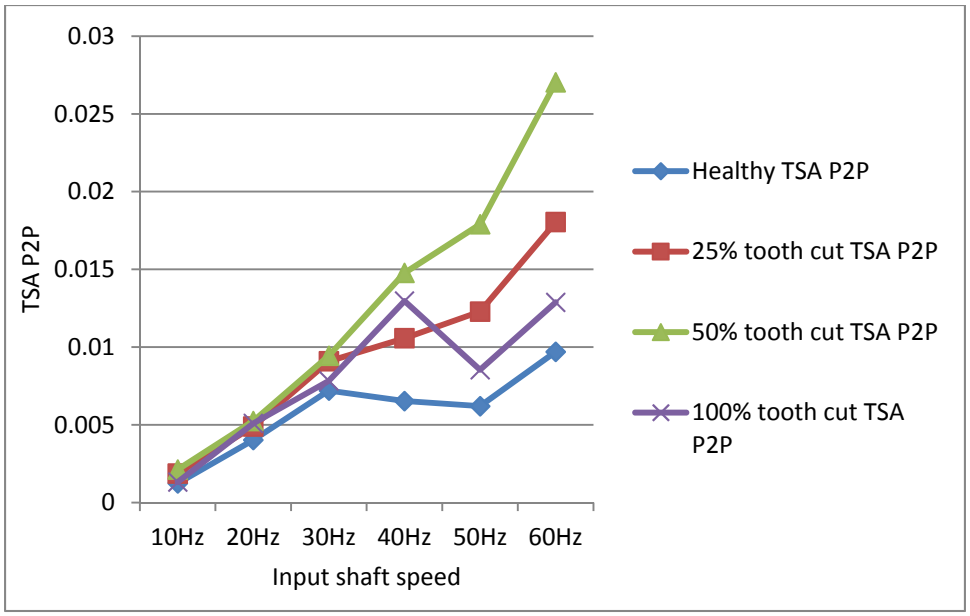


Figure 59. P2P of the axial vibration TSA signals

Figure 60 shows the FM0 of the axial vibration signals. FM0 could detect the anomalies in most of the cases. However, it has a lot of fluctuation at different speeds. Again it is not effective for damage level separation.

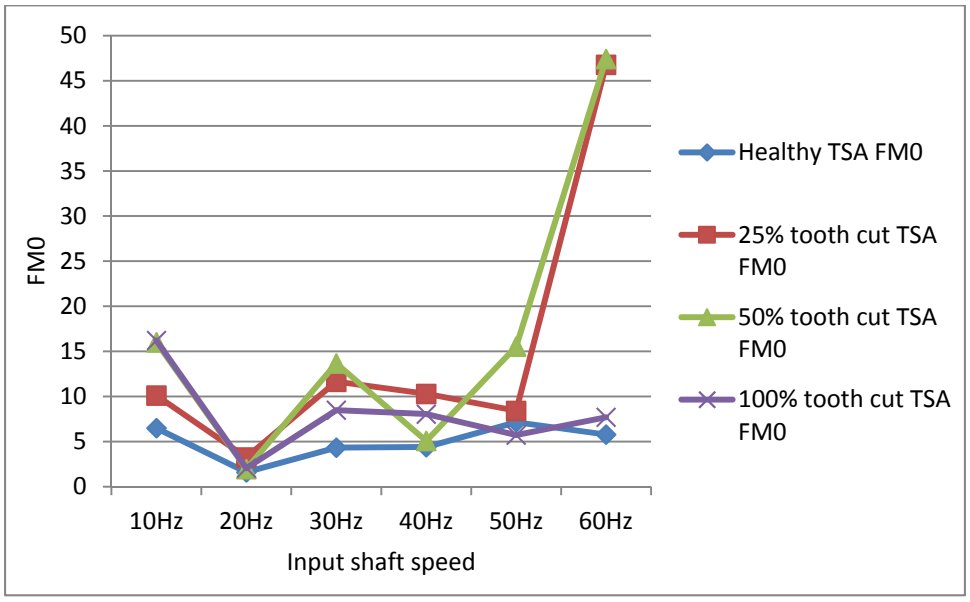


Figure 60. FM0 of the axial vibration TSA signals

Figure 61 shows the condition indicator SLF plots of the axial sensors. It can be seen that at 10 Hz, 30 Hz, and 60 Hz, the healthy SLF are all lower than faulty ones. But for the other speeds, some of the faulty signals SLFs are lower than healthy. This result shows that SLF of axial vibration is not effective for fault detection.

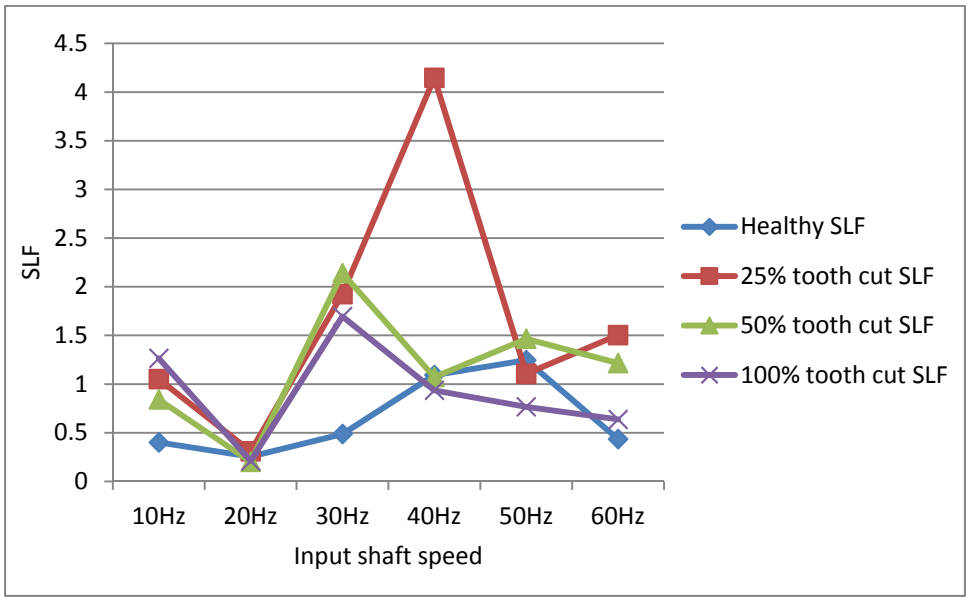


Figure 61. SLF of axial vibration TSA signals

Figure 62 shows the RMS plots of the radial vibration TSA signals. It can be seen from the plot that the radial vibration signal are seriously affected by the mechanical resonance, especially at 30 Hz. Basically, the RMS of radial vibration does not give a good indication for gear tooth cut fault and the level of the cut.

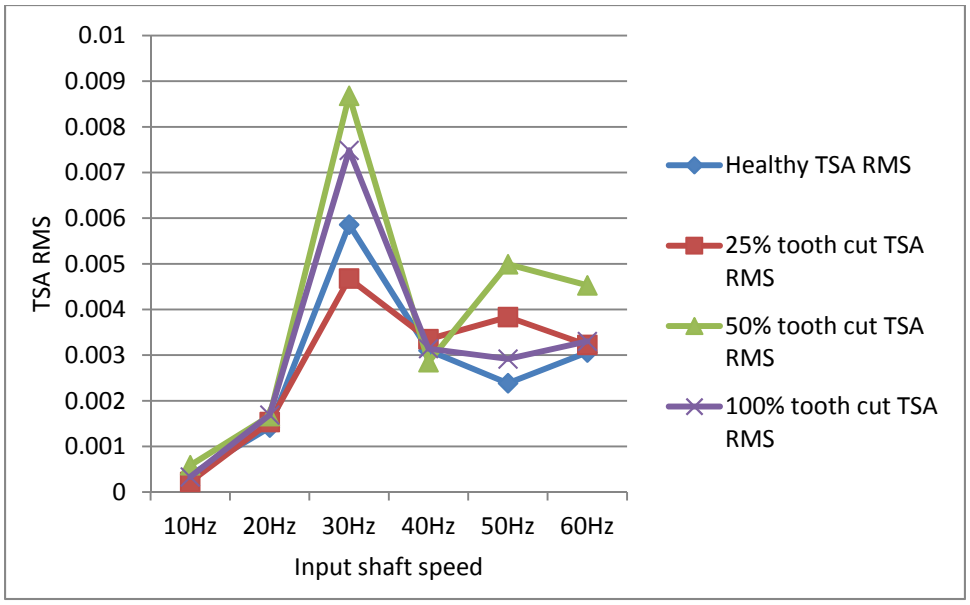


Figure 62. RMS of radial vibration TSA signals

Similarly, the P2P of the radial vibration does not give a good indication neither, as shown in Figure 63.

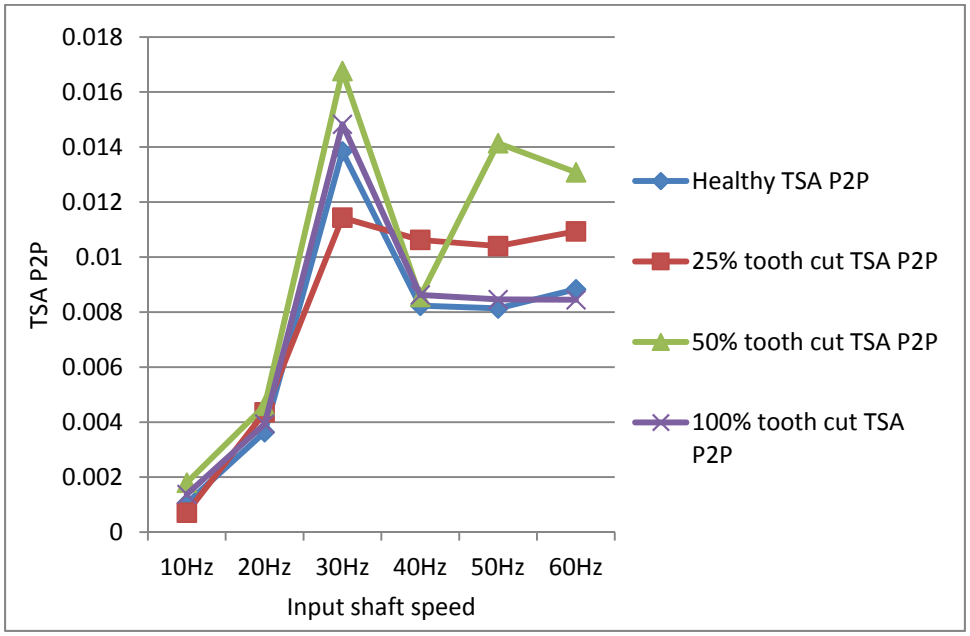


Figure 63. P2P of radial vibration TSA signals

Figure 64 shows the condition indicator FM0 of the radial vibration sensors. It can be see that except at 20 Hz and 30 Hz, the FM0 of the faulty signals are all higher than the healthy ones. At 30 Hz, FM0 for all cases dropped to a low level and overlapped each other. At the same time, RMS and P2P from Figure 62 and Figure 63 show that the peaks and energy levels for all cases increased significantly. It is highly likely to be caused by mechanical resonance. Other than that, the healthy FM0 is relatively stable with the bound of approximately 10, while the faulty signals can go as high as 40, which makes FM0 a good condition indicator for tooth cut fault detection purpose.

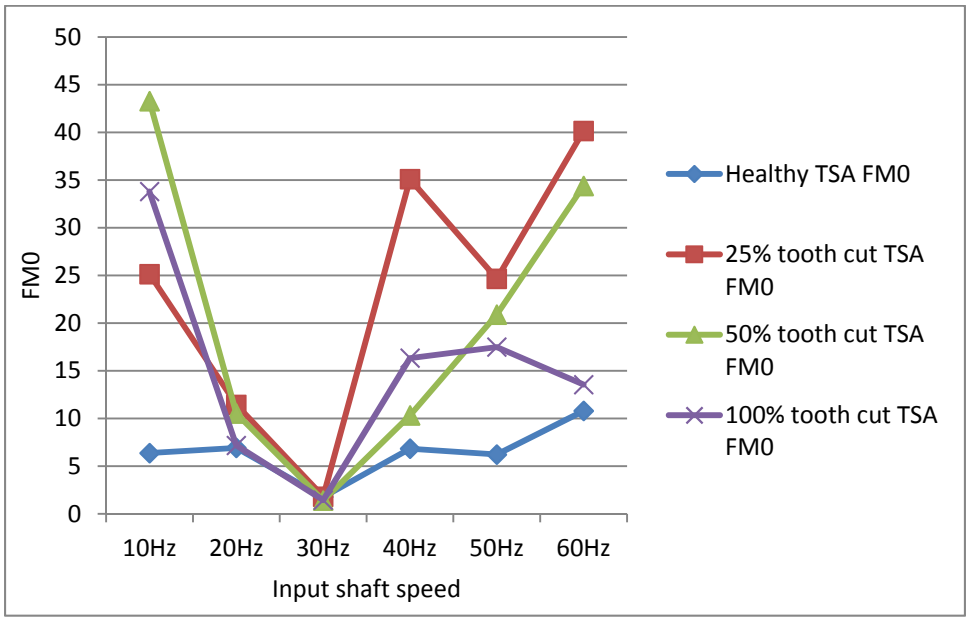


Figure 64. FM0 of radial vibration TSA signals

Figure 65 shows the condition indicator of SLF. SLF works similarly as FM0, it could separate the healthy signals from the faulty one clearly in the low speed at 10 Hz as well as high speed 30 Hz and above. But it fails to distinguish the fault at 20 Hz and 30 Hz.

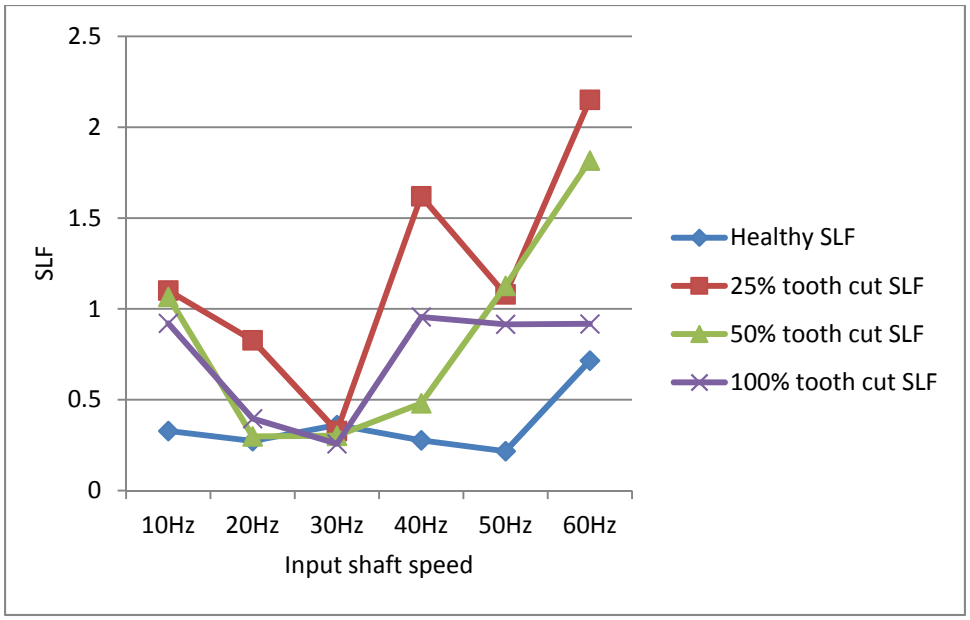


Figure 65. SLF of vibration TSA signals

In summary, it can be seen that for axial vibration sensor mounted on the bearing house, the RMS and P2P show good fault detection potential. FM0 and SLF of the axial sensor work in most cases but not stable. On the other side, for the radial sensor mounted on the top of the gearbox, RMS and P2P fail to work, while FM0 and SLF work for fault detection purpose. Compared with AE results, none of the vibration condition indicators could detect the tooth cut level. The vibration signals are highly affected by background noise or mechanical resonance, making it unstable in performance. AE RMS and P2P show a roughly linear relationship against shaft speed. They could clearly indicate the tooth cut levels for diagnostics. Also, kurtosis of AE signals offers another effective index for fault detection.

It is also needed to point out that vibration signals offer better frequency domain resolution as both FM0 and SLF are calculated based on gear meshing frequency. AE offers better time domain features related to energy levels, such as RMS and P2P.

As explained in Section 5.1, the tooth cut fault is the direct cause of larger backlash and reduction in contact ratio. Both the large backlash and low contract ratio introduce more looseness during gear meshing and therefore cause higher impact and gear noise. From this perspective, it can be inferred that AE sensors are much more sensitive to impact energy. Vibration measured by accelerometer is the velocity signal, which is less sensitive to direct impact energy.

## 5.4 Conclusions

Previous results have shown that AE sensor based approach using a sampling rate that was comparable to that of vibration analysis gave good gear fault diagnostic results. However, it is questionable if an AE based technique would give a better or at least the same performance as the vibration analysis based techniques using the same sampling rate. To answer the question, this section presented a comparative study for gearbox tooth damage level diagnostics using AE and vibration measurements. Three different levels of tooth cut fault were artificially seeded and tested on a notational STG. For AE based gear fault diagnostic approach, the proposed heterodyne technique was used before AE data collection. Both the AE signals and vibration signals were collected with the same sampling rate of 100 kHz. TSA was applied to both types of signals. Condition indicators were then calculated respectively for AE and vibration signals. Experimental results were provided and explained. Based on the experimental results, several conclusions can be drawn:

1) AE condition indicators, such as RMS, residual RMS, P2P, and kurtosis are effective to detect tooth cut faults. Also, RMS and P2P are sensitive to tooth damage levels.
2) Vibration condition indicators, such as P2P, FM0 and SLF are effective for tooth cut damage detection. However, all of the vibration condition indicators cannot distinguish the tooth damage levels.

3) AE condition indicators, such as RMS and P2P are approximately proportion to the shaft speed despite of the presence of fault or not. The experimental study validated that AE condition indicators are less sensitive to mechanical resonance, while vibration condition indicators are seriously affected by mechanical resonance. Therefore, AE condition indicators have more stable performance for gear damage level diagnosis.

# CHAPTER 6
# INVESTIGATION OF LOW SAMPLING RATE AE ANALYSIS

In Section 5, a sampling rate of 100 kHz was chosen to sample AE signals. This sampling rate is still considered higher than normal vibration sampling rate. In order to evaluate that whether the AE sampling rate could be further reduced for effective fault diagnosis and still maintain acceptable performance compared with vibration signals, this section further investigate the performance of AE analysis under an even lower sampling rate. A comparative study using AE and vibration measurements under a low sampling rate for the same case study as in Section 5 was presented. The tested gear conditions and processing methods remained the same. A sampling rate of 20 kHz, which is the typical sampling rate in industry for vibration data collection, is chosen to evaluate the AE based diagnosis technique. The performance of the AE based analysis is compared again with vibration based analysis at 20 kHz sampling rate. The results will be shown in the following sections.

## 6.1 Results of AE analysis

After heterodyning, TSA was performed on the AE signals first to get the TSA signals using tachometer signal as the phase reference. Then the AE signal condition indicators were calculated on the TSA signals. Three condition indicators as introduced above are tested on the AE TSA signals, i.e., RMS, P2P, and kurtosis.

Figure 66 shows the average results of RMS comparison at each speed. It can be seen that the RMS provided a good trend for the energy level when speed increase. For different level of tooth cut, the RMS could roughly separate from each other. This indicates that AE signals are sensitive to the gear meshing impact due to both speed and severity level of the tooth fault. More

importantly, the separation between the faulty signals and the healthy ones is clear. A carefully chosen threshold could easily indicate the presence of a fault.

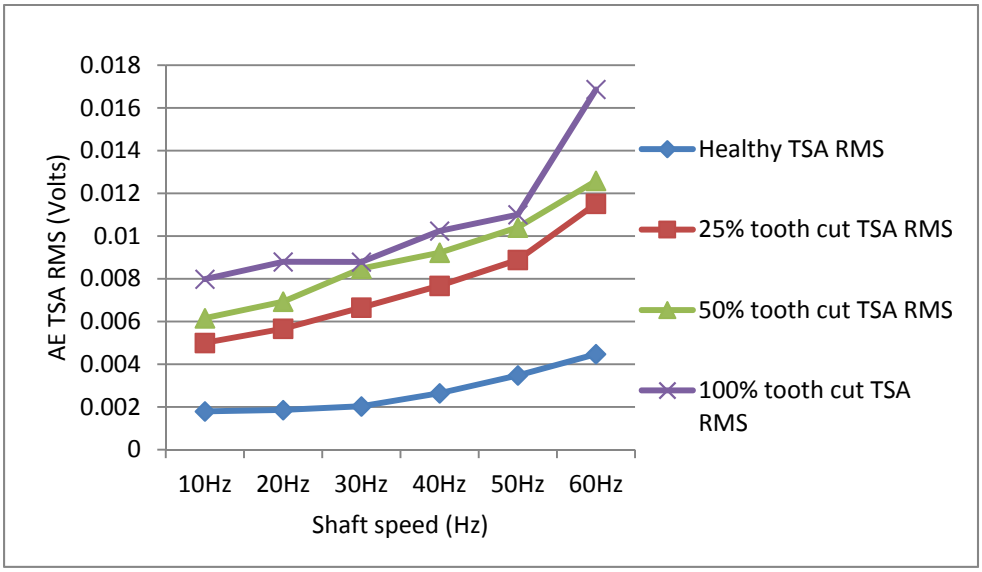


Figure 66. RMS average of AE TSA signals

Figure 67 shows the P2P plots of AE TSA signals. As can be seen from here, P2P generally shows a trend as the speed increases, but contains some fluctuation compared with RMS. Nonetheless, P2P also gives a good separation for different levels of the tooth damage.

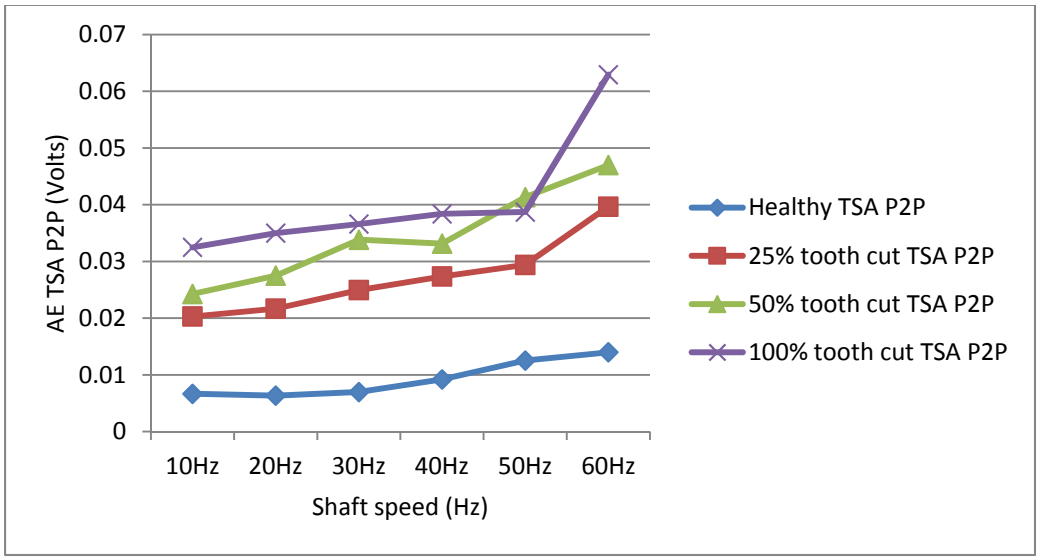


Figure 67. P2P average of AE TSA signals

Figure 68 shows the kurtosis plots of the AE TSA signals. Although kurtosis cannot reliably distinguish the fault levels, it acts as a good condition indicator for fault detection. Kurtosis measures the peakiness of the signals. It is a non-quantitative parameter, which means it is independent of the magnitude of the signal. For any Gaussian distribution, the value of kurtosis is calculated as 3. As one can see from Figure 69, the kurtosis of the healthy signals is close to 3. When a tooth fault is presented, the value will increase. In addition, kurtosis is not affected largely by speed. Therefore it is useful for making fault detection decisions under varying speed condition.

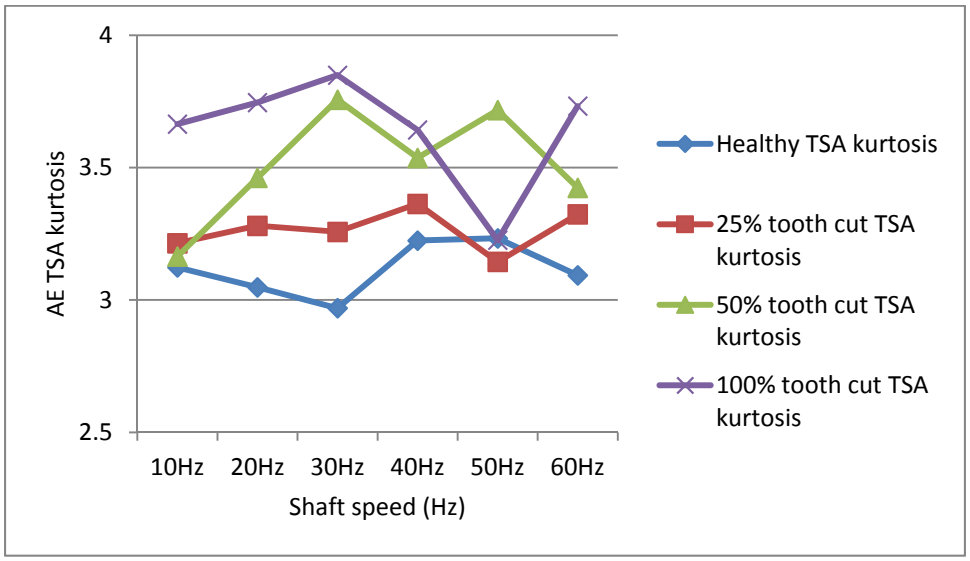


Figure 68. Kurtosis average of AE TSA signals

## 6.2 Results of vibration analysis

Vibration sensors, typically accelerometers, measure the velocity signals, which is the second derivation of displacement. The frequency response range of vibration signals is much lower than that of AE sensors. So vibration, in a sense, has the advantage of representing the mechanical behaviors more closely. However, it also has the disadvantage of being easily effected by mechanical resonance. Similar to processing of the AE signals, TSA was performed

on raw vibration signals first, and then the condition indicators were computed. P2P, kurtosis and FM0 are investigated for vibration signals.

During the seeded fault tests, both axial and radial direction vibration signals were collected and analyzed. Figure 69 to Figure 74 provide the results from the axial direction vibration sensor. Figure 75 and Figure 76 give the results from the radial vibration sensor.

In order to make a comparison with the AE results, condition indicators were first calculated on the vibration TSA signals. Since RMS generally does not work for vibration signal in the case of single tooth damage, it is not shown here.

Figure 69 shows the P2P plots of the TSA for the axial direction vibration sensor. The healthy TSA overlap with P2P of 100% tooth cut TSA. Also, the healthy TSA P2P is above that of 25% tooth cut. In order to get a better result, the residual signal was taken from the TSA signals to remove the low frequency background machine noises and the meshing components. The TSA residual P2P plots of the axial direction vibration sensor are shown in Figure 70.

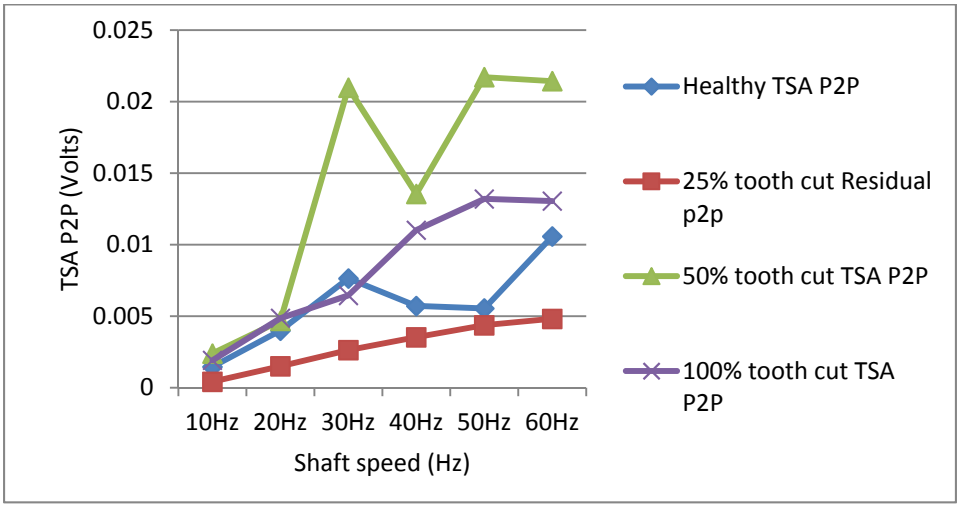


Figure 69. P2P average of axial vibration sensor

In comparison with the results shown in Figure 69, taking the TAS residuals significantly removed the noise and improved the fault detectability from the healthy signals, see Figure 70. It can be seen that in the low speed range, below 30 Hz input shaft speed, the vibration residual P2P has some overlap with 25% tooth cut. In the high speed range, the vibration residual P2P with tooth faults increases significantly and can be used for fault detection purpose for all damage levels. However, vibration residual P2P is not sensitivity to the level of tooth cut as the level of 50% tooth cut is higher than that of 100% tooth cut.

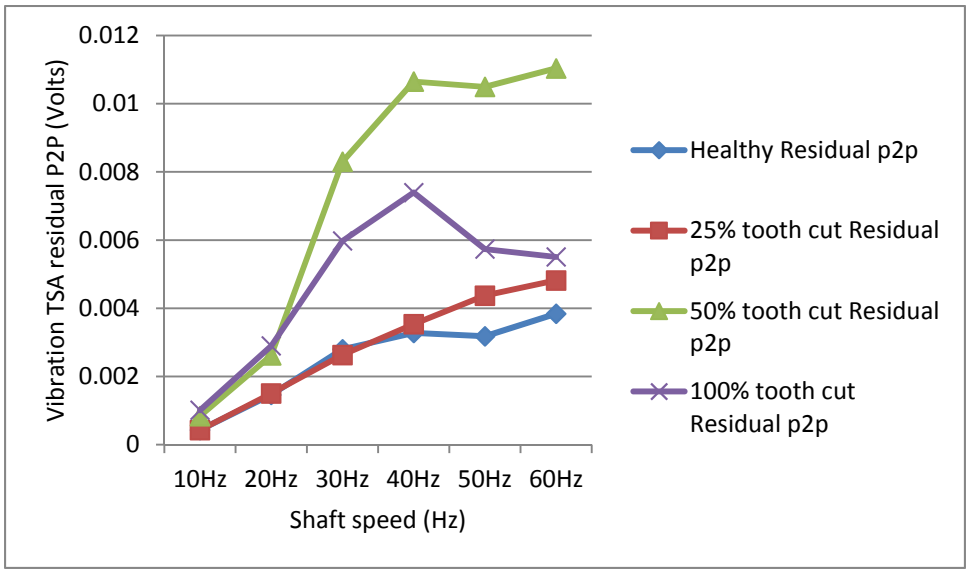


Figure 70. Residual P2P average of axial vibration sensor

Similar with P2P, taking the residual of the vibration TSA would improve the fault detection using kurtosis condition indicator. Figure 71 and Figure 72 show the kurtosis of the TSA and TSA residuals, respectively. From Figure 71, it can be seen that TSA kurtosis does not work for fault detection.

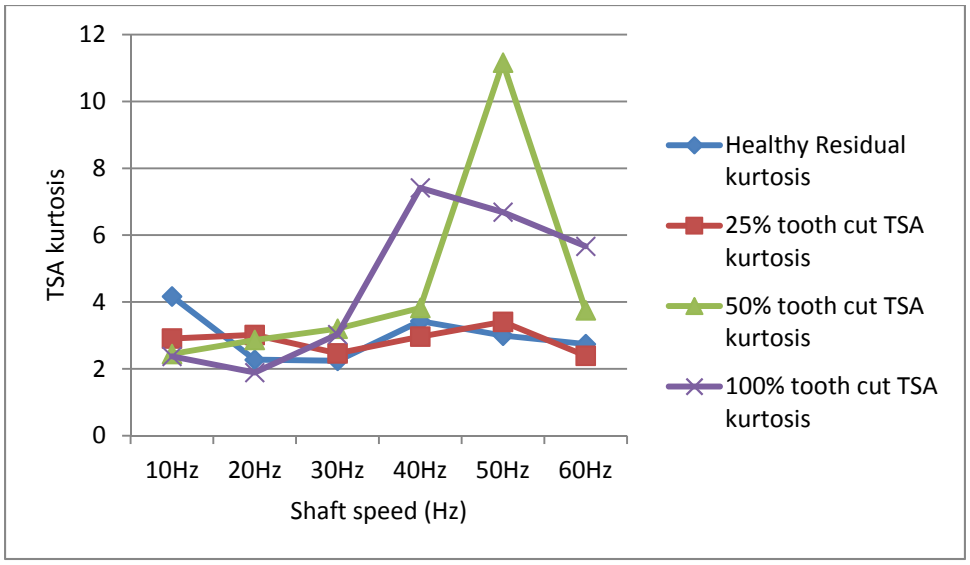


Figure 71. Kurtosis average of the axial vibration sensor

Figure 72 gives the kurtosis plots of the TSA residual signals. Compared with direct TSA kurtosis, it gives better separation between the healthy ones and faulty ones. Kurtosis values of 50% and 100% tooth cut are mostly higher than the healthy counterpart. However, the 25% tooth cut kurtosis is lower than healthy ones which make it unable to detect the 25% tooth fault. Also, vibration kurtosis is not effective for level differentiation.

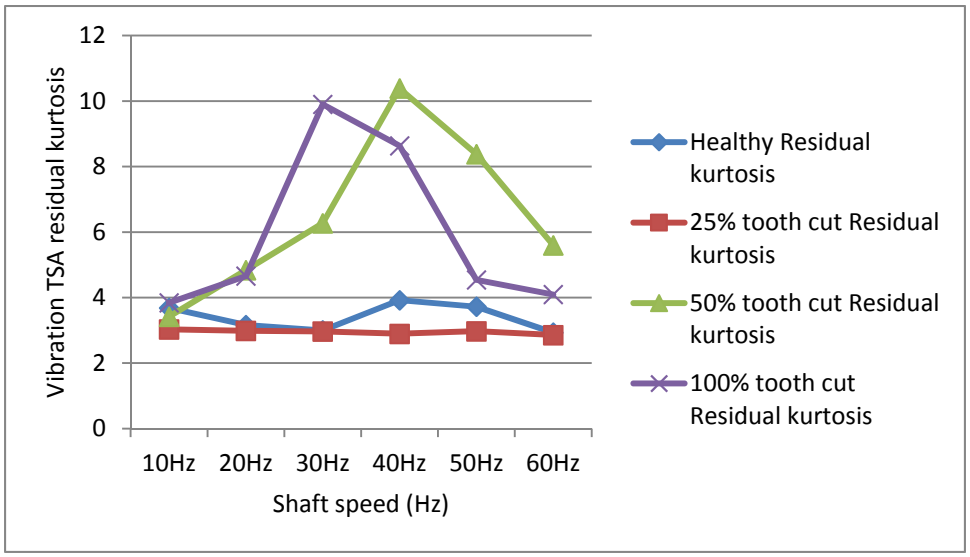


Figure 72. Residual kurtosis average of axial vibration sensor

In order to investigate other condition indicators, P2P and kurtosis were also computed on the EO signals. Figure 73 shows the P2P of the TSA EO signals from axial direction vibration sensors. Similar with the P2P of the residual signals, it works in high speed cases for fault detection purpose but not in the low speed cases.

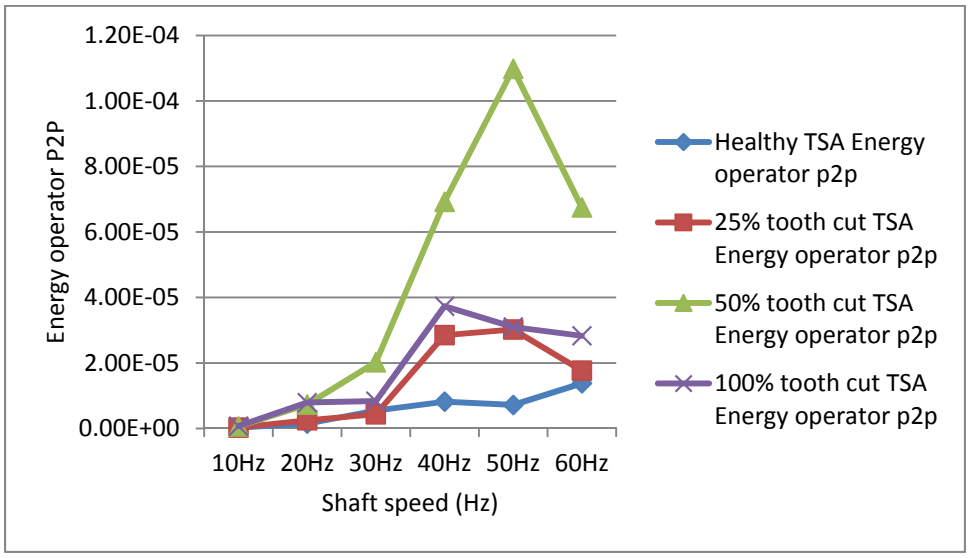


Figure 73. EO P2P average of axial vibration sensor

Figure 74 shows the kurtosis plots of the TSA EO signals of axial direction sensor. It can be seen that healthy signal EO kurtosis overlap that of 25% tooth cut making the 25% tooth fault undetectable. For 50% and 100% tooth cut, it mostly works.

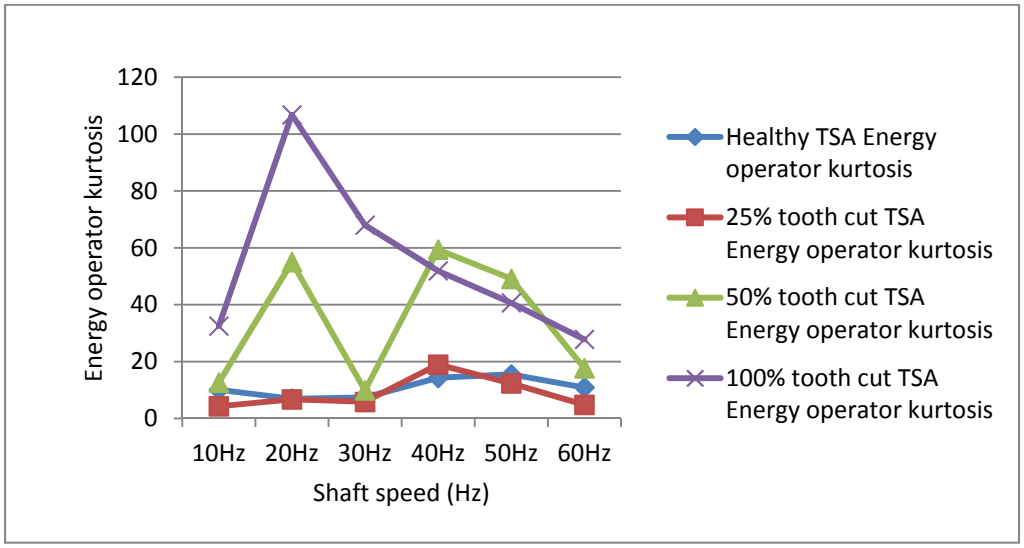


Figure 74. EO kurtosis average of axial vibration sensor

The results shown above are based on the axial direction vibration sensor. Figure 75 shows the P2P of the radial direction vibration TSA signals. It can be seen from the plots that the radial vibration signal are affected by the mechanical resonance. The P2P trends are inconsistent with speed increasing. Basically, the healthy P2P of radial vibration overlap the faulty ones, especially with 25% tooth cut. It is not reliable for fault detection and damage level separation.

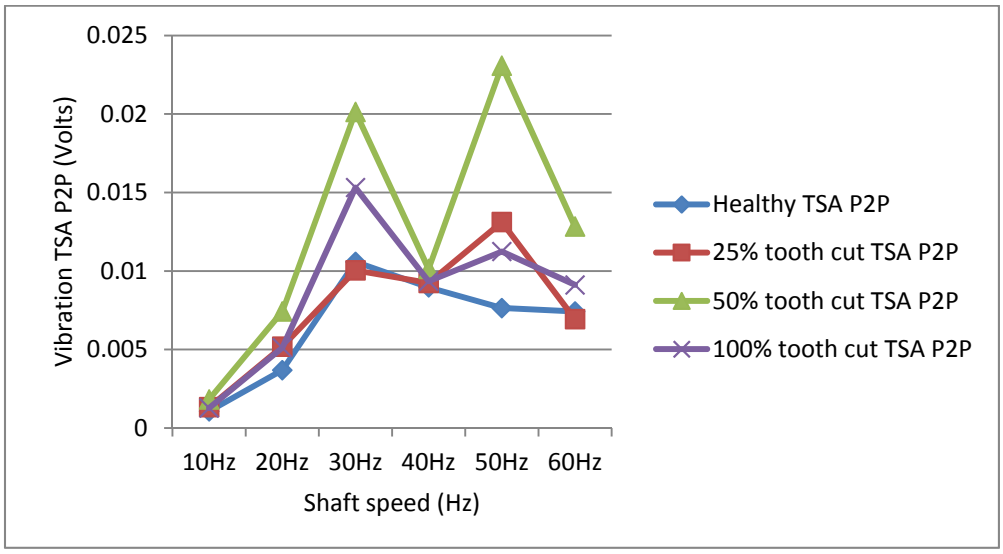


Figure 75. P2P average of radial vibration sensor

Figure 76 shows FM0 plots of the radial vibration sensors. It can be seen that FM0 of the faulty signals are mostly higher than the healthy ones. At 30 Hz, FM0 for all cases dropped to a low level and overlapped each other. This was likely caused by the resonance. Other than that, the healthy FM0 is relatively effective for fault detection.

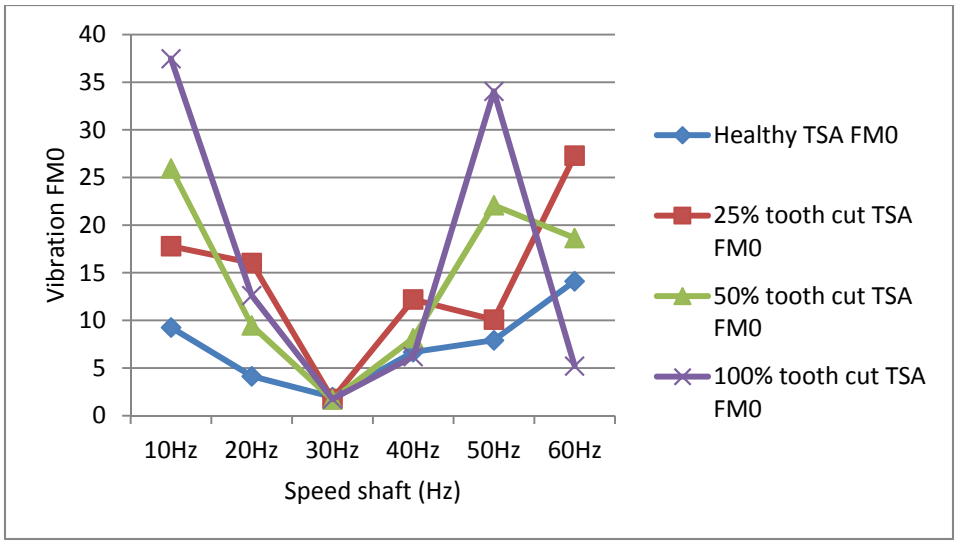

Figure 76. FM0 average of radial vibration sensor

In summary, it can be seen that for axial direction vibration sensor mounted on the gearbox housing, the P2P and kurtosis of the residual signals and EO show good fault detection potential, although most of them do not work for 25% tooth cut. On the other hand, for the radial sensor mounted on the top of the gearbox housing, both P2P and FM0 are highly affected by the machine resonance. FM0 might act as a good condition indicator in the speed range that was not heavily affected by resonance. Compared with AE results, none of the vibration condition indicators could detect all the faults and separate the damage levels. The vibration signals are highly affected by background noise and mechanical resonance, making it unstable in diagnostic performance. AE RMS and P2P show a roughly linear relationship against shaft speed. They could clearly indicate the tooth cut levels for diagnostics. Also, the kurtosis of AE signals offers another effective indication for fault detection.

As explained in Section 5.1, the tooth cut fault is the direct cause of larger backlash and reduction in contact ratio. Both the large backlash and low contract ratio introduce more looseness during gear meshing and therefore cause higher impact and gear noise. From this perspective, it can be

inferred that AE sensors are much more sensitive to impact energy. Vibration measured by accelerometer is the velocity signal, which is less sensitive to direct impact energy.

## 6.3 Conclusions

Based on the experimental results, the following conclusions can be drawn:

1) AE signals could be sampled at as low as 20 kHz while maintaining the capability of distinguishing tooth damage levels using TSA RMS and P2P.
2) Vibration signal condition indicators are not consistent with gear tooth damage level. Vibration is less sensitive than AE to small tooth damage in the low speed range.

# CHAPTER 7
# CONCLUSIONS

In this dissertation, effective and efficient AE based methods and tools for gearbox fault diagnosis were developed and validated with gearbox seeded fault tests on a notational split torque gearbox. Specifically, a frequency reduction method was developed based on the heterodyne technique to reduce the AE data sampling rate to as low as 20 kHz. By heterodyning, the AE signal frequency could be down shifted from several hundred kHz to below 50 kHz. Also through heterodyning, the AE signals could be demodulated to remove less useful high frequency components while keeping the fault characteristic frequency components in the demodulated AE signals. As a result, the demodulated AE signals could be sampled at a low rate comparable to that of vibration sensors. In order to extract useful features from AE signals sampled at a low rate, an effective AE signal processing method for gearbox fault diagnosis based on time synchronous average was developed. This was the first reported research effort in developing a physics based gearbox fault diagnosis method using AE sensors.

The developed AE based gearbox fault diagnosis methods and tools have several significant advantages. First, the heterodyne based frequency reduction method could down shift the sampling rate to that comparable to the vibration signals. The original meshing frequencies of the gearbox could be retained in the AE signals sampled at a low rate. This enabled well developed vibration analysis methods to be applied efficiently in practice to the AE signals for gearbox fault diagnosis, which is one of the major contributions of this work. Also, this could reduce the storage and computational burden for further signal processing; thus, great cost reduction can be achieved. By using TSA, the knowledge of the physical structure of the gearbox could be utilized

effectively and efficiently for fault diagnosis. This is different from any of the previous data driven methods which completely rely on a black box type of reasoning.

A comparative study between vibration analysis and AE analysis was also performed. Different levels of tooth cut faults were seeded and tested with both vibration and AE data collected. Results showed that AE based approach has the potential to differentiate gear tooth damage levels in comparison with vibration based approach. While vibration signals were easily affected by mechanical resonance, the AE signals showed more stable performance.

The effectiveness of AE analysis under low sampling rate has also been investigated. The results have shown that AE sampling rate could be as low as 20 kHz without serious performance degradation.

In summary, this dissertation presented an effective and efficient approach to process AE signals for gear fault diagnosis, which could be used in industrial applications with low cost. It showed that AE signals could be processed in a similar way as vibration signals using the heterodyne technique. TSA was applied to AE signal processing for the first time as known in literature. The methods and tools developed in this dissertation were validated by experimental investigation.

## REFERENCES


Åkerblom M., 2001, *Gear Noise and Vibration - A Literature Survey*, Maskinkonstruktion, Stckholm, Sweden.

Al-Balushi K. R. and Samanta B., 2002, "Gear Fault Diagnosis using Energy-based Features of Acoustic Emission Signals", *Proceedings of the Institution of Mechanical Engineers. Part I: Journal of Systems and Control Engineering*, Vol.216, No. 3, pp. 249 - 263.

Al-Ghamd A. M. and Mba D., 2006, "A Comparative Experimental Study on the Use of AE and Vibration Analysis for Bearing Defect Identification and Estimation of Defect Size", *Mechanical Systems and Signal Processing*, Vol. 20, No. 7, pp. 1537 - 1571.

Andrade F. A., Esat I., and Badi M. N. M., 1999, "Gearbox Fault Detection using Statistical Methods, Time–Frequency Methods (STFT and Wigner–Ville Distribution) and Harmonic Wavelet—A Comparative Study", *Proceedings of the COMADEM*, Jul. 6 - 9, Sunderland, England, pp. 77 - 85.

Antolick L. J., Branning J. S., Wade D. R., and Dempsey P. J., 2010, "Evaluation of Gear Condition Indicator Performance on Rotorcraft Fleet, *Proceedings of the American Helicopter Society 66th Annual Forum*, May 11 – 13, Phoenix, AZ.

Antoni J. and Randall R. B., 2006, "The Spectral Kurtosis: Application to the Vibratory Surveillance and Diagnostics of Rotating Machines", *Mechanical Systems and Signal Processing*, Vol. 20, No. 2, pp. 308 - 331.

Antoni J., 2006, "The Spectral Kurtosis: a Useful Tool for Characterizing Non-stationary Signals", *Mechanical Systems and Signal Processing*, Vol. 20, No. 2, pp. 282 - 307.

Arthur N. and Penman Inverter J., 1997, "Inverter Fed Induction Machine Condition Monitoring using the Bispectrum", *Proceedings of the IEEE Signal Processing Workshop on Higher-Order Statistics*, Jul 21 - 23, Banff, Alta., Canada, pp. 67 - 71.

Astridge D. G., 1989, "Helicopter Transmissions - Design for Safety and Reliability", *Proceedings of the Institution of Mechanical Engineers, Part G: Journal of Aerospace Engineering*, Vol. 203, No.2, pp. 123 - 138.

Baillie D. C. and Mathew J., 1996, "A Comparison of Autoregressive Modeling Techniques for Fault Diagnosis of Rolling Element Bearings", *Mechanical Systems and Signal Processing*, Vol. 10, No.1, pp. 1 - 17.

Bains M. and Kumar R., 2009, "Detection of Missing Ball in Bearing using Decomposition of Acoustic Signal", *Asian Journal of Chemistry*, Vol. 21, No.10, pp.143 - 147.

Bassiuny A. M., Li X. L., and Du R., 2007, "Fault Diagnosis of Stamping Process Based on Empirical Mode Decomposition and Learning Vector Quantization", *International Journal of Machine Tools Manufacture*, Vol. 47, No.15, pp. 2298 - 2306.

Baydar N. and Ball A., 2001, "A Comparative Study of Acoustic and Vibration Signals in Detection of Gear Failures using Wigner–Ville Distribution", *Mechanical Systems and Signal Processing*, Vol. 15, No.6, pp. 1091 - 1107.

Baydar N., Chen Q., Ball A., and Kruger U., 2001, "Detection of Incipient Tooth Defect in Helical Gears using Multivariate Statistics", *Mechanical Systems and Signal Processing*, Vol. 15, No.2, pp. 303 - 321.

Bechhoefer E., Qu Y., Zhu Z., and He D., 2013, "Signal Processing Techniques to Improve an Acoustic Emissions Sensor", Annual Conference of the Prognostics and Health Management Society, Oct. 14 - 17, New Orleans, LA.

Blankenship G. W. and Singh R., 1995, "Analytical Solution for Modulation Sidebands Associated with a Class of Mechanical Oscillators", *Journal of Sound and Vibration*, Vol. 179, No.1, pp. 13 - 36.

Bonnardot F., El Badaoui M., Randall R.B., Daniere J., and Guillet F., 2005, "Use of the Acceleration Signal of a Gearbox in Order to Perform Angular Resampling (with Limited

Speed Fluctuation) ", *Mechanical Systems and Signal Processing*, Vol. 19, No. 4, pp. 766 - 785.

Bosch Rexroth, 2011, "Designing for Wind Turbine Reliability", DesignNews Online, May 5, http://www.designnews.com/document.asp?doc_id=230485.

Braun S., 1975, "The Exaction of Periodic Waveforms by Time Domain Averaging", *Acustica*, Vol. 32, No.2, pp. 69 – 77.

Braun S., 2011, "The Synchronous (Time Domain) Average Revisited", *Mechanical Systems and Signal Processing*, Vol. 25, No.4, pp. 1087 - 1102.

Budynas R. G. and Nisbett J. K., 2011, *Shigley's Mechanical Engineering Design*, 9th Edition, McGraw Hill, New York, NY.

Capdevielle V., Servie`re C., and Lacoume J. L. 1996, "Blind Separation of Wide-Band Sources: Application to Rotating Machine Signals", *Proceedings of the Eighth European Signal Processing Conference*, Vol. 3, pp. 2085 – 2088, Sep. 10 - 13, Trieste, Italy.

Chen D., 2002, "Classification of Wavelet Map Patterns using Multi-layer Neural Networks for Gear Fault Detection", *Mechanical Systems and Signal Processing*, Vol. 16, No. 4, pp. 695 - 704.

Chiementin X., Mba D., Charnley B., Lignon S., and Dron J. P., 2010, "Effect of the Denoising on AE Signals", *Journal of Vibration and Acoustics*, Vol.132, No.3, pp. 1 - 9 .

Choudry A. and Tandon N., 2000, "Application of AE Technique for the Detection of Defects in Rolling Element Bearings", *Tribology International*, Vol. 33, No.1, pp. 39-45.

Chow T. W. S. and Fei G., 1995, "Three Phase Induction Machines Asymmetrical Faults Identification using Bispectrum", *IEEE Transactions on Energy Conversion*, Vol. 10, No.4, pp. 688 - 693.

Combet F. and Gelman L., 2007, "An Automated Methodology for Performing Time Synchronous Averaging of a Gearbox Signal Without Speed Sensor", *Mechanical Systems and Signal Processing*, Vol. 21, No. 6, pp. 2590 - 2606.

Craig, G. A., Heath, G. F., and Sheth V. J., 1998, Split Torque Proprotor Transmission, McDonnell Douglas Helicopter Co., U.S. Patent Number 5,823,470.

Dalpiaz G., Rivola A., and Rubini R., 2000, "Effectiveness and Sensitivity of Vibration Processing Techniques for Local Fault Detection in Gears", *Mechanical Systems and Signal Processing*, Vol. 14, No. 3, pp. 387 - 412.

De la Cruz M. and Rahnejat H., 2008, "Impact Dynamic Behaviour of Meshing Loaded Teeth in Transmission Drive Rattle". *Proceedings of the Sixth EUROMECH Nonlinear Dynamics Conference*, Jun. 30 – Jul. 4, Saint Petersburg, RUSSIA, pp. 418 - 430.

DeLange, G., 2000, "Failure Analysis for Gearing", *Maintenance Technology online*, Jan. 1, http://www.mt-online.com/january2000/failure-analysis-for-gearing.

Donzey J. P., 2006, "Helicopter Bristol 171 Sycamore Main Gear Box and Rotor Head.jpg", Deutsches Museum, Munich, Germany.

Dron J. P., Rasolofondraibe L., Couet C., and Pavan A., 1998, "Fault Detection and Monitoring of a Ball Bearing Bench Test and a Production Machine via Autoregressive Spectrum Analysis", *Journal of Sound and Vibration*, Vol. 218, No.3, pp. 501 - 525.

Dwyer R.F., 1983, "Detection of Non-Gaussian Signals by Frequency Domain Kurtosis Estimation", *Proceedings of the International Conference on Acoustic, Speech, and Signal Processing*, Apr. 14 – 16, Boston, MA, Vol. 8, pp. 607 - 610.

Eftekharnejad B. and Mba D., 2009, "Seeded Fault Detection on Helical Gears with AE", *Applied Acoustics*, Vol. 70, No.4, pp. 547 - 555.

Elmaleeh M. A. and Saad N., 2008, "Development of AE Diagnostic System for Condition Monitoring of Rotating Machines", 2nd IEEE International Conference on Power and Energy (PECon 08), Dec. 1 - 3, 2008, Johor Baharu, Malaysia.

Elmaleeh M.A., Saad N., Ahmed N., and Awan M., 2007, "On-line Fault Detection & Diagnosis of Rotating Machines using Acoustic Mission Monitoring Techniques" , International

Conference on Intelligent and Advanced Systems, Nov. 25 – 28, 2007, Kuala Lumpur, Malaysia.

Feldman M., 2011, "Hilbert Transform in Vibration Analysis", *Mechanical Systems and Signal Processing*, Vol. 25, No.3, pp. 735 - 802.

Feng Y., Thanagasundrum S., and Schlindwein F. S., 2006, "Discrete Wavelet-based Thresholding Study on AE Signals to Detect Bearing Defect on a Rotating Machine" ICSV13-Vienna, the 13th International Congress on Sound and Vibration, Vienna , Austria.

Gao L., Zai F., Su S., Wang H., Chen P., and Liu L., 2011, "Study and Application of AE Testing in Fault Diagnosis of Low-speed Heavy-duty Gears", *Sensors*, Vol.11, No.1, pp. 599 - 611.

Gmirya, Y. and Kish J.G., 2003, "Split-Torque Face Gear Transmission", Sikorsky Aircraft Corporation, U.S. Patent Number 6,612,195.

Gmirya, Y. and Vinayak, H., 2004. "Load Sharing Gear for High Torque, Split-path Transmissions". Sikorsky Aircraft Corporation. International Patent PCT. WO 2004/094093.

Gmirya, Y., 2005, "Split Torque Gearbox with Pivoted Engine Support", Sikorsky Aircraft Corp., U.S. Patent Number 6,883,750.

Gnanakumarr M., Theodossiades S., Rahnejat H., and Menday M., 2005, "Impact-induced Vibration in Vehicular Driveline Systems: Theoretical and Experimental Investigations". *Proceedings of the Institution of Mechanical Engineers, Part K: Multibody Dynamics*, Vol. 219, No.1, pp. 1 - 12.

Guo Y.B. and Ammula S.C., 2005, "Real-time AE Monitoring for Surface Damage in Hard Machining", *International Journal of Machine Tools & Manufacture*, Vol. 45, No.14, pp. 1622 - 1627.

Hall L. D. and Mba D., 2004, "AEs Diagnosis of Rotor-Stator Rubs using the Ks Statistic", *Mechanical Systems and Signal Processing*, Vol. 18, No. 4, pp. 849 - 868.

He D., Li R., Zhu J., and Zade M., 2011, "Data Mining Based Full Ceramic Bearing Fault Diagnostic System using AE Sensors", *IEEE Transactions on Neural Network*, Vol. 22, No. 12, pp. 2022 - 2031.

He D., Manon P., Li R., Seçkiner S., and Bechhoefer E., 2010, "Gear Fault Location Detection for Split Torque Gearbox using AE Sensors", Annual Conference of the Prognostics and Health Management Society, Oct. 10 – 14, Portland, OR.

He Y., Zhang X., and Friswell M. I., 2009, "Defect Diagnosis for Rolling Element Bearings using AE", *Journal of Vibration and Acoustics*, Vol.131, No.6, pp. 102 - 111.

Hellier C., 2003, *Handbook of Nondestructive Evaluation*, McGraw Hill Professional.

Ho D. and Randall R.B., 2000, "Optimisation of Bearing Diagnostic Techniques using Simulated and Actual Bearing Fault Signals", *Mechanical Systems and Signal Processing*, Vol. 14, No.5, pp. 763 - 788.

Holroyd T., 2000, *AE & Ultrasonics Monitoring Handbook*, Oxford, U.K.: Coxmoor Publishing Co. 2000.

Huang N. E, Wu M. L., Steven R. L., Shen S. P., Qu W. D., Gloersen P., and Fan K. L., 2003, "A Confidence Limit for the Empirical Mode Decomposition and Hilbert Spectral Analysis", *Proceedings of the Royal Society of London A*, Vol. 459, No.2037, pp. 2317 - 2345.

Huang N. E., Shen Z., Long S. R., Wu N. C., Zheng Q., Yen N. C., Tung C. C., and Liu H. H., 1998, "The Empirical Mode Decomposition and the Hilbert Spectrum for Nonlinear and Non-stationary Time Series Analysis", *Proceedings of the Royal Society of London A*, Vol. 454, No.1791, pp. 903 - 995.

ISO 12713, 1998a, "AE Inspection-Primary calibration of Transducers", ISO.

ISO 12713, 1998b, "AE Inspection-Secondary Calibration of Transducers", ISO.

ISO 22096, 1996, "Condition Monitoring and diagnostics of machines-AE", ISO.

Jardine A. K. S. , Lin D., and Banjevic D., 2006, "A review on machinery diagnostics and prognostics implementing condition-based maintenance", *Mechanical Systems and Signal Processing*, Vol. 20, No. 7, pp. 1483 – 1510.

Jong J., McBride J., Jones J., Fiorucci T., and Zoladz T., 1996 , "Synchronous Phase Averaging Method for Machinery Diagnostics", Defense Technical Information Center, Proceedings of a Joint Conference, Mobile, Alabama, April 22-26, 1996.

Kaiser J. F., 1990, "On Teager's Energy Algorithm and Its Generalization to Continuous Signals", Proc. 4th IEEE Digital Signal Processing Workshop, Mohonk (New Palts), NY.

Kilundu B., Chiementin X., Duez J., and Mba D., 2011, "Cyclostationarity of AEs for Monitoring Bearing Defects", *Mechanical Systems and Signal Processing*, Vol. 25, No.6, pp. 2061 - 2072.

Kish J. G. and Webb L. G. 1992, "Elastomeric Torsional Isolator. United Technologies Corporation", U.S. Patent Number 5,117,704.

Kish J. G., 1993a, Sikorsky Aircraft Advanced Rotorcraft Transmission (ART) Program – Final Report. NASA CR-191079, NASA Lewis Research Center, Cleveland, OH.

Kish J. G., 1993b, Comanche Drive System. Proceedings of the Rotary Wing Propulsion, Specialists Meeting, American Helicopter Society, Williamsburg, VA, pp. 7.

Krantz T. L. and Delgado I. R., 1996, Experimental Study of Split-Path Transmission Load Sharing, Technical Memorandum 107,202, NASA Lewis Research Center, Cleveland, Ohio. Army Research Laboratory Technical Report ARL-TR-1067.

Krantz T. L., 1994, Dynamics of a Split Torque Helicopter Transmission, in: Technical Memorandum 106,410, NASA Lewis Research Center, Cleveland, Ohio. Army Research Laboratory Technical Report ARL-TR-291.

Krantz T. L., 1996, A Method to Analyze and Optimize the Load Sharing of Split Path Transmissions, Technical Memorandum 107,201, NASA Lewis Research Center, Cleveland, Ohio. Army Research Laboratory Technical Report ARL-TR-1066.

Krantz T. L., Rashidi M., and Kish J. G. 1992. Split Torque Transmission Load Sharing, in: Technical Memorandum 105,884, NASA Lewis Research Center, Cleveland, Ohio. Army Research Laboratory Technical Report 92-C-030.

Kwak J. S. and Ha M. K., 2004, "Neural Network Approach for Diagnosis of Grinding Operation by AE and Power Signals", *Journal of Materials Processing Technology*, Vol.147, No.1, pp. 65 - 71.

Lebold M., McClintic K., Campbell R., Byington C., and Maynard K., 2000, "Review of Vibration Analysis Methods for Gearbox Diagnostics and Prognostics", Proceedings of the 54th Meeting of the Society for Machinery Failure Prevention Technology, Virginia Beach, VA, May 1-4, p. 623 - 634.

Lebold M., McClintic K., Campbell R., Byington C., and Maynard K., 2000, "Review of Vibration Analysis Methods for Gearbox Diagnostics and Prognostics", *Proceedings of the 54th Meeting of the Society for Machinery Failure Prevention Technology*, Virginia Beach, VA, May 1-4, pp. 623 - 634.

Lei Y., Lin J., He Z., and Zuo M. J., 2012, "A review on empirical mode decomposition in fault diagnosis of rotating machinery", *Mechanical Systems and Signal Processing*, Vol. 35, No. 1-2, pp. 108 - 126.

Li H. L., Deng X. Y., and Dai H. L., 2007, "Structural Damage Detection using the Combination Method of EMD and Wavelet Analysis", *Mechanical Systems and Signal Processing*. Vol. 21, No.1, pp. 298 - 306.

Li R. and He D., 2012, "Rotational Machine Health Monitoring and Fault Detection using EMD-Based AE Feature Quantification", *IEEE Transactions on Instrumentation and Measurement*, Vol. 61, No.4, pp. 990 - 1001.

Li S., 2013, "Effects of Centrifugal Load on Tooth Contact Stresses and Bending Stresses of Thin-rimmed Spur Gears with Inclined Webs", *Mechanism and Machine Theory*, Vol. 59, No.1, pp. 34 - 47.

Li X. L., 2002, “A Brief Review: AE Method for Tool Wear Monitoring During Turning”, *International Journal of Machine Tools and Manufacture*, Vol. 42, No.2, pp. 157 - 165.

Liao B., 1995, “Mechanical Fault Diagnosis Fundamental”, Metallurgical Industry Press, Beijing, China (in Chinese).

Link H., LaCava, W., van Dam J., McNiff B., Sheng S., Wallen R., McDade M., Lambert S., Butterfield S., and Oyague, F., 2011, "Gearbox reliability collaborative project report: findings from phase 1 and phase 2 testing," NREL technical report: NREL/TP-5000-51885.

Liu B., Riemenschneider S., and Xu Y., 2006, “Gearbox Fault Diagnosis using Empirical Mode Decomposition and Hilbert Spectrum”, *Mechanical Systems and Signal Processing*, Vol. 20, No.3, pp. 718 - 734.

Loutas T. H., Roulias D., Pauly E., and Kostopoulos V., 2011, “The Combined Use of Vibration, AE and Oil Debris On-line Monitoring Towards A More Effective Condition Monitoring of Rotating Machinery”, *Mechanical Systems and Signal Processing*, Vol. 25, No. 4, pp. 1339 - 1352.

Loutas T. H., Sotiriades G., Kalaitzoglou I., and Kostopoulos V., 2009, “Condition monitoring of a single-stage gearbox with artificially induced gear cracks utilizing on-line vibration and AE measurements”, *Applied Acoustics*, Vol. 70, No.9, pp. 1148 - 1159.

Mathews J. R., 1983, *Acoustic Emission*, Gordon and Breach Science Publishers Inc., New York, NY.

Mba D., 2003, “AEs and monitoring bearing health”, *Tribology Transactions*, Vol.46, No.3, pp. 447 - 451.

McFadden P. D. and Toozhy M., 2000, “Application of Synchronous Averaging to Vibration Monitoring of Rolling Element Bearing”, *Mechanical Systems and Signals Processing*, Vol. 14, No. 6, pp. 891 - 906.

McFadden P. D., 1986, "Detecting Fatigue cracks in Gears by Amplitude and Phase Demodulation of the Meshing Vibration", *ASME Transactions*, *Journal of Vibration, Acoustics, Stress, and Reliability in Design*, Vol. 108, No.2, pp. 165 - 170.

McFadden P. D., 1987, "A Revised Model for the Extraction of Periodic Waveforms by Time Domain Averaging", *Mechanical Systems and Signal Processing*, Vol. 1, No. 1, pp. 83 - 95.

McFadden P. D., 1987, "Examination of a Technique for The Early Detection of Failure in Gears by Signal Processing of The Time Domain Average of The Meshing Vibration", *Mechanical Systems and Signal Processing*, Vol. 1, No. 2, pp. 173 - 183.

McFadden P. D., 1991, "Technique for Calculating The Time Domain Averages of The Vibration of the Individual Planet Gears and the Sun Gear in An Epicyclic Gearbox", *Journal of Sound and Vibration*, Vol. 144, No. 1, pp. 163 - 172.

Mechefske C. K. and Mathew J., 1992, "Fault Detection and Diagnosis in Low Speed Rolling Element Bearing. Part I: The Use of Parametric Spectra", *Mechanical Systems and Signal Processing*, Vol. 6, No. 4, pp. 297 - 307.

Mechefske C. K. and Mathew J., 1992, "Fault Detection And Diagnosis in Low Speed Rolling Element Bearings part II: The Use of Nearest Neighbor Classification", *Mechanical Systems and Signal Processing*, Vol. 6, No. 4, pp. 309 – 316.

Miller R. K. and McIntire P., *Non-destructive testing handbook, Volume 5 – Acoustic Emissions*, Chapter 1, American Society of Non-destructive Testing, 1987.

Mirhadizadeh S. A., 2008, "Observations of AE in a hydrodynamic bearing", The 2nd International Conference on Technical Inspection and NDT, Oct. 21 - 22, Tehran, Iran.

Morhain A. and Mba D., 2003, "Bearing defect diagnosis and AE", *Proceedings of the Institution of Mechanical Engineers, Part J, Journal of Engineering Tribology*, Vol 217, No. 4, pp. 275 - 272.

Nooli P. K., 2011, *A Versatile and Computationally Efficient Condition Indicator for AH-64 Rotorcraft Gearboxes*, Master thesis, Department of Mechanical Engineering, University of South Carolina, Columbia, SC.

Ogbonnah V., 2007, Condition Monitoring of Gear Failure with AE, Master's Degree Thesis, Department of Mechanical Engineering, Blekinge Institute of Technology, Karlskrona, Sweden.

Ognjanović M. and Snežana Ć. K., 2012, "Gear Unit Housing Effect on the Noise Generation Caused by Gear Teeth Impacts", *Journal of Mechanical Engineering*, Vol. 58, No. 5, pp. 327-337.

Pan M. C., Van Brussel H., Sas P., and Verbeure B., 1998, "Fault Diagnosis of Joint Backlash", *Journal of Vibration and Acoustics*, Vol. 120, No. 1, pp. 13 - 24.

Parker B. E., Ware H. A., Wipf D. P., Tompkins W. R., Clark B. R., Larson E. C., and Poor H. V., 2000, "Fault Diagnostics using Statistical Change Detection in the Bispectral Domain", *Mechanical Systems and Signal Processing*, Vol. 14, No. 4, pp. 561 - 570.

Poyhonen S., Jover P., and Hyotyniemi H., 2004, "Signal processing of vibrations for condition monitoring of an induction motor", ISCCSP: 1st International Symposium on Control, Communications and Signal Processing, New York, NY, pp. 499–502.

Propulsion M., 2012, "Vibration & AEs", Kittiwake Company News, http://www.kittiwake.com/news/2012/02.

Randall R. B., Antoni J., and Chobsaard S., 2001, "The Relationship Between Spectral Correlation And Envelope Analysis in the Diagnostics of Bearing Faults and Other Cyclostationary Machine Signals", *Mechanical Systems and Signal Processing* Vol. 15, No. 5, pp. 945–962.

Sarkar N., Ellisb R. E., and Mooreb T. N., 1997, "Backlash Detection in Geared Mechanisms: Modeling, Simulation, and Experimentation", *Mechanical Systems and Signal Processing*, Vol. 11, No. 3, pp. 391–408.

Segade-Robleda A., Vilán-Vilán J., López-Lago M., and Casarejos-Ruiz E., 2012, "Split Torque Gearboxes: Requirements, Performance and Applications", *Mechanical Engineering,* InTech, Rijeka, Croatia.

Shen Z. X., Huang X.Y., and Ma X.X., 2008, "An Intelligent Fault Diagnosis Method Based on Empirical Mode Decomposition and Support Vector Machine", *Proceedings of the Third International Conference on Convergence and Hybrid Information Technology*, Busan, Korea, Nov. 11–13, pp. 865 - 869.

Sheng S., Oyague F., and Butterfield S., 2009, "Investigation of Various Wind Turbine Drive Train Condition Monitoring Techniques", 7th International Workshop on Structural Health Monitoring, Stanford, California.

Shiroishi J., Li Y., Liang S., Kurfess T. and Danyluk S., 1997, "Bearing Condition Diagnostics Via Vibration and AE Measurements", *Mechanical Systems and Signal Processing*, Vol. 11, No. 5, pp. 693 - 705.

Sikorska J. Z. and Mba D., 2008, "Challenges and Obstacles in The Application of AE to Process Machinery", *Proceedings of the Institution of Mechanical Engineers, Part E: Journal of Process Mechanical Engineering*, Vol. 222, No. 1, pp.1-19.

Smith J. D., 2003, *Gear Noise and Vibration*, Marcel Dekker Inc., New York, NY.

Soua S., Lieshout P., Perera A., Gan T. H., and Bridge B., 2013, "Determination of the Combined Vibrational and AE Signature of a Wind Turbine Gearbox and Generator Shaft in Service as a Pre-requisite for Effective Condition Monitoring", *Renewable Energy*, Vol. 51, No. 3, pp. 175 – 181.

Stack J. R., Harley R. G., and Habetler T. G., 2004, "An Amplitude Modulation Detector for Fault Diagnosis in Rolling Element Bearings", *IEEE Transactions on Industrial Electronics*, Vol. 51, No. 5, pp. 1097 - 1102.

Stewart R. M., 1977, “Some Useful Analysis Techniques for Gearbox Diagnostics”, Technical Report MHM/R/10/77, Machine Health Monitoring Group, Institute of Sound and Vibration Research, University of Southampton.

Tan C. K. and Mba D., 2005, “Experimentally Established Correlation between AE Activity, Load, Speed, and Asperity Contact of Spur Gears under Partial Elastohydrodynamic Lubrication”. *Proceedings of the Institute of Mechanical Engineers, Part J*: *Journal of Engineering Tribology,* Vol. 219, No. 6, pp. 401 - 409.

Tan C. K. and Mba D., 2006, “A Correlation between Acoustic Emission and Asperity Contact of Spur Gears under Partial Elastohydrodynamic Lubrication”, International Journal of COMADEM, Vol. 9, No. 1, pp. 9 - 14.

Tandon N. and Nakra B. C., 1992, Comparison of Vibration and Acoustic Measurements Techniques for the Condition Monitoring of Rolling Element Bearings. *Tribology International*, Vol. 25, No. 3, pp. 205 - 212.

Teager H. M. and Teager S. M., 1992, “Evidence for Nonlinear Sound Production Mechanisms in the Vocal Tract”, Speech Production and Speech Symposium Time-Frequency and Time-Scale Analysis, Victoria, British Columbia, Canada, pp. 345-348.

Theodossiades S. and Natsiavas S., 2000, “Nonlinear Dynamics of Gear-pair Systems with Periodic Stiffness and Backlash”. *Journal of Sound and Vibration*, Vol. 229, No. 2, pp. 287 - 310.

Tiwari S. K. and Joshi U. K., 2012, “Stress Analysis of Mating Involute Spur Gear Teeth”, *International Journal of Engineering Research & Technology (IJERT)* , Vol. 1, No. 9, pp. 2173 - 2180.

Tomoya M., Katsumi I., and Masana K., 1994, “Acoustic Emission during Fatigue Crack Growth in Carburized Gear Tooth”, *Transactions of the Japan Society of Mechanical Engineers*, Part C, Vol. 60, No. 575, pp. 2456 - 2461.

Tse P. W., Yang W. X., and Tam H. Y., 2004, "Machine Fault Diagnosis through an Effective Exact Wavelet Analysis". *Journal of Sound and Vibration*, Vol. 227, No. 5, pp. 1005 - 1024.

Tuma J., 2009, "Gearbox Noise and Vibration Prediction and Control". *International Journal of Acoustics and Vibration*, Vol. 14, No. 2, pp. 99 - 110.

Vallen H., 2002, "AE Testing Fundamentals, Equipment, Applications", NDT.net, Vol. 7, No. 9, Icking (Munich), Germany.

Večeř P., Kreidl M., and Šmíd R., 2005, "Condition Indicators for Gearbox Condition Monitoring Systems", *Journal of Advanced Engineering,* Vol. 45, No. 6, pp. 35 - 43.

Verbruggen T.W., 2003, "Wind Turbine Operation and Maintenance Based on Condition Monitoring", ECN Project Report, www.ecn.nl/publicaties/PdfFetch.aspx?nr=ECN-C--03-047.

Vilán Vilán J. A., Robleda A. S., Lago M. L., and Vilán A. M. F., 2009, "Configurations to Increase Power Density in Split Torque Gearboxes With Idler Pinions", 3rd International Conference on Integrity, Reliability and Failure, Jul. 20 - 24, Porto, Portugal.

Wang C. C. and Too G. P. J., 2002, "Rotating Machine Fault Detection Based on HOS and Artificial Neural Networks", *Journal of Intelligent Manufacturing*, Vol. 13, No. 4, pp. 283 - 293.

Wang K. S. and Heyns P. S., 2011, "Application of Computed Order Tracking, Vold - kalman Filtering and EMD in Rotating Machine Vibration", *Mechanical Systems and Signal Processing,* Vol. 25, No. 1, pp. 416 - 430.

Wang W. J. and Lin R. M., 2003, "The Application of Pseudo-phase Portrait in Machine Condition Monitoring", Journal of Sound and Vibration, Vol. 259, No. 1,pp. 1 - 16.

Wang W. J. and McFadden P. D., 1993, "Early Detection of Gear Failure By Vibration Analysis i. Calculation of the Time - Frequency Distribution", *Mechanical Systems and Signal Processing,* Vol.7, No. 3, pp. 193 - 203.

Wang W. J., Chen J., Wu X. K., and Wu Z. T., 2001, "The Application of Some Non-linear Methods in Rotating Machinery Fault Diagnosis", *Mechanical Systems and Signal Processing*, Vol. 15, No. 4, pp. 697 - 705.

Wang W., 2001, "Early Detection of Gear Tooth Cracking using the Resonance Demodulation Technique", *Mechanical Systems and Signal Processing*, Vol. 15, No. 5, pp. 887 - 903

Wang Z., Willett P., De Aguiar P.R., and Webster J., 2001, "Neural Network Detection Of Grinding Burn from AE", *International Journal of Machine Tools & Manufacture*, Vol. 41, No. 2, pp. 283 - 309.

White G., 1974, "New Family of High-Ratio Reduction Gear with Multiple Drive Paths", *Proceedings of the Institution of Mechanical Engineers*, Vol. 188, No.1, pp. 281 - 288.

White G., 1983, "A 2400 kW Lightweight Helicopter Transmission Whit Split Torque Gear Trains", ASME Paper 84-Det-91.

White G., 1989, "Split-Torque Helicopter Transmission With Widely Separated Engines". *Proceedings of the Institution of Mechanical Engineers*, *Part G: Journal of Aerospace Engineering*, Vol. 203, No. 1, pp. 53 - 65.

White G., 1993, "3600 HP Split-Torque Helicopter Transmission", *Mechanical Systems Technology Branch Research Summary*, 1985-1992, NASA Technical Memorandum.

White G., 1998, "Design Study of a Split-torque Helicopter Transmission, in: Proceedings of the Institution of Mechanical Engineers", *Part G: Journal of Aerospace Engineering*, Vol. 212, No. 2, pp. 117 - 123.

Xiong L., Shi T., Yang S., and Rao R. B. K. N., 2002, "A Novel Application Of Wavelet-based Bispectrum Analysis to Diagnose Faults in Gears", *International Journal of COMADEM* , Vol. 5, No. 3, pp. 31 - 38.

Yan R. Q. and Gao R. X., 2006, "Hilbert-Huang Transform-Based Vibration Signal Analysis for Machine Health Monitoring", *IEEE Transactions on Instrumentation and Measurement*, Vol. 55, No. 6, pp. 2320 - 2329.

Yang D. M., Stronach A. F., Macconnell P., and Penman J., 2002, "Third-order Spectral Techniques for the Diagnosis of Motor Bearing Condition using Artificial Neural Networks", *Mechanical Systems and Signal Processing*, Vol. 16, No. 2-3, pp.391 - 411.

Zakrajsek J. J., Townsend D. P., and Decker H. J., 1993, "An Analysis of Gear Fault Detection Methods As Applied To Pitting Fatigue Failure Data", Technical Report NASA TM-105950, AVSCOM TR-92-C-035, NASA and the US Army Aviation Systems Command.

Zhan Y., Makis V., and Jardine A. K. S., 2003, "Adaptive Model For Vibration Monitoring of Rotating Machinery Subject to Random Deterioration", *Journal of Quality in Maintenance Engineering*, Vol. 9, No.4, pp. 351 - 375.

# VITA

NAME: Yongzhi Qu

EDUCATION: B.S., Wuhan University of Technology, 2008
M.S., Wuhan University of Technology, 2011

EXPERIENCE: Research Assistant, Intelligent System Modeling and Development Laboratory, Department of Mechanical & Industrial Engineering, University of Illinois at Chicago, January 2012 – December 2013.

Teaching Assistant, ECE 265 Introduction to Logic Design, University of Illinois at Chicago, Fall, 2010.

Teaching Assistant, ECE 365 CAD-Based Digital Design, University of Illinois at Chicago, Spring, 2011.

Teaching Assistant, IE 467 Discrete Event Computer Simulations, University of Illinois at Chicago, Fall, 2013.

Teaching Assistant, 201 Financial Engineering, University of Illinois at Chicago, Fall, 2013.

HONORS: Best Academia Paper Award, IEEE International Conference on Prognostics and Health Management, 2013, "Time Synchronous Average Based Acoustic Emission Signal Analysis on Gear Fault Detection".

Best Student Paper Runner-up Award, Machine Failure Prevention Technology Society (MPFT), 2013, "Development and Validation of Lubrication Oil Particle Contamination Models".

PUBLICATIONS: **Qu Y.**, Bechhoefer E., He D., and Zhu J., 2013, "A New Acoustic Emission Sensor Based Gear Fault Detection Approach", *The International Journal of Prognostics and Health Management* (*IJPHM*), *Special Issue on Wind Turbine PHM*, Vol. 4, pp. 32- 45.

Zhu J., Yoon J., He D., **Qu Y**., and Bechhoefer E., 2013, "Lubrication Oil Condition Monitoring and Remaining Useful Life Prediction with Particle Filtering", *International Journal of Prognostics and Health Management, Special Issue Wind Turbine PHM*, Vol. 4, pp. 1 – 15.

**Qu Y.**, Zhu J., Bechhoefer E., and He D., 2013, "Gear Fault Detection using Acoustic Emission Spectrum Kurtosis", *Proceedings of the 2013 Conference of the Society for Machinery Failure Prevention Technology (MFPT)*, May 13-17, Cleveland, OH.

**Qu Y.**, Zhu J., Bechhoefer E., and He D., 2013, "Gear Fault Detection using Time Synchronous Average based Acoustic Emission Condition

Indicators", American Helicopter Society conference, May 21-23, Phoenix, AZ.

**Qu Y**., Zhu J., He D., Qui B., and Bechhoefer E., 2013, "Time Synchronous Average Based Acoustic Emission Signal Analysis on Gear Fault Detection", Proceedings of 2013 IEEE International Conference on Prognostics and Health Management (PHM), June 24 – 27, Gaithersburg, MD.

Bechhoefer E., **Qu Y**., Zhu J., and He D., 2013, "Analog Signal Processing to Improve Acoustic Emission Sensing", Proceedings of the 2013 Conference of the Society for Machinery Failure Prevention Technology (MFPT), May 13 – 17, Cleveland, OH.

Bechhoefer E., **Qu Y.**, Zhu J., and He D., 2013, "Signal Processing Technique to Improve an Acoustic Emissions Sensor", Annual Conference of the Prognostics and Health Management Society, Oct. 14 -17, New Orleans, LA.

Zhu J., He D., **Qu Y**., and Bechhoefer E., 2012, "Lubrication Oil Condition Monitoring and Remaining Useful Life Prediction with Particle Filtering", Proceedings of 2012 American Wind Energy Association (AWEA), Wind Power Conference, June 3 – 6, Atlanta, GA.